Poisson's ratio and Young's modulus of weft-knitted fabrics

A study on the influence of using and combining different knitting patterns

Emma de Groen

Delft University of Technology

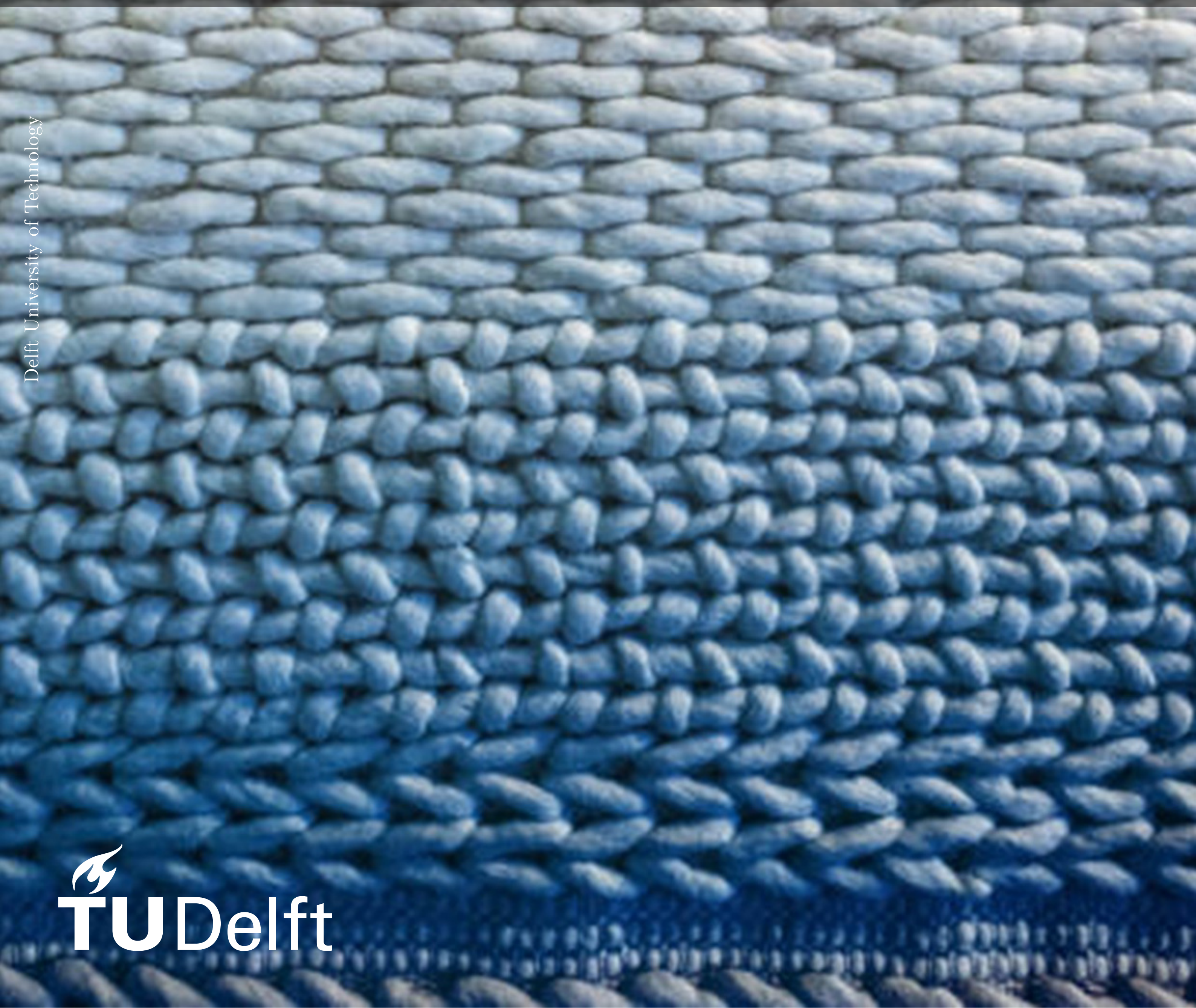

TU Delft

Poisson's ratio and Young's modulus of weft-knitted fabrics

A study on the influence of using and combining different knitting patterns

by

Emma de Groen

to obtain the degree of Master of Science
at the Delft University of Technology,

Project duration:	February, 2024 – August, 2024	
Thesis committee:	Dr. M.A. Popescu,	TU Delft, chair
	N. Christidi	TU Delft, daily supervisor
	Dr. Ir. F.P. van der Meer	TU Delft, secondary supervisor

Cover: Picture by Studio Light and Shade, 2018

TU Delft

Abstract

Membrane structures are material efficient structures made with a lightweight flexible membrane. Usually the membrane is made out of a woven textile. Because of the size restrictions of the woven patches of fabric, the membrane will contain multiple seams. This will not be the case when the membrane is a knitted fabric. Membrane structures are suitable for making lightweight formworks for concrete structures with complex geometries.

Knitted fabrics can be made using a CNC knitting machine which uses weft-knitting. This machine uses two needle beds with needles which can catch the yarn and perform different knitting operations like a plain stitch, a float stitch, a tuck stitch, a transfer stitch and an interlock stitch. Different configurations of these knitting operations create different knitting patterns.

The mechanical properties of the knitted textiles that are considered during this research are the Poisson's ratio and Young's modulus. Since knitted fabrics show orthotropic behaviour, the fabrics have to be tested in both directions (wale and course direction). The properties can be determined when fabrics are tested in a uniaxial tensile test, a wide jaw test or a biaxial tensile test. Digital image correlation can be used to measure the strain of the fabric in lateral direction.

This research addresses the effect of different knitting patterns on the Poisson's ratio and Young's modulus of weft-knitted fabrics. To achieve this objective, homogeneous fabrics of multiple knitting patterns have been tested. The knitting patterns that are considered in this thesis are interlock, eightlock, hexagon, tuck, interlock_1float and interlock_2float. Afterwards, non-homogeneous textiles have been fabricated in which two knitting patterns have been combined. This is done with interlock as a primary pattern and tuck or eightlock as a secondary knitting pattern. The secondary knitting pattern is applied as a circle in the centre of the fabric.

The results of the tensile tests show large differences in mechanical properties for the fabrics with different knitting patterns. In wale direction the Poisson's ratios for the interlock, tuck, interlock_1float and interlock_2float pattern are between 0.5 and 0.65, while the ratios for the eightlock and hexagon patterns are larger; between 0.8 and 0.9. In course direction, the ratios are smaller than in wale direction. For the interlock, tuck and interlock_1float show a Poisson ratio between 0.45 and 0.5 while the ratio for the eightlock pattern is around 0.6.

In wale direction, the Young's modulus for the interlock, tuck and interlock_1float are between 0 and 2.5 MPa, while the Young's modulus for the eightlock and interlock_2float pattern are between 8 and 12 MPa. The hexagon pattern is even more stiff, with a Young's modulus around 30 MPa. In course direction, the Young's moduli are way lower (between 0 and 0.5 MPa for all fabrics). In this direction, the stress-strain curves of the fabrics do not reach the elastic region because of rotation of the clamps in the test setup.

For the non-homogeneous interlock_tuck fabrics, the Poisson's ratio in wale direction is larger than the homogeneous interlock and tuck fabrics. This is caused by the interaction between the different knitting patterns. This effect is not visible in course direction. For the non-homogeneous interlock_eightlock fabrics, this is the other way around. The interaction between the knitting patterns plays a role in course direction, but is not visible to the same extent in wale direction.

The Young's modulus of the secondary knitting pattern is larger for both the interlock_tuck and interlock_eightlock fabrics. Therefore the Young's modulus increases when the diameter of the circle containing the secondary knitting pattern increases.

Acknowledgements

First of all, I want to express my gratitude to my chair Dr. Mariana Popescu. If it wasn't for your enthusiasm regarding knitted fabrics, I would have never started my thesis on this topic. I want to thank you for your critical view on my topic during our meetings and for always being willing to help find solutions to challenges I encountered throughout this research. I want to thank my daily supervisor Nikoletta Christidi for always being willing to help me with the setup, making fabrics, figuring out solutions for the challenges we encountered and always being available to answer my never-ending amount of questions. You have been a great help! I would like to extend my appreciation to my secondary supervisor Dr. Ir. Frans van der Meer for his critical questions and technical advise during our meetings.

Furthermore, I want to acknowledge Giorgos Stamoulis for being a great help with the implementation of the DIC software and providing a camera. It might seem of less importance, but without you I would not have been able to present the results I have now.

Last but not least, I want to thank my friends and family who have supported me throughout not only this thesis period but throughout my whole time at this university. Thank you for listening to my stories even though they might have been a bit too technical.

Emma de Groen
Delft, August 2024

Contents

Part I

Introduction

1
Background

1.1. Context

Membrane structures are structures that are made with a lightweight flexible membrane which is tensioned to create the shape of the structure. The membrane is usually supported by columns or cables and carries the applied loads primarily in tension (LSAA, 2010). An advantage of these structures is that they are able to cover large spans without the need for supporting members. Since the membrane is very light-weight, but still is able to cover a large free span and carry large loads, this type of structures is very material efficient. This creates a low environmental footprint which has nowadays become more and more important (LSAA, 2010).

The membranes that are used are thin and flexible. Therefore fabrics are a suitable material to make membranes. The fabrics are kept in the desired shape by using structural elements like columns or cables or by inflating the membrane. Examples of this are shown in Figure 1.1. Due to the double curved shape of the membrane, forces can be distributed to the foundations (Heslop, 2010). The membrane has to be prestressed to ensure that the structure will remain tensioned under all load conditions. Architectural membrane structures are usually made out of coated woven fabrics (Gosling et al., 2013).

A disadvantage of woven textiles is that the size of the patches is limited to the size of the machinery that is used to fabricate the textile. Because of this, the length and width of the patches are not infinite. To connect the different patches, the fabrics need to be sewn together which results in large seams. This is not the case for knitted fabrics, where there is no length restriction of the fabric. Furthermore, the properties of knitted fabrics can be locally altered by using different yarns or different knitting patterns.

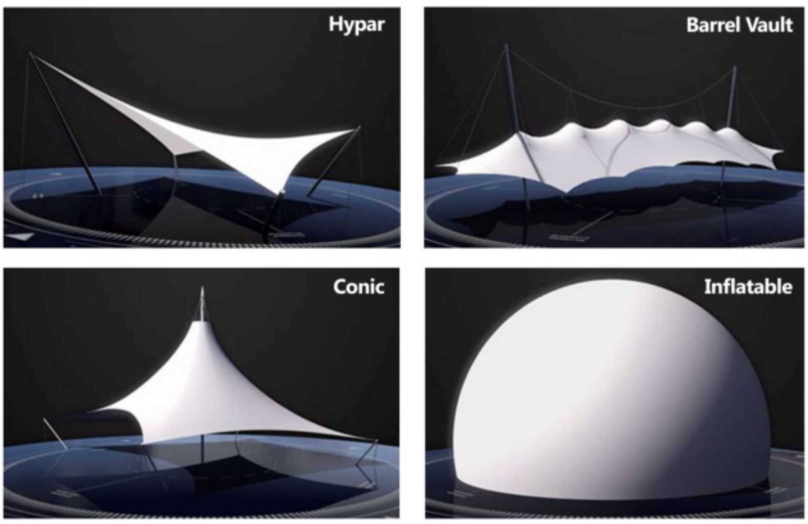

Figure 1.1: Membrane structures (Heslop, 2010)

Membrane structures are suitable for making flexible formworks for concrete structures with complex geometries. This is not limited to more or less flat structures, but also double-curved structures can be fabricated. Figure 1.2 shows the formwork of the roof of the NEST HiLo building. The formwork of this roof structure consists of a steel cable-net in combination with woven membrane (Echenagucia et al., 2019). This figure clearly shows that the woven formwork consists of multiple patches which are sewn together. Figure 1.3 shows a knitted membrane that is used as a lightweight formwork. This structure is made by using strips of fabric which can be assembled to make the final shape (Popescu, 2019).

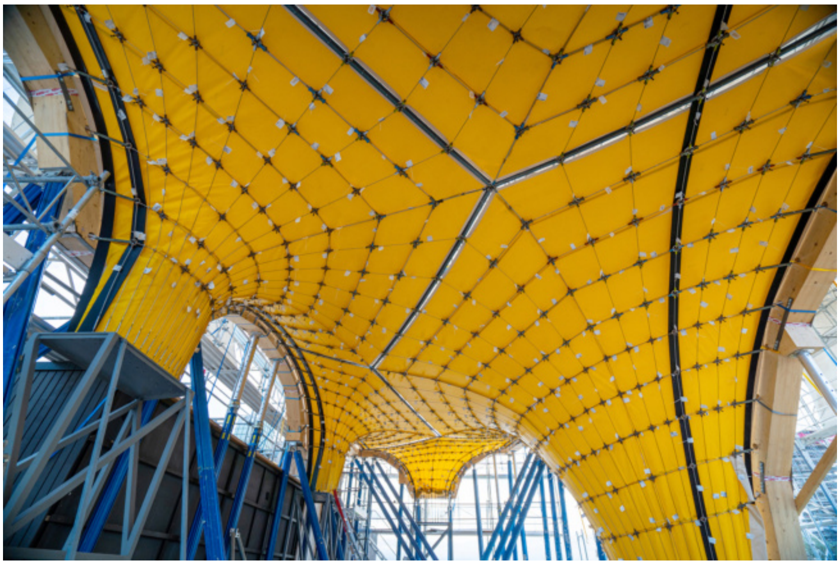

Figure 1.2: NEST HiLo roof structure (photo credit: Juney Lee)

Compared to conventional formwork made with timber panels or EPS moulds, knitted formwork has multiple advantages. The knitted formwork is way lighter than conventional formwork since there is not much falsework needed to keep the fabric in the right position. The weight of conventional formwork is dependent on the dimensions and thickness of the panels, but is generally between 20 and 40 kg per meter squared (OKorder, n.d.). For comparison, according to Popescu et al. (2021) it is possible to make a 50 m^2 knitted formwork which weighs only 55 kg. Besides that, the production process of conventional formwork for double-curved structures is very costly because the moulds have to be custom made. This accounts for approximately 70% of the total costs for the structure (García de Soto et al., 2018).

Figure 1.3a shows the knitted textile when it is tensioned. This shape was achieved by inserting a steel cable net into pockets in the fabric and tensioning the cables. After the fabric is tensioned to the desired shape, the fabric needs to be stiffened to make sure the structure will not deform when applying the concrete. This is done with a cement-paste coating which hardens rapidly (Popescu et al., 2021), see Figure 1.3b. After the stiffening of the shell, multiple layers of concrete could be applied to finish the structure as shown in Figure 1.3c (Popescu et al., 2021).

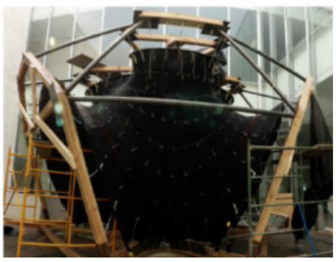

(a) Knitted geometry

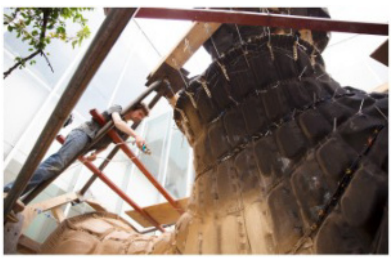

(b) Applying cement-paste coating

(c) Applying concrete

Figure 1.3: KnitCandela (Popescu, 2019)

A form finding process is needed to determine the equilibrium shape of the fabric. This can be done by physical or computational form finding. Form finding is independent of the material properties of the elements that are used (Gosling et al., 2013). Once the process is completed, a structural analysis can be performed. For this analysis it is essential to know the mechanical properties of the membrane material.

1.2. Problem statement

The material and mechanical properties of unconventional building materials are often either unknown or difficult to predict. For knitted fabrics, the latter is the case. Especially, the Young's modulus and Poisson's ratio are important properties to predict correctly because these are used to determine other elastic material properties (Poplavko, 2019). Besides that, these properties are crucial information that is needed to perform a structural analysis on a membrane structure. It is known that the properties strongly depend on the type of yarn and the pattern that is used (Weeger et al., 2018). Previous studies have been performed on the Young's modulus and Poisson's ratio of knitted fabrics, but these studies were limited to homogeneous textiles of only one knitting pattern (Jinyun et al., 2010). A study of the effect of two or more different knitting patterns has not yet been performed. Besides that, previous studies have not clearly documented the method that was used to test the knitted fabrics.

2

State-of-the-art

This chapter provides an overview of the current methods used to obtain the mechanical properties of knitted fabrics. Section 2.1 goes into depth about the fabrication process of knitted fabrics. Subsection 2.1.1 discusses the general fabrication process while subsection 2.1.2 revolves around the production of different knitting patterns. section 2.2 elaborates on the mechanical properties of fabrics, existing testing methods (subsection 2.2.1 and 2.2.2) and the factors that influence the mechanical properties of fabrics (subsection 2.2.3).

2.1. Knitted fabrics

2.1.1. Fabrication process of knitted fabrics

Fabrics in general are made out of yarn. Knitted fabrics are composed of several loops of yarn which are interlocking. This interlocking mechanism can be achieved in two different ways, by weft knitting or warp knitting (Chauhan and Ghosh, 2023). Weft knitting uses only one piece of yarn for all the needles in the knitting machine while warp knitting uses one piece of yarn per needle. Apart from that, in weft knitting the yarn is entered more or less perpendicular to the direction in which the fabric is produced. In warp knitting the yarn is entered in the direction parallel to the production direction (ISO 8388:1998). A visualization of both knitting categories is shown in Figure 2.1. This research will only focus on weft knitted fabrics.

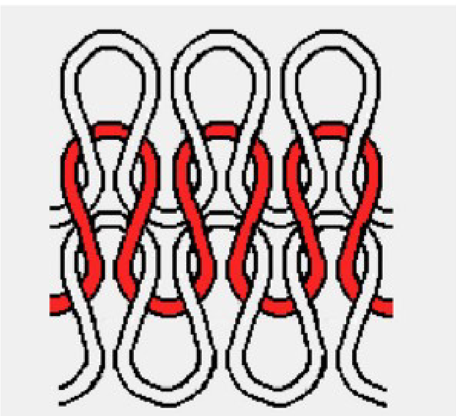

(a) Weft knitting

(b) Warp knitting

Figure 2.1: Weft and warp knitting (Chauhan and Ghosh, 2023)

To understand how knitted fabrics behave, some terminology needs to be known. First of all, a knitted fabric is made out of loops. These loops together make a wale and a course direction of the fabric. This is shown in Figure 2.2. The loops have a certain loop length which can be calculated by dividing the course length of the fabric by the number of loops. Furthermore, a fabric has a wale and a course density which are the amount of wales and courses per centimeter respectively (Chauhan and Ghosh, 2023).

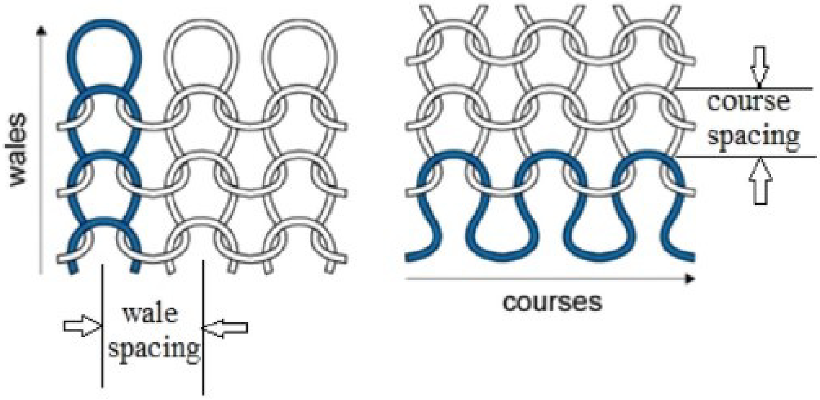

Figure 2.2: Wale and course direction (Chauhan and Ghosh, 2023)

Knitted fabrics can be made with computer numerically controlled (CNC) knitting machines. This type of machinery can produce a variety of different knitting patterns as long as the machine receives the right code to do so. It is also possible to combine different knitting patterns when producing a fabric.

Figure 2.3 shows the components of a flat-bed knitting machine. This type of machine contains two needle beds with needles. The needles are activated when the carriage passes by. This makes the needles catch the yarn which creates loops to make knits. The yarn guides are moved by the carriages and bring the yarn to the right position. The take-down catches the fabric when it reaches a certain length and pulls it down (Popescu, 2019).

During the knitting process, the fabric is made course after course. As a consequence of this, there is no restriction on the length of the fabric. The width however is limited by the width of the machine. When making large pieces of fabric, the fabric needs to be divided into strips or patches which can be made individually. The individual pieces of fabric can be assembled to make the final geometry. When designing a structure with knitted fabric, it should always be kept in mind that there will be seams in the fabric at the places where the different strips/patches are combined (Chauhan and Ghosh, 2023).

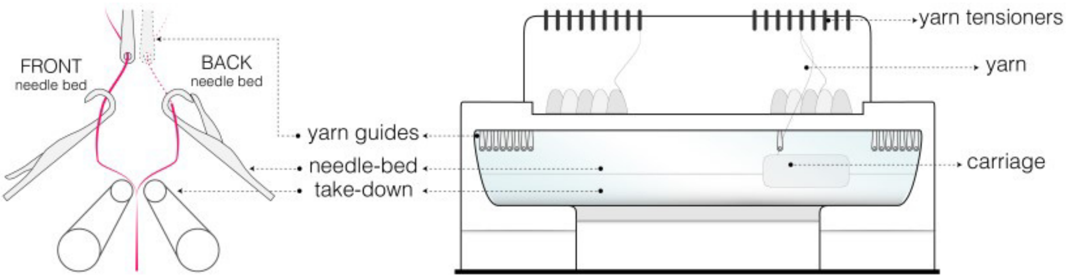

Figure 2.3: Components of a knitting machine (Popescu, 2019)

2.1.2. Stitches and knitting patterns

A piece of knitted fabric is made out of various courses of stitches. The configuration of the stitches determines which pattern will be produced by the knitting machine. Four of the most common stitches are shown in Figure 2.4. These stitches are suitable for making single-layered fabrics. When making double-layered fabrics, both needle beds on the knitting machine are used. An example of a stitch of a double-layered fabric is the interlock stitch shown in Figure 2.5. The names of the stitches are according to ISO 4921:2000.

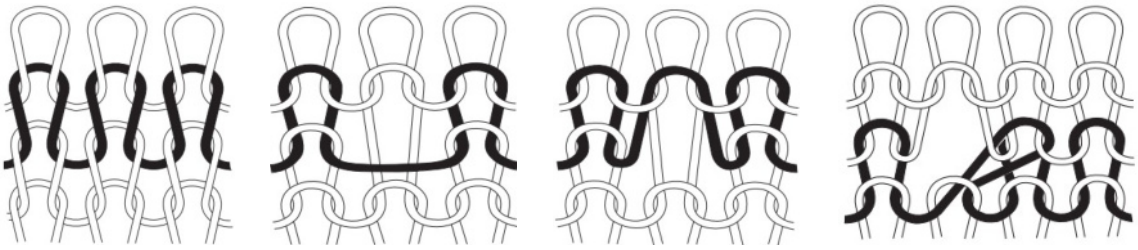

(a) Plain stitch **(b)** Float stitch **(c)** Tuck stitch **(d)** Transfer stitch

Figure 2.4: Overview of stitches for single-layered fabrics (Wilson, 2001)

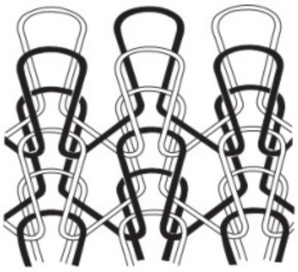

Figure 2.5: Interlock stitch (Wilson, 2001)

2.2. Mechanical properties

An important mechanical property in structural engineering is the Poisson's ratio. This factor describes how much a material will expand or contract perpendicular to the loading direction, see Figure 2.6. The ratio can be calculated using Equation 2.1.

For homogeneous solids out of isometric materials, the Poisson's ratio is limited between -1 and 0.5 (Gercek, 2006). These limits are based on the thermodynamic restrictions of the materials, which suggests that the Young's, shear and bulk moduli should be positive (Gercek, 2006). However, due to their structure, non-homogeneous materials may have a Poisson's ratio that will exceed the limit mentioned before. This is known to be the case for woven fabrics (Brnada et al., 2019).

$$\nu = -\frac{\varepsilon_y}{\varepsilon_x} \tag{2.1}$$

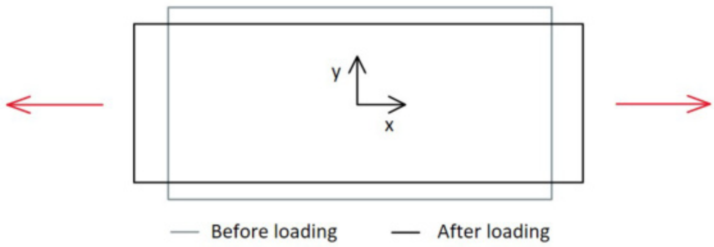

Figure 2.6: Positive Poisson's ratio of a solid

Another important property is the Young's modulus. This property represents the elasticity of a material. A material with a small Young's modulus is very elastic while a material with a large Young's modulus is very stiff. The Young's modulus can be determined by calculating the slope of the stress-strain diagram of a material.

The stress-strain diagram for woven fabrics shows four distinct regions, see Figure 2.7. In the first region, the crimp region, a large increase in strain results in a small increase in stress. In this region, geometric deformation occurs to straighten the yarns. The second region represents the elastic region of the fabric. In this region, the yarns are straightened and can take more load. The third region is the nonlinear failure region. In this region, failure of the individual yarns starts to occur. The last region represents the post-peak region where progressive failure of the yarns starts to occur. This leads to a steep negative slope of the stress-strain curve (Zhu et al., 2011).

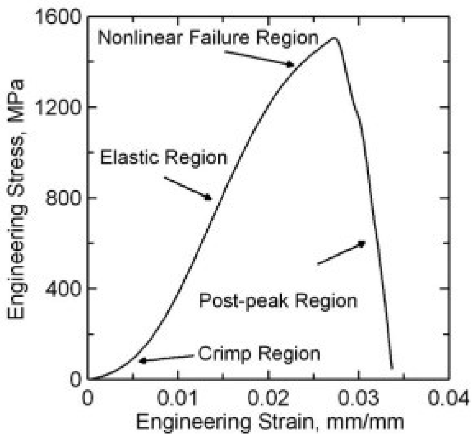

Figure 2.7: Typical stress-strain curve of fabrics (Zhu et al., 2011)

2.2.1. Testing methods

Several testing methods exist to obtain the Poisson's ratio and Young's modulus of fabrics.

Uniaxial tensile test

Figure 2.8 shows the test setup for a uniaxial tensile test. During this test, the sample is clamped at both ends and is then stretched. A camera is placed exactly in front of the sample and from that footage, the length of the sample in both directions can be obtained. From the lengths, the Poisson's ratio can be calculated. The Young's modulus can be calculated using the loads recorded during the test.

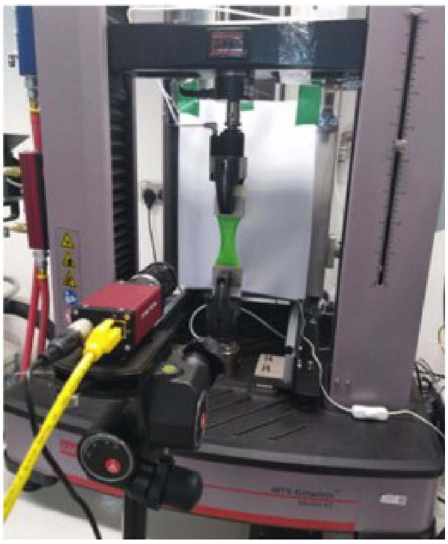

Figure 2.8: Test setup uniaxial tensile test (Weeger et al., 2018)

Wide jaw test

This testing method is a special case of an uniaxial test and is mainly used for woven textiles. Because for woven textiles the strain perpendicular to the loading direction is not easily visible, the test specimen needs to be wide but short in length (Lloyd and Hearle, 1977). The test setup of this type of test is shown in Figure 2.9.

To obtain an accurate result with this testing method, specimens with a small length/width ratio are needed. However, this introduces errors since the flexibility of the clamping device will have a relatively large influence on the results (Lloyd and Hearle, 1977). Therefore, this testing method is not considered accurate.

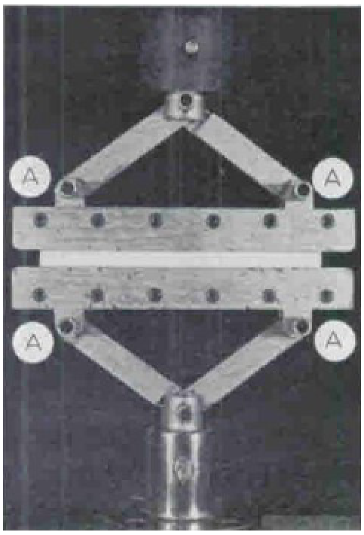

Figure 2.9: Test setup wide jaw test (Lloyd and Hearle, 1977)

Biaxial tensile test
A biaxial tensile test is the most accurate testing method to determine the Poisson's ratio of knitted fabrics (Jinyun et al., 2010). With this testing method, the Young's moduli in both wale and course direction can be measured simultaneously as well as the Poisson's ratio in both directions (Jinyun et al., 2010).

An example of a test setup is shown in Figure 2.10. The specimen is stretched in two perpendicular directions and the strain is measured with sensors that are placed on top of the fabric (Kariouh, 2023). The Poisson's ratio of the fabric can be determined in both wale and course direction from the data obtained from these sensors.

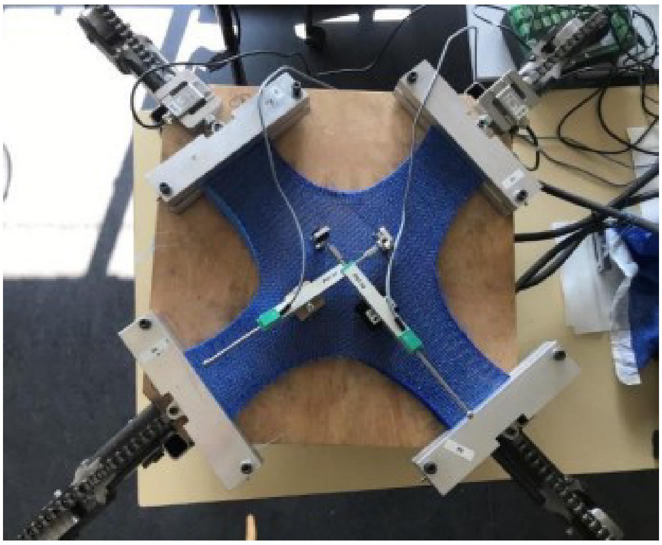

Figure 2.10: Test setup biaxial tensile test (Kariouh, 2023)

2.2.2. Strain measuring methods

There are various options to measure the longitudinal and lateral strain of test specimens. Some are easy to use, while others use more advanced technologies. Besides that, the complexity of the post-processing of the raw data is not the same for all options.

Grid

A rather simple way to measure the strain is by placing a grid below the specimen while a camera is placed exactly perpendicular to the surface of the specimen. An impression of how this will look for a uniaxial test is shown in Figure 2.11.

This method is the most easy to use, but it is prone to errors. When the camera is not placed exactly perpendicular to the specimen, the strain can not be measured correctly. Furthermore, the strain of the specimen needs to be determined visually which is likely to not be very accurate. Besides that, this method is time-consuming since the images/videos of the camera need to be processed by hand. When a large number of experiments will be performed, this method is not efficient to use.

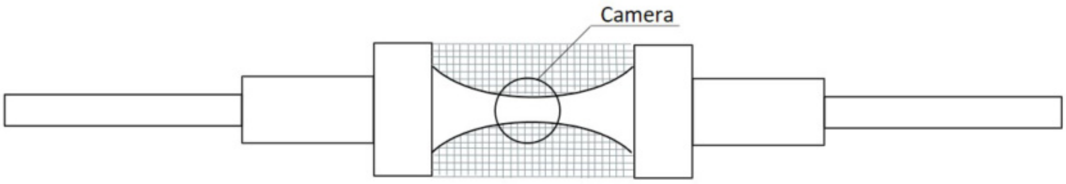

Figure 2.11: Uniaxial test setup with grid

Strain gauges

A commonly used method to measure the strain of a material is by using strain gauges. These sensors are made of a long conductive film which is placed in a zigzag pattern of parallel lines, see Figure 2.12. The resistance of the gauge is measured by making use of the two metal wires shown on the right of Figure 2.12. When the material to which the sensor is attached deforms, the resistance of the strain gauge will change. From the resistance data, the strain of the test specimen can be obtained (Zhang, 2010).

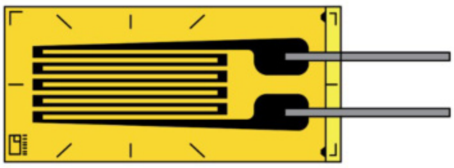

Figure 2.12: Strain gauge (IQSdirectory, n.d.)

Digital Image Correlation (DIC)

Another possibility of measuring the strain in the centre of the specimen is by using DIC (Jadhav et al., 2023). Figure 2.13a shows the test setup of this kind of experiment. The camera is placed vertically above the test sample. The camera captures multiple images of the specimen and with special software they can be compared to get the result shown in Figure 2.13b (Jadhav et al., 2023).

Usually, a high-resolution camera is used when DIC is applied, but it is also possible to make use of a phone camera. However, by using a phone several errors need to be corrected to obtain the correct result (Yu and Pan, 2014).

To obtain a single value for the Poisson's ratio of a specimen, the values of all points need to be averaged (Cerbu et al., 2018). Before doing that, outliers must be removed to prevent them from influencing the results.

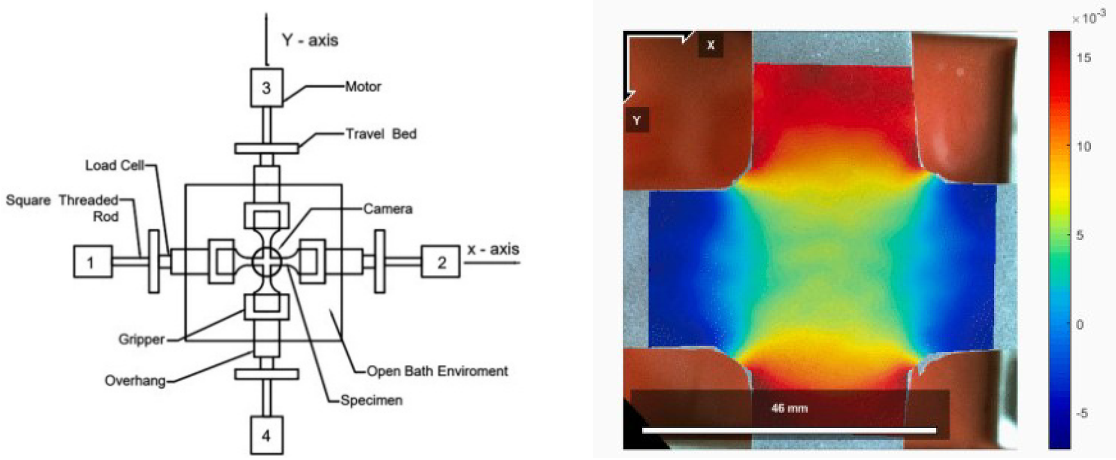

(a) Schematic test setup

(b) Result

Figure 2.13: Experiment using DIC (Jadhav et al., 2023)

2.2.3. Influencing factors

The mechanical properties of a material can be influenced by several aspects. Some of them are relevant for all types of materials while others are specifically relevant for knitted fabrics. Below a short overview of the parameters is given.

General	**Fabrics**
Temperature	Yarn type
Moisture content	Knitting pattern
Direction of testing	Loop length
	Orientation of the sample

Temperature

For some materials, temperature influences the mechanical properties. In essence, the Poisson's ratio will increase if the temperature of the material becomes higher (Carneiro and Puga, 2018). This thesis will not focus on this effect. To control this variable, all tests will be performed at room temperature.

Moisture content

Furthermore, the moisture content could influence the properties of fabrics. For timber, it is known that the moisture content has a large impact (Mizutani and Ando, 2015). For fabrics this is also the case. After laundering of fabrics, they tend to shrink and become more stiff which means the Young's modulus has become larger. This also impacts the Poisson's ratio; this property of the fabric increased after laundering (Fletcher and Roberts, 1954). This is beyond the scope of this thesis.

Direction of testing

Another variable is the dependency of material properties on the direction of testing. The properties are usually different for a specimen tested in tension compared to one tested in compression (Poplavko, 2019). For fabrics this is not relevant since they cannot resist any compressive forces.

Yarn type

The type of yarn that is used has a large influence on the performance of the fabric as a whole. The radius of the yarn impacts the contact surface between the individual yarns which influences the behaviour of the fabric (Weeger et al., 2018). Besides that, the Young's modulus of the yarn in combination with the knitting pattern will determine the stiffness of the fabric. In general, the fabric will behave more elastically when a more elastic type of yarn is used (Weeger et al., 2018). This thesis only focuses on a single yarn type that remains constant throughout all experiments.

Knitting pattern
The material properties of knitted fabric also strongly depend on the knitting pattern that is used. In the clothing industry, the knitting pattern determines the comfort and durability of a garment (Tiwari et al., 2013). Besides that, it influences the density and elasticity of a piece of fabric. Both factors also have an impact on the Poisson's ratio of the fabric.

Loop length
The loop length in itself does not say much about how a piece of fabric behaves, but it does affect the wale and course density. These properties influence the behaviour of the fabric and thus the mechanical properties. This is the case for warp knitted fabrics (Dabiryan and Jeddi, 2012) as well as for weft knitted fabrics (Weeger et al., 2018). For auxetic knitted fabrics, the effect of the negative Poisson's ratio increases when the loop length becomes larger (Osman and Mohamed, 2020).

Orientation of the sample
Because of the fabrication process, a piece of knitted fabric has a wale and course direction. This results in an orthotropic behaviour of the material and therefore the Poisson's ratio in both directions of the fabric is likely to not be the same (Chauhan and Ghosh, 2023). During this research, the fabrics will be tested in both directions.

2.3. Summary

This chapter provided an overview of the current state-of-the-art regarding the use of knitted fabrics and their mechanical properties. Starting with the fabrication process of knitted textiles where different knitting operations can be combined to create 3D geometries, distinct knitting patterns and functional features.

A standardised testing method to determine the Poisson's ratio and Young's modulus of knitted fabrics does not exist so multiple methods have been mentioned. Testing possibilities include a uniaxial tensile test, a wide jaw test and a biaxial tensile test. When using these testing methods, the Young's modulus of the fabrics can be directly determined. To calculate the Poisson's ratio, the strain parallel and perpendicular to the loading direction has to be measured. This can be done using a grid, strain gauges or digital image correlation.

3

Research framework

3.1. Research objectives

Currently there is little data available on the mechanical properties of knitted fabrics, including the Poisson's ratio and Young's modulus. It is known that the knitting pattern is one of the main factors that influences these properties. This thesis explores the possibility of gaining more insight into how the knitting pattern influences the behaviour of knitted fabrics.

The main objective of this research is to:

Determine the effect of different knitting patterns on the Poisson's ratio and Young's modulus of weft-knitted fabrics.

To complete this objective, three subquestions have been formulated.

1. *What methods can be used to determine the Poisson's ratio and Young's modulus of weft-knitted fabrics?*
   This subquestion focuses on the method that will be used to determine the properties of the knitted fabrics. Since a standardised testing method does not yet exist, multiple options are explored (see section 2.2).

2. *What are the Poisson's ratios and Young's moduli for weft-knitted fabrics with a uniform pattern?*
   This question addresses the properties of fabrics with a uniform pattern. During this research six different knitting patterns are considered. These are: interlock, eightlock, hexagon, tuck, interlock-1float and interlock-2float. Chapter 5 goes more into depth about how these knitting patterns are defined.

3. *What is the effect of combining knitting patterns on the Poisson's ratios and Young's moduli of weft-knitted fabrics?*
   The last question addresses the effect on the material properties of the fabrics when multiple knitting patterns are combined in one fabric. This research mostly focuses on combining the interlock and eightlock pattern, but shortly mentions a combination of interlock with tuck as well.

As mentioned before, this research is limited to using six distinct knitting patterns. Besides that, the material that the fabrics are made of strongly influences the properties. During this research, all fabrics are made out of Diolen polyester yarns.

3.2. Thesis outline

This thesis is structured into four parts. Part I served as an introduction to the topic of this research. Chapter 1 provided an overview of the context of this research and the problem statement. Afterwards, chapter 2 gave insight into the current state-of-the-art. Part I concludes with the current chapter, chapter 3, about the research framework.

Part II delves into the methods that are used during this research. Chapter 4 presents an overview of the methodology. In chapter 5 the knitting patterns that are used in this thesis are defined. Chapter 6 describes the fabric preparation that has to take place before the fabrics can be tested. Chapter 7 elaborates on the test setup and procedure that are used for testing the fabrics.

In Part III the results of the material tests are presented. This contains both the results of the homogeneous fabrics (section 8.1) and the non-homogeneous fabrics in which the knitting patterns are combined (section 8.2).

Part IV presents a reflection on the contributions made by this research. This includes chapter 9 which critically discusses the limitations of this research. Chapter 10 presents the conclusions that can be drawn from this research. This chapter also provides recommendations for future work.

Part II

Approach

4
Methodology

4.1. Overview

To achieve the main objective of this research, knitted fabrics with different knitting patterns are tested in a uniaxial tensile test. This is done for both homogeneous and non-homogeneous fabrics containing only one or two different knitting patterns respectively. Before the testing procedure can start, the fabrics and setup have to be prepared. This is further explained in section 4.2. After the tests have been performed, the results can be processed. This is elaborated on in section 4.4. An overview of the research methodology is given in Figure 4.1.

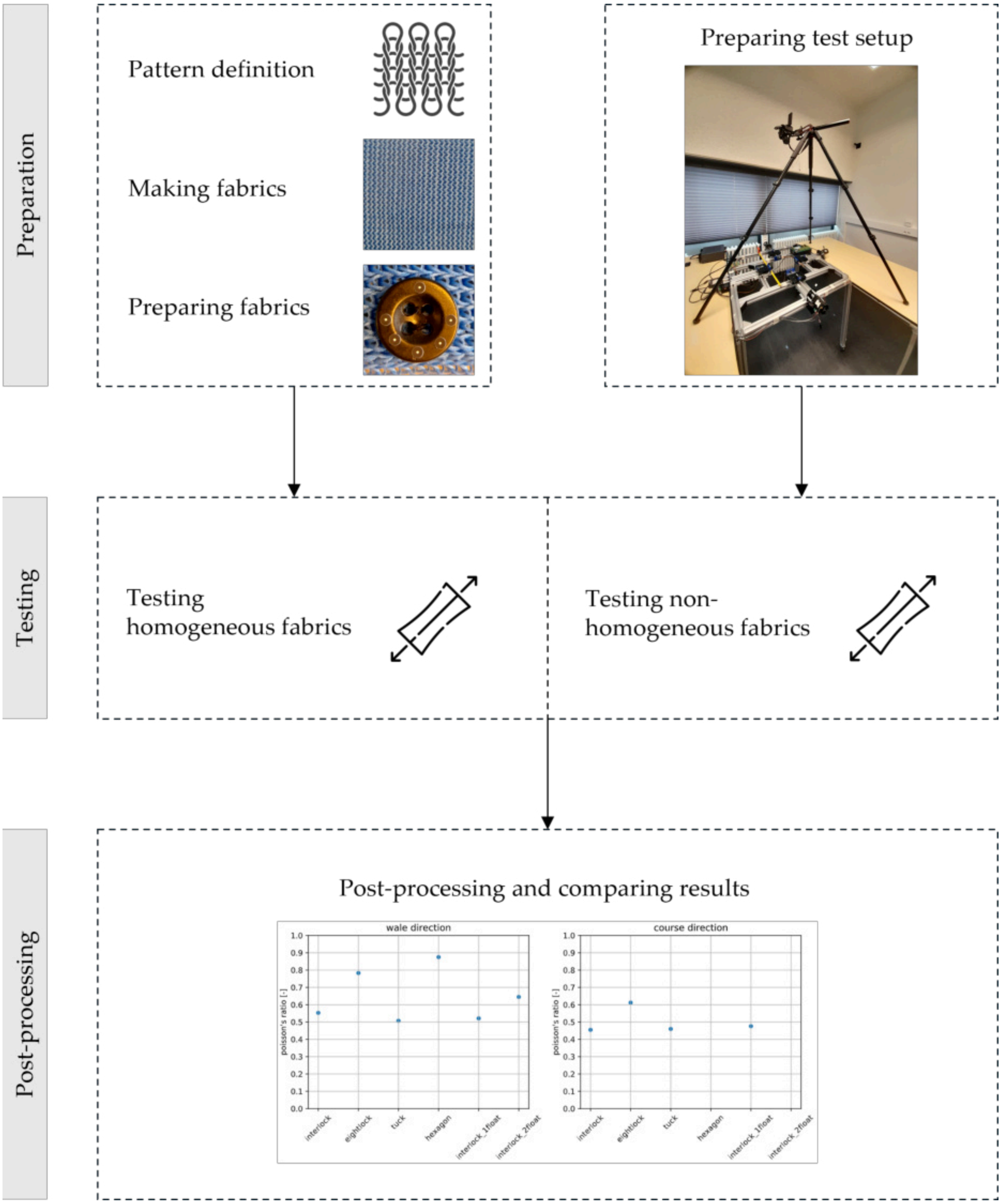

Figure 4.1: Methodology

4.2. Preparation

The preparation phase consists of two parts: the preparation related to the fabrics and the preparation related to the setup used for the tensile tests.

Since the fabrics are made by a CNC knitting machine, a fabrication file has to be generated to control the machine. This is done by using knitting software in which every knitting operation is represented by a pixel. A coloured bitmap image of a certain amount of pixels is used to define which pixel represents which knitting operation.

Channels have to be included in the fabrics to be able to insert rods which can be clamped in the setup. The channels do not affect the test results since they are placed inside the clamps. Furthermore, the size of the fabrics has to be calibrated to fit in the tensile test setup. This is further explained in section 6.1. To be able to determine the Poisson's ratio of the fabrics, the displacement of four points on the fabric needs to be known. This is realised by attaching four buttons to the fabric, see section 6.3.

A standardised testing procedure to obtain the Poisson's ratio and Young's modulus of knitted textiles does not yet exist. Therefore a lot of preparation is needed to design a working test setup and procedure. The fabrics are tested uniaxially. Hence, a setup with two moving axes is used.

To measure the Poisson's ratio, the displacement of the fabrics in both lateral and longitudinal direction needs to be measured throughout the test. This is achieved by positioning a camera precisely levelled above the centre of the fabric. The camera captures a picture at multiple timesteps during the tensile test.

4.3. Testing

After the homogeneous fabrics are made and the test setup is ready to use, the testing can take place. First, the homogeneous fabrics are tested. The results of these tests are analysed and when necessary, the test setup or procedure is revised. Three tests are performed on each knitting pattern to obtain a distribution of the properties of the fabrics. This is done in both wale and course direction.

After the results of the homogeneous fabrics are processed, it is decided which knitting patterns will be combined into non-homogeneous fabrics. This choice is based on the behaviour of the different knitting patterns.

4.4. Post-processing

After the fabrics are tested, the results can be post-processed. This applies to the measurements of the load cells as well as the pictures taken with the camera. A summary of the post-processing is given below and a more elaborate explanation can be found in chapter 8.

The measured values of the load cells are processed with a Python script. The values are plotted against the displacement of the clamps, which results in a force-displacement diagram. This diagram is converted into a stress-strain diagram from which the Young's modulus of the fabrics can be determined.

The digital image correlation (DIC) software "Zeiss Inspect Correlate" is used to process the images captured by the camera. This software can recognise points in a series of images. This functionality is used to track the displacement of points on the fabric during testing. The data extracted from the DIC software is processed with a Python script. The script plots the Poisson's ratio of the fabric throughout the test. This shows the relationship between the amount of strain and the Poisson's ratio. Furthermore, the script makes a figure of the distribution of the measured values for the Poisson's ratio of the knitted fabrics with the same knitting pattern.

When the results of all tests are post-processed, the results can be compared. A comparison is made between the properties of the homogeneous fabrics, and also between the homogeneous and non-homogeneous fabrics. Especially the comparison of the results of the non-homogeneous fabrics is interesting because no research has yet been performed on this topic. An attempt is made to establish a relationship between the results of the homogeneous and non-homogeneous fabrics.

5

Pattern definition

This research only focuses on double-layered fabrics. The patterns are based on the conventional interlock pattern mentioned in ISO 8388:1998 but make use of different arrangements of the float, tuck and transfer stitches mentioned in subsection 2.1.2.

Firstly, patterns are defined to make homogeneous fabrics (section 5.1). Afterwards, the patterns are combined to make non-homogeneous fabrics (section 5.2). To combine the patterns, a primary and secondary pattern are defined.

5.1. Homogeneous fabrics

Interlock

The interlock pattern consists of two repeating knitting operations, see Figure 5.1. Firstly, the first yarn guide guides a string of yarn to the needles on the front needle bed and the second yarn guides another string of yarn to the needles on the back needle bed. Afterwards, the operations are the other way around, the first string of yarn makes a loop on the back needle bed and the second string of yarn makes a loop at the front needle bed. After these two pairs of operations, this process repeats itself. This knitting pattern is included in ISO 8388:1998. A close-up of a fabric containing this knitting pattern is presented in Figure 5.2.

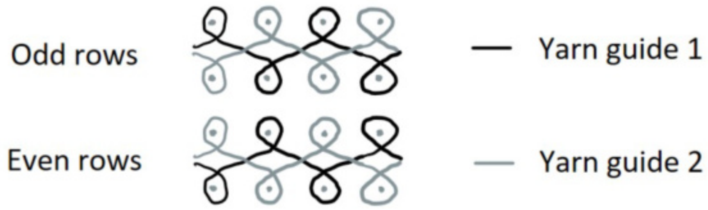

Figure 5.1: Knitting operations interlock

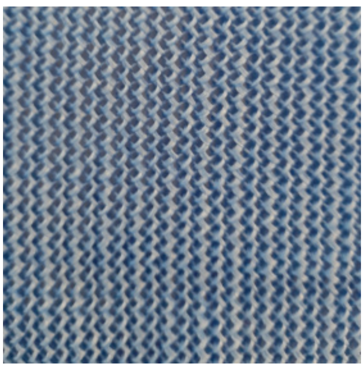

Figure 5.2: Interlock fabric

Interlock-1float

A variation of the interlock pattern is the interlock-1float pattern. The scheme of the knitting operations used to fabricate this pattern is shown in Figure 5.3. After every plain stitch, a float is placed on both needle beds. A close-up of a fabric containing this knitting pattern is presented in Figure 5.4. This knitting pattern looks similar to the interlock pattern, but the loops are slightly looser.

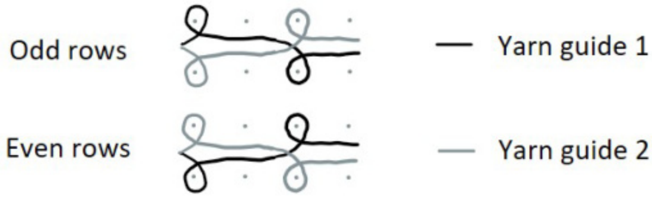

Figure 5.3: Knitting operations interlock-1float

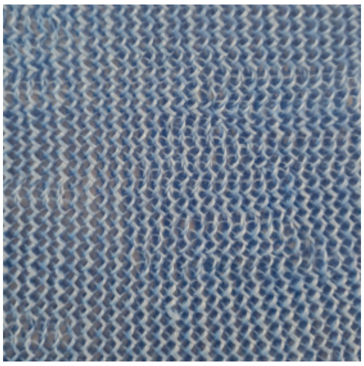

Figure 5.4: Interlock_1float fabric

Interlock-2float

Similar to the interlock-float pattern, the interlock-2float pattern is a variation of the interlock pattern. Instead of one float stitch in between the interlock stitches, this pattern has a double float, see Figure 5.5. A close-up of a fabric containing this knitting pattern is presented in Figure 5.6. For this knitting pattern, the loops are a bit looser than for the interlock_1float fabric. Furthermore, it looks similar to the interlock fabric.

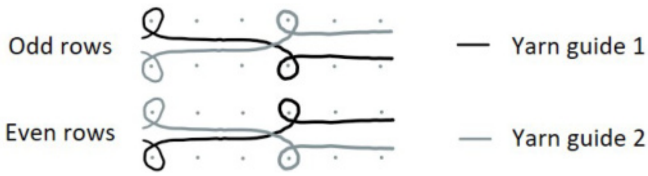

Figure 5.5: Knitting operations interlock-2float

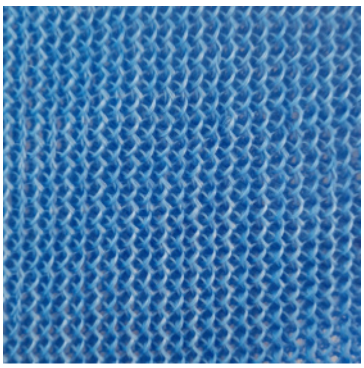

Figure 5.6: Interlock_2float fabric

Eightlock

Similar to the interlock pattern, eightlock is also an existing pattern according to ISO 8388:1998. The knitting operations used to make this pattern are similar to the ones used for the interlock pattern, but it consists of four knitting operations that are repeated, see Figure 5.7. Because of the knitting architecture of this pattern, the fabric is slightly ribbed. A close-up of a fabric containing this knitting pattern is presented in Figure 5.8.

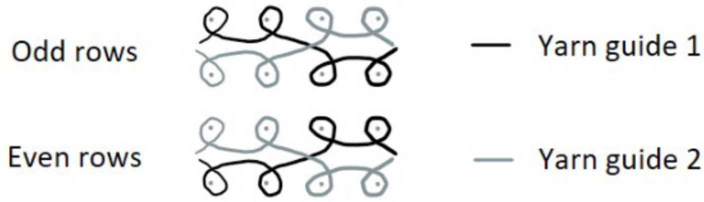

Figure 5.7: Knitting operations eightlock

Figure 5.8: Eightlock fabric

Tuck

The tuck pattern used during this research contains an interlock stitch followed by a tuck stitch on one needle bed and an interlock stitch on the other. Since the tuck stitch is always made on the same needle bed, this creates a fabric that includes a one-sided tuck. Figure 5.9 shows a visualisation of the knitting operations. A close-up of a fabric containing this knitting pattern is presented in Figure 5.10. These images clearly show that the fabric has a different appearance on the front and back.

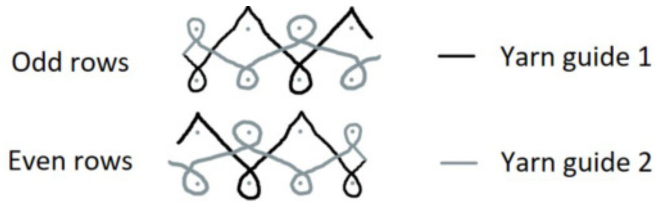

Figure 5.9: Knitting operations tuck

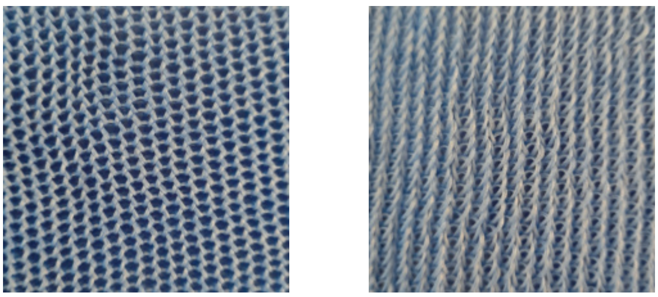

(a) Front **(b)** Back

Figure 5.10: Tuck fabric

Hexagonal
The hexagonal pattern does not only contain plain knitting stitches but also transfer stitches which are made by shifting the needle bed into a different position. This is explained by the different images in Figure 5.11. Every row in the knitting software contains the four operations shown in Figure 5.11. An explanation of the four operations is given below. A close-up of a fabric containing this knitting pattern is shown in Figure 5.12.

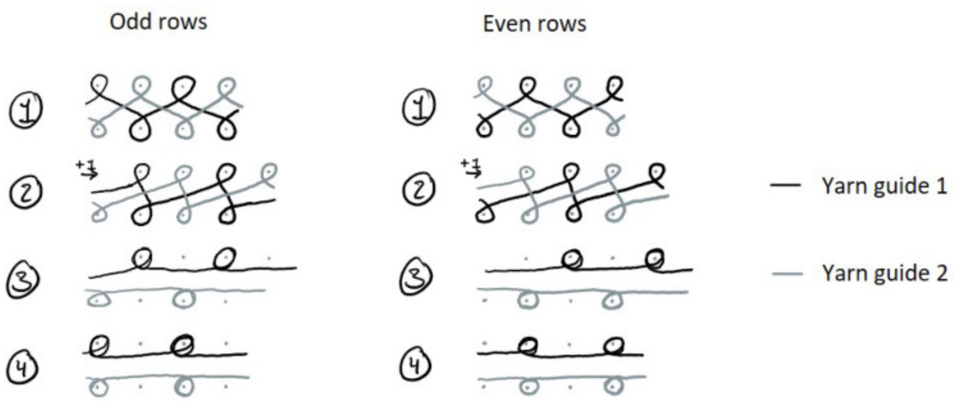

Figure 5.11: Knitting operations hexagon

Step 1	:	Knit interlocking stitches
Step 2	:	Shift needle bed on the back to the right
Step 3	:	Transfer loops of yarn guide 1 to the needle bed on the back and the loops of yarn guide 2 to the needle bed on the front to create double loops
Step 4	:	Shift needle bed on the back to its original position

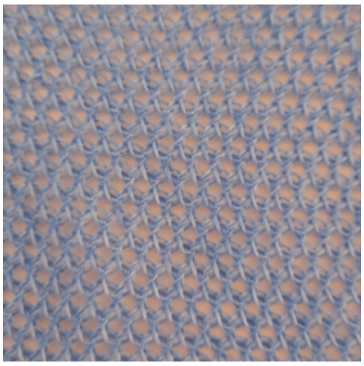

Figure 5.12: Hexagon fabric

5.2. Non-homogeneous fabrics

As stated before, the knitting patterns are combined to make non-homogeneous fabrics. This is done with a mask similar to the one shown in Figure 5.13. This figure shows a mask for a fabric made with a squared bitmap file. The image size of the mask corresponds with the size of the bitmap file that is used for the fabric. The black (outer) part of the bitmap, which is marked in black in the mask, corresponds to the primary pattern while the white (inner) part corresponds to the secondary pattern. In this research, the interlock pattern is chosen as the primary pattern. The secondary pattern is either tuck or eightlock. In section 8.2 the choice of these patterns is explained.

A circle is chosen as a shape for the secondary pattern since this shape does not result in singularities. Due to singularities, peak stresses can develop at sharp corners. This, for example, would be the case if the secondary pattern was applied as a square. Peak stresses could cause a different mechanical behaviour of the fabric and that should be prevented.

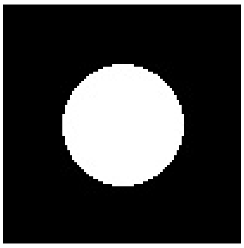

Figure 5.13: Circular mask

6

Fabric preparation

Before the fabric could be tested some preparation had to be done. First, the size of the fabric had to be determined. This is elaborated on in section 6.1. Section 6.2 delves into the preparation that was needed before the fabrics could be tested in course direction. Section 6.3 explains the necessary preparation for the use of digital image correlation.

6.1. Size calibration

The different knitting operations mentioned in subsection 2.1.2 affect the size of the fabric. As stated before, the knitting software uses a bitmap file containing pixels of different colours for each knitting operation. When bitmap files of 100x100 pixels are used for distinct patterns, the size of the fabric can be completely different, see Figure 6.1.

Not only does the knitting pattern influence the fabrics' size, but the channels do so as well. When the channels are placed on the top and bottom of the fabric, the size is different compared to when the channels are placed on the sides, see Figure 6.2.

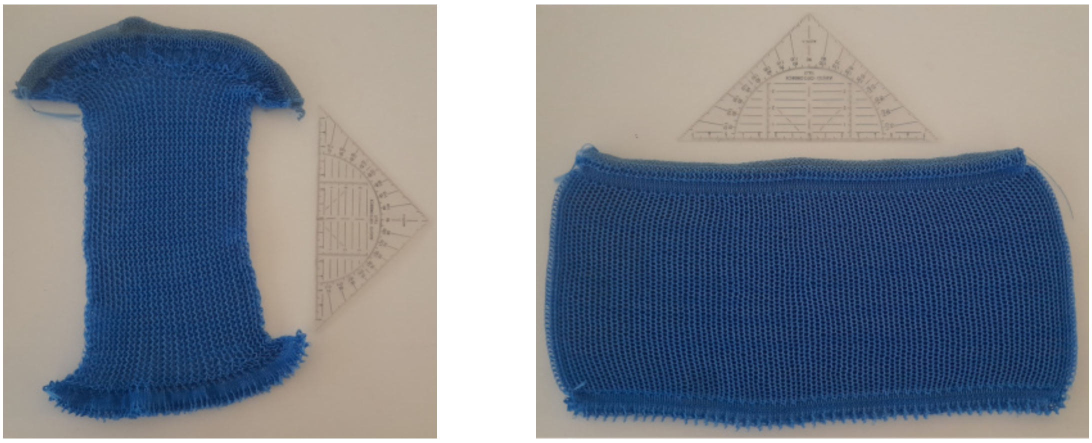

(a) Interlock_2float **(b)** Tuck

Figure 6.1: Fabrics made of 100x100 pixel bitmap files with channels on the top and bottom

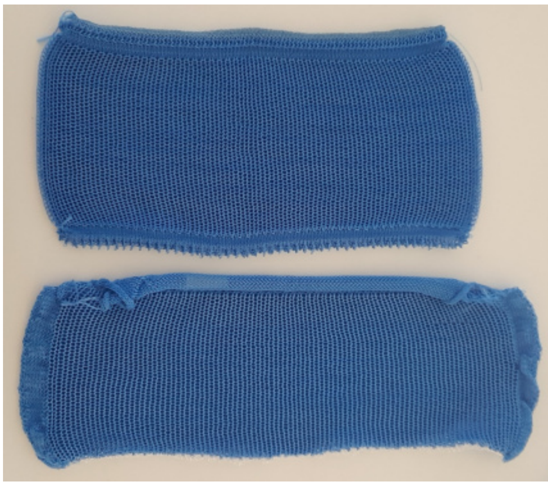

Figure 6.2: Size comparison 100x100 pixel tuck fabrics (top: channels on top and bottom, bottom: channels on sides)

To determine the needed size of each pattern, firstly fabrics are made of 100x100 pixels. The length and width of these fabrics are compared to the length of the test setup and the width of the clamps respectively.

6.2. Testing in course direction

Because the behaviour of knitted textiles is orthotropic, the fabrics were tested in both wale and course direction. When the fabrics were tested in the wale direction, the channels were placed on the top and bottom of the fabric. When the fabrics were tested in course direction, the channels were placed on the sides of the fabric. This is shown in Figure 6.3.

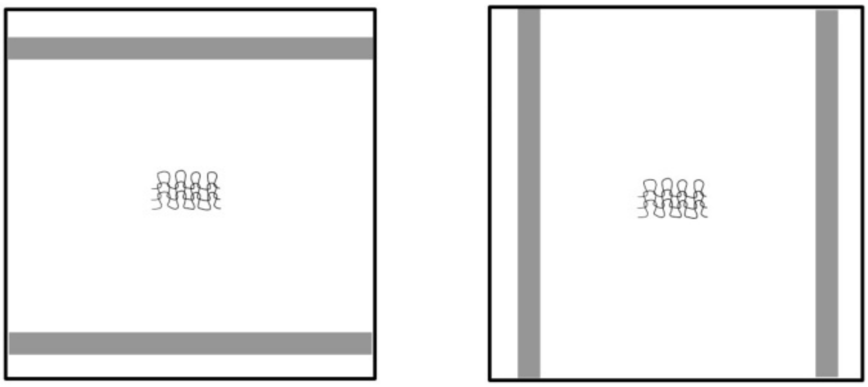

(a) Wale direction **(b)** Course direction

Figure 6.3: Location of channels

When the fabrics are made, a start and a closing are needed to prevent the unravelling of the fabrics. For the fabrics tested in wale direction, the start and closing were positioned outside of the channels and thus outside of the area that was tested. For the tests in course direction, the start and closing were positioned along the edge of the area that was tested. This means that the behaviour of the start and closing would influence the behaviour of the fabric itself if the properties are too different. During this research, multiple options for starting and closing the fabrics have been considered, see Figure 6.4.

Figure 6.4a shows a fabric with a start and a single-layered finishing. This type of finishing is relatively easy and fast to fabricate. The finishing doesn't close the fabric directly at the end of the double-layered part, but it creates an additional single-layered part which can unravel before the unravelling influences the double-layered part. A disadvantage of this type of closing is that the single-layered part influences the behaviour and size of the double-layered part of the fabric. Besides that, the start and finishing did not have the same stiffness, which caused the clamps to rotate. This causes inconsistencies in the results.

Figure 6.4b shows a fabric with both a start and a closing. When this fabric was tested, the start and closing seemed to be stiffer than the fabric itself. This means that the loadcells recorded forces that were more representative of the start and the closing than of the fabric itself. Besides that, the stiffness of the start and closing was not the same, which caused the clamps to rotate.

As a way to avoid the influence of the overly stiff start and closing on the test results, the start and closing were placed further away from the edge of the fabric. This resulted in a diamond-shaped fabric as shown in Figure 6.4c. Since the start was stiffer than the closing, the start was placed at a larger distance from the centre of the fabric. Because of the additional material, the core of the fabric could not deform freely. This caused the fabric to wrinkle when a certain amount of strain is applied which would lead to unrealistic and unrepresentative results.

The final option that was considered for the start and closing of the fabrics is shown in Figure 6.4d. In this case, it was decided to fully remove the start of the fabric. This was possible for most patterns that are used within the scope of this research except for the eightlock pattern. For that pattern, the first row was replaced with a row of the interlock pattern. This prevented the unravelling of the fabric. Since the closing was in this case also stiffer than the fabric itself, the clamps did start to rotate.

During this research, it was chosen to use the option shown in Figure 6.4d. As stated before, the clamps are going to rotate. Since it was not known beforehand when this was going to happen, the tests were performed as usual and stopped after the clamps had started to rotate. Due to this effect, the strain that can be applied to the fabrics made of different knitting patterns was not the same.

(a) Start and single layer end

(b) Start and closing

(c) Diamond shaped fabric

(d) Only closing, no start

Figure 6.4: Closing considerations (for every image the start is located at the bottom and the closing at the top)

6.3. DIC preparation

To calculate the Poisson's ratio of the fabrics, the displacement of four points needs to be known. If the material is expected to behave symmetrically, the maximum lateral contraction is expected to be in the centre of the fabric. Because the clamping of the fabric at the edges resulted in a bilinear stress state, the longitudinal strain of the fabric was measured close to the centre of the fabric. In this area, the fabric was loaded purely uniaxial.

To be able to track the displacements of the four points of the fabric, buttons were attached. This was done at the locations shown in Figure 6.5a. On each button, six small stickers were placed (Figure 6.5b). These points could be recognised and followed by the DIC software. The orientation of the stickers on the buttons needed to be different for each button, so the software could distinguish between them.

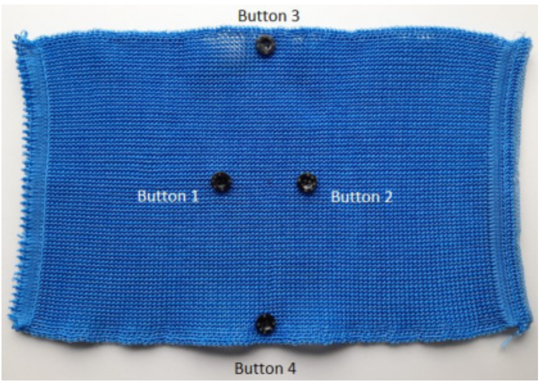

(a) Buttons on fabric

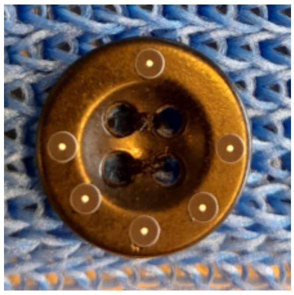

(b) Button with stickers

Figure 6.5: Prepared fabrics

7

Test setup and procedure

A biaxial test setup was used to perform tensile tests on the fabrics. Since the fabrics were tested uniaxially, only two of the four axes were used. These were two axes which are opposite of each other. In section 7.1 an overview of the most important features of the test setup is given. Afterwards, section 7.2 describes the test procedure.

7.1. Test setup

Figure 7.1 shows an overview of the test setup. The use of every highlighted element is elaborated on in the paragraphs. The list is divided into two categories; elements needed for controlling the movements and elements needed for the post-processing of the results.

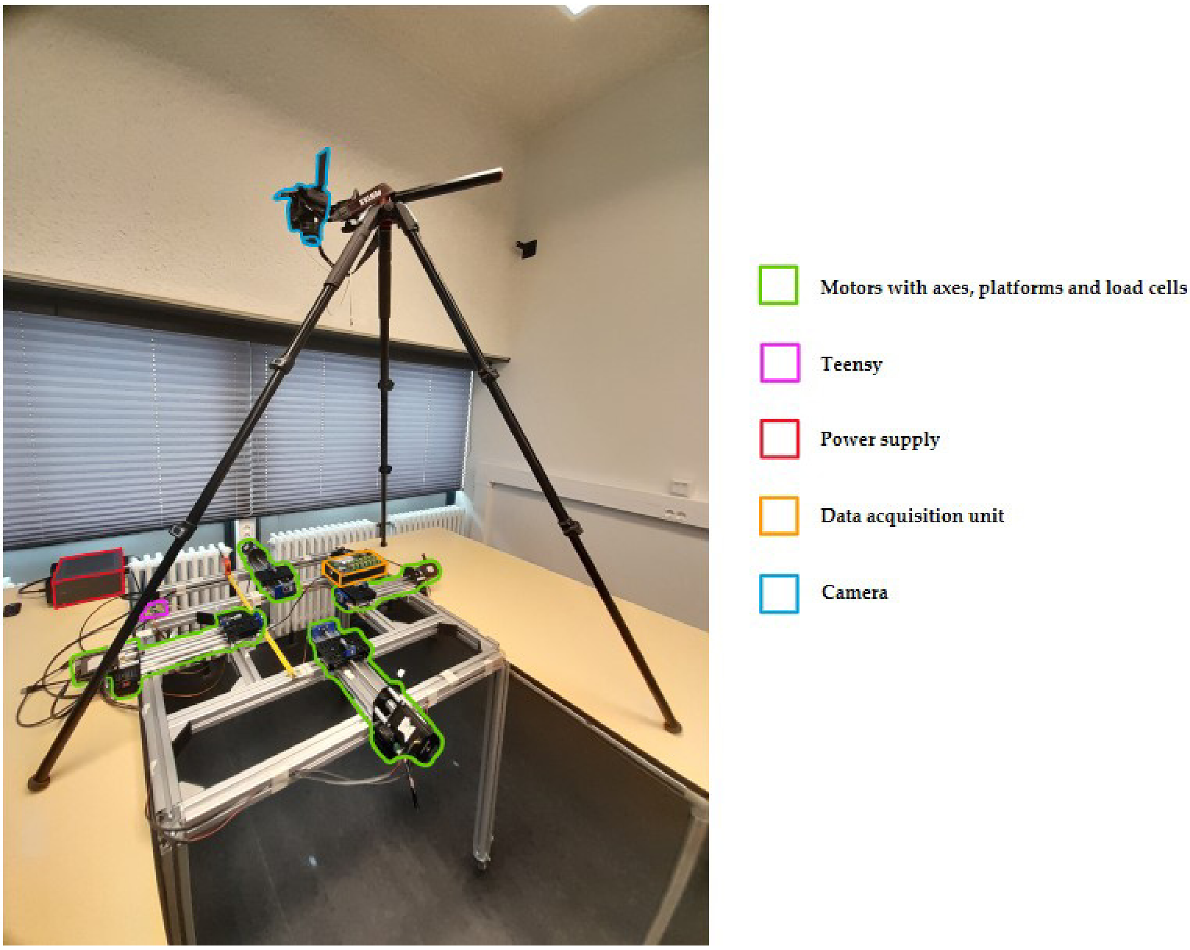

Figure 7.1: Overview of test setup

7.1.1. Controlling the movements

Frame with motors

The biggest part of the test setup consists of the aluminium frame with four motors (see Figure 7.1). The motors control the rotation of the axes on which a platform is located (see Figure 7.2). When an axis rotates, the platform that is attached to it moves back or forth.

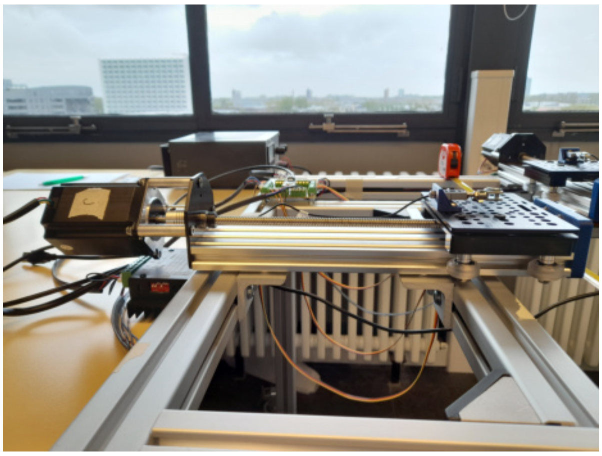

Figure 7.2: Axis with motor

Teensy

The motors are controlled via a Teensy (see Figure 7.3) which is controlled with an Arduino code. With this code, it is possible to move each axis individually as well as simultaneously. Another feature of the code is that it is possible to choose to do a uniaxial test (controlling only two opposite motors) or a biaxial test (controlling all four motors). The full Arduino code can be found in Appendix A.

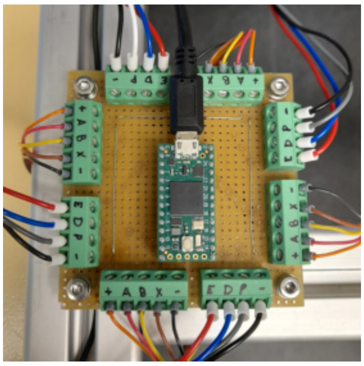

Figure 7.3: Teensy

Clamps

The fabrics were attached to the setup by clamps. The clamps make sure the fabric does not slip during the tensile test. To distribute the forces evenly to the fabric, rods are inserted in the channels of the fabrics. The clamps fit perfectly around the rods due to the intrusions that are visible in Figure 7.4a.

Figure 7.4b shows the top view of one of the clamps. A black tape is placed over the full length of the top of the clamp to ensure no shadows are visible on the pictures taken during testing. Shadows will be recognised as points in the software used to process the images, which could influence the results of the displacements.

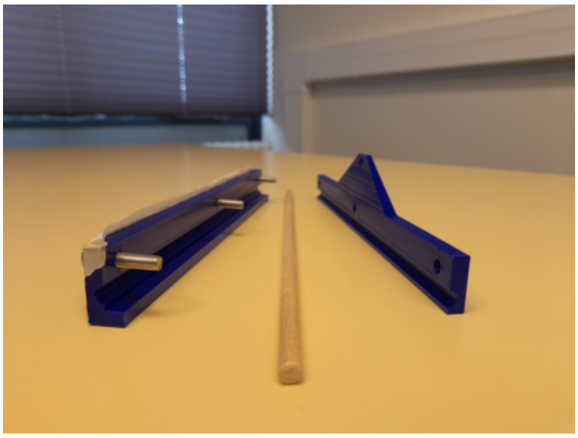

(a) Parts of a clamp

(b) Top view

Figure 7.4: Clamp

Power supply
The power supply unit provides power for the motors. When something does not go to plan while testing, the power can be switched off to prevent accidents from happening.

7.1.2. Post-processing

Load cells
A load cell is placed on each of the four moving platforms. When a load is applied, these sensors record a certain value which can be converted to a load in Newton. The clamps are attached to the load cells with fork supports, see Figure 7.5. This connection type allows the clamp to rotate, which is useful if asymmetrical deformation of the tested fabric is expected.

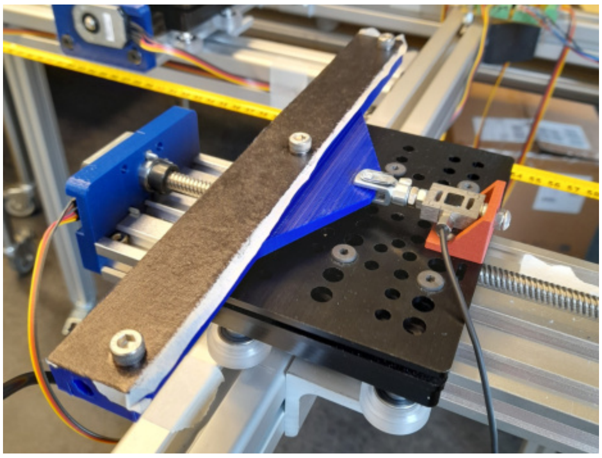

Figure 7.5: Platform with load cell and clamp

Data acquisition unit
The data acquisition unit is used to retrieve the data from the load cells. The measured values were retrieved with a Python script.

Camera
A camera is placed exactly levelled above the centre of the setup, and thus above the centre of the fabrics. The camera captures the fabric during the whole range of displacements. The images from the camera can be imported into the Zeiss Correlate software to track the displacements of the buttons. To control the camera, a remote is used. This prevents any movements of the camera while testing.

7.2. Test procedure

The tests were performed using the Python code shown in Appendix B. Before the test could take place, the Teensy and the data acquisition unit must be connected to a computer that could run the Python code.

First, the Python code zeroed the load cells. This was done to ensure the load recorded at the start of the test was not influenced by the result of the previous test. Besides that, this could show the difference in tension working on the fabrics at the start of the test. After zeroing the load cells, the clamps with the fabric could be placed.

When the fabric was in place, the camera had to be focused on the fabric and not on a surrounding part of the setup. This had to be done to ensure that the pictures captured by the camera were of good enough quality to let the Zeiss Correlate software recognise the stickers on the buttons. Focusing the camera had to be done with the "autofocus" setting because this is more accurate than manually focusing the camera. After the focus of the camera was correct, the settings had to be changed to "manual focus" to ensure that the focus does not shift during the test.

When the test started, a picture had to be taken with the camera. This represented the fabric at the zero strain stage. After this, the platforms could be moved step by step. After every movement, a new picture had to be captured by the camera. The Python code was programmed to move each platform in steps of 5 mm. Since the uniaxial test used two moving platforms, the total strain applied to the fabrics at each step was 10 mm. This procedure was repeated until the platforms reached the end of the axes or until the recorded loads got too large (above 150 N).

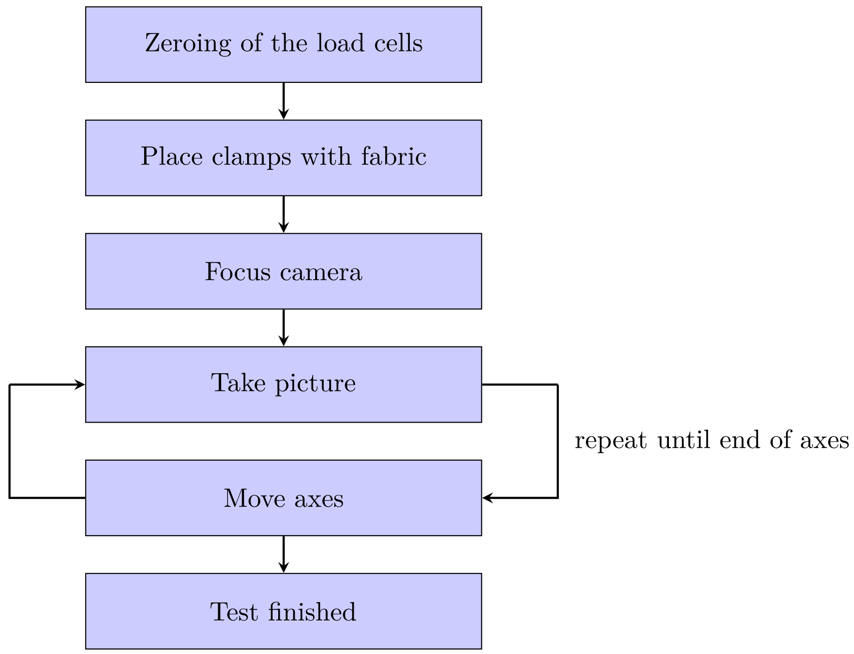

Figure 7.6: Test procedure

Part III

Results

8 Results

In this Chapter, the results of the tensile tests are presented. Section 8.1 goes into depth about the results of the tests on the homogeneous fabrics, while section 8.2 focuses on the test results of the non-homogeneous fabrics. In both sections, first the deformation curves are addressed. Afterwards, the results of the measured Poisson's ratios are presented. Lastly, the results of the measured Young's modulus are elaborated on.

8.1. Homogeneous fabrics

8.1.1. Deformation curves

The displacement of the points is recorded by the Zeiss Correlate software. The software produces a diagram with the displacement of the defined points. The data of this diagram is exported as a .csv file and is processed in a Python script. A full overview of how the displacement diagrams are obtained can be found in Appendix C.

Figure 8.1 shows the displacement data of the four buttons that were placed on a fabric with the "interlock" pattern. Button 1 and 2 move in x-direction, which is the longitudinal direction. The figure shows that the displacement of buttons 1 and 2 is not smooth if the strain that is applied to the fabric is small. This is caused by the geometric deformation of the fabric. However, for the displacement in y-direction (perpendicular to the loading direction) the displacement curves do look smooth. The displacement diagrams of all tested fabrics can be found in Appendix D.

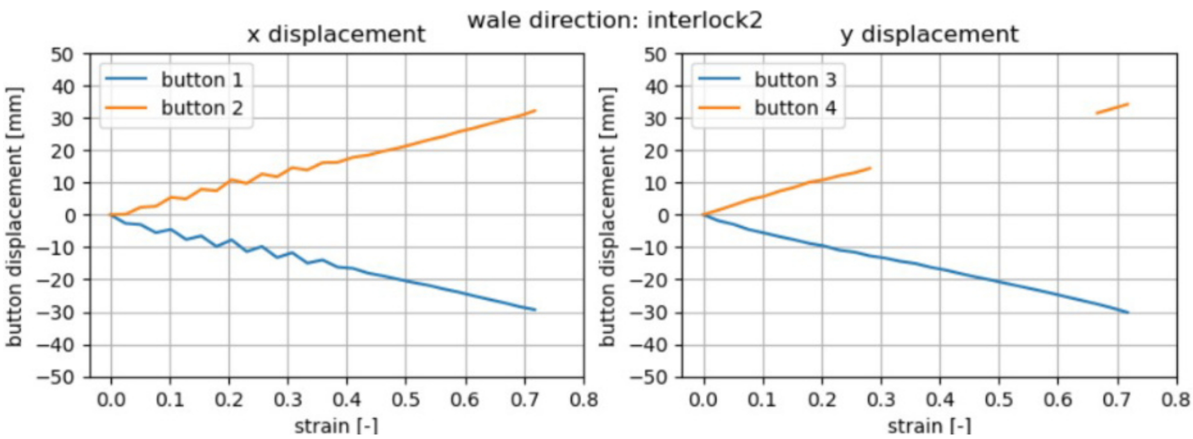

Figure 8.1: Displacement curves interlock pattern

8.1.2. Poisson's ratio

To calculate the Poisson's ratio, a linear curve is fitted through the data points of the displacement of the buttons. In this way, missing data points can be interpolated. Besides that, the interpolated curves of buttons 1 and 2 are added to each other to obtain a single curve for the total strain in longitudinal direction. The same principle is used for buttons 3 and 4 to obtain a single curve for the lateral displacement of the fabrics.

As mentioned in section 2.2, the Poisson's ratio of a material can be calculated using Equation 8.1. To obtain the strain, Equation 8.2 can be used. The original length in this formula represents the distance between the buttons. This distance is measured in the Zeiss Correlate software. An overview of these lengths can be found in Appendix D. When Equation 8.1 and 8.2 are applied with the data from the displacement-strain curves (Figure 8.1), the Poisson's ratio can be plotted against the strain of the fabric. This is shown in Figure 8.2 for a sample of the "interlock" pattern. The figure shows two plots. The first plot shows a large peak in the Poisson's ratio which is caused by the geometric deformation of the fabric. In the second plot, the datapoints that are highly affected by the geometric deformation are not included. This gives a distribution of the Poisson's ratio which is more representative of the fabric itself. The plots for all tests that have been performed can be found in Appendix E.

$$\nu = -\frac{\varepsilon_y}{\varepsilon_x} \tag{8.1}$$

$$\varepsilon = \frac{\Delta L}{L} \tag{8.2}$$

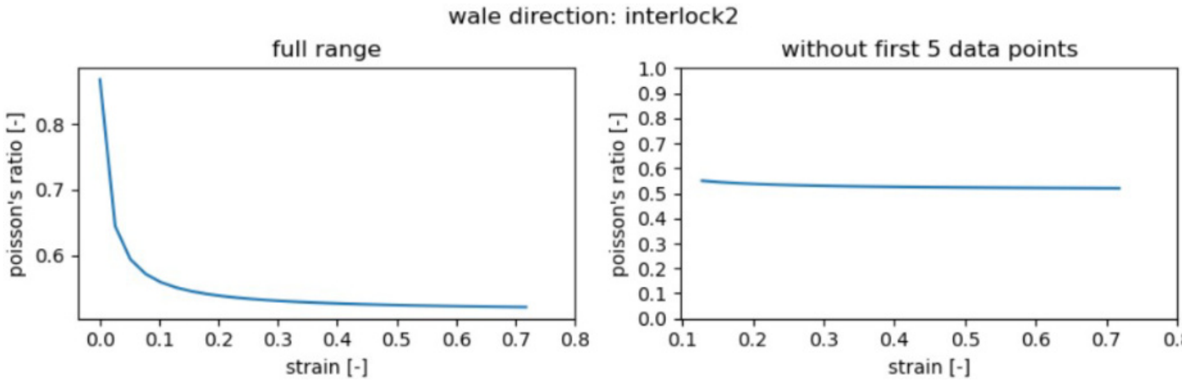

Figure 8.2: Poisson's ratio interlock pattern

Three samples are fabricated and tested for every knitting pattern. Because the sample size is smaller than 30, the t-distribution is used to determine the confidence intervals for the Poisson ratios (Boston University, 2021). The confidence intervals are calculated with Equation 8.3. Because the sample size equals three, the t-value is rather large. For a 90% confidence interval $t = 2.920$ and for a 95% confidence interval $t = 4.303$.

$$Confidence\ Interval = \mu \pm t \cdot \frac{\sigma}{\sqrt{n}} \tag{8.3}$$

μ	:	Sample mean
t	:	Value dependent on degree of freedom ($df = n - 1$)
σ	:	Standard deviation of sample
n	:	Sample size

Since the Poisson's ratio depends on the amount of strain applied to the specimen, the standard deviation also depends on the strain and therefore is not constant. Lots of factors influence the geometric deformation of the fabrics, therefore the standard deviation will be larger in the region where the applied strain is small. An overview of the characteristic values for the distributions of the Poisson ratios is given in Table 8.1 and 8.2. A visual representation of the distribution of the Poisson's ratios is shown in Figure 8.3 and Figure 8.4 for the wale and course direction respectively.

Wale direction

Table 8.1: Overview characteristic values Poisson's ratio wale direction

	Interlock		Eightlock		Tuck		Hexagon		Interlock-1float		Interlock-2float	
	$\varepsilon = 0.13$	$\varepsilon = 0.72$	$\varepsilon = 0.13$	$\varepsilon = 0.72$	$\varepsilon = 0.13$	$\varepsilon = 0.72$	$\varepsilon = 0.13$	$\varepsilon = 0.44$	$\varepsilon = 0.13$	$\varepsilon = 0.72$	$\varepsilon = 0.13$	$\varepsilon = 0.72$
μ	0.589	0.553	0.689	0.783	0.316	0.507	0.897	0.875	0.434	0.521	0.535	0.645
σ_{90}	0.086	0.055	0.064	0.011	0.122	0.065	0.098	0.081	0.085	0.034	0.142	0.051
σ_{95}	0.127	0.081	0.095	0.017	0.180	0.096	0.144	0.119	0.125	0.050	0.210	0.074

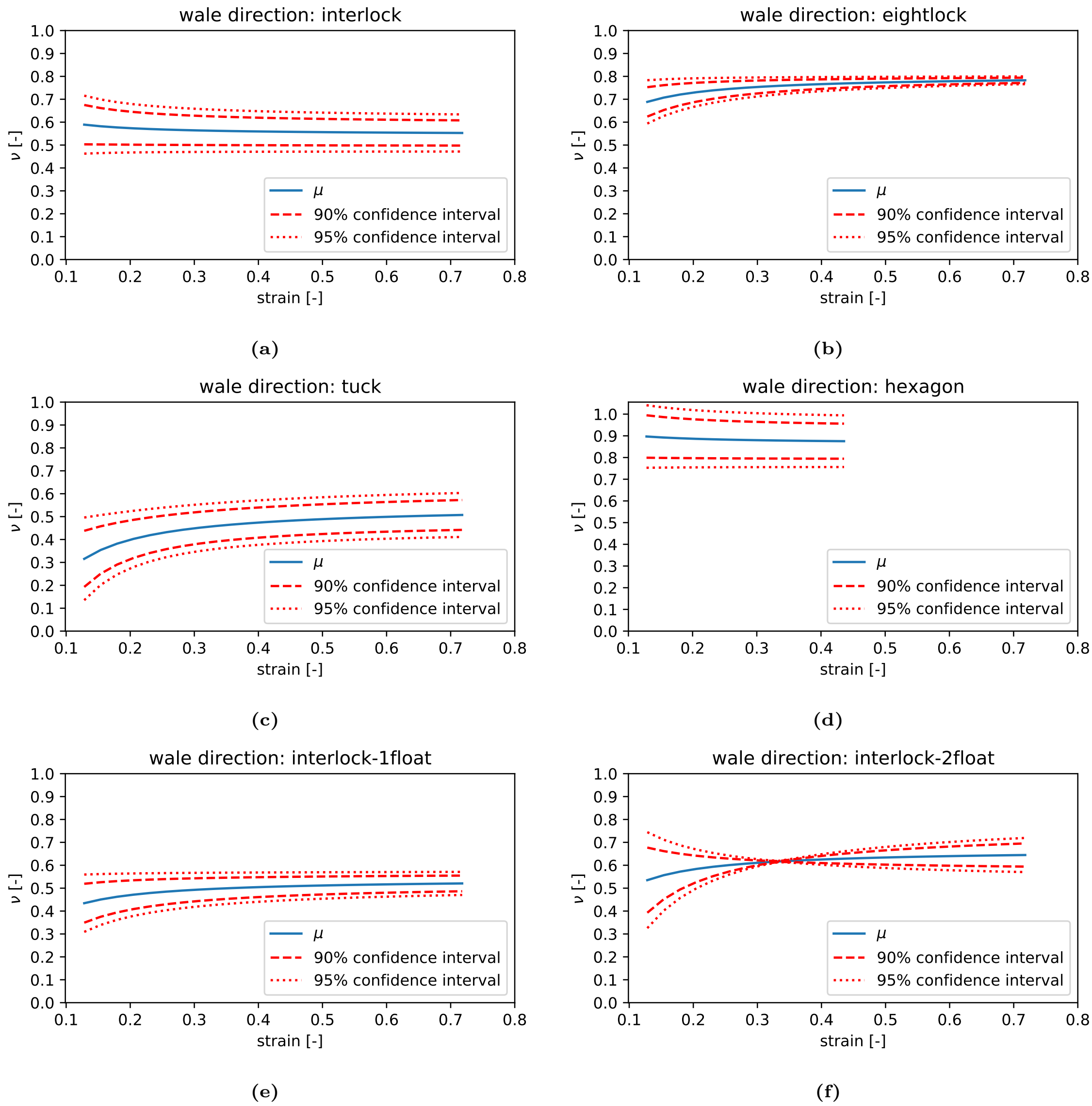

Figure 8.3: Confidence intervals Poisson's ratios wale direction

Remark: the results for the interlock_2float pattern are not considered representative of the behaviour of this knitting pattern. The clamps started rotating very suddenly when performing tests on fabrics containing this knitting pattern. This is visible in the displacement diagrams in Figure D.6 in Appendix D.

Course direction

Table 8.2: Overview characteristic values Poisson's ratio course direction

	Interlock		Eightlock		Tuck		Hexagon		Interlock-1float		Interlock-2float	
	$\varepsilon = 0.13$	$\varepsilon = 0.38$	$\varepsilon = 0.13$	$\varepsilon = 0.49$	$\varepsilon = 0.13$	$\varepsilon = 0.31$	$\varepsilon = -$	$\varepsilon = -$	$\varepsilon = 0.13$	$\varepsilon = 0.72$	$\varepsilon = -$	$\varepsilon = -$
μ	0.420	0.455	0.475	0.612	0.458	0.460	-	-	0.196	0.476	-	-
σ_{90}	0.167	0.174	0.142	0.154	0.019	0.016	-	-	0.097	0.030	-	-
σ_{95}	0.247	0.257	0.209	0.227	0.029	0.024	-	-	0.143	0.044	-	-

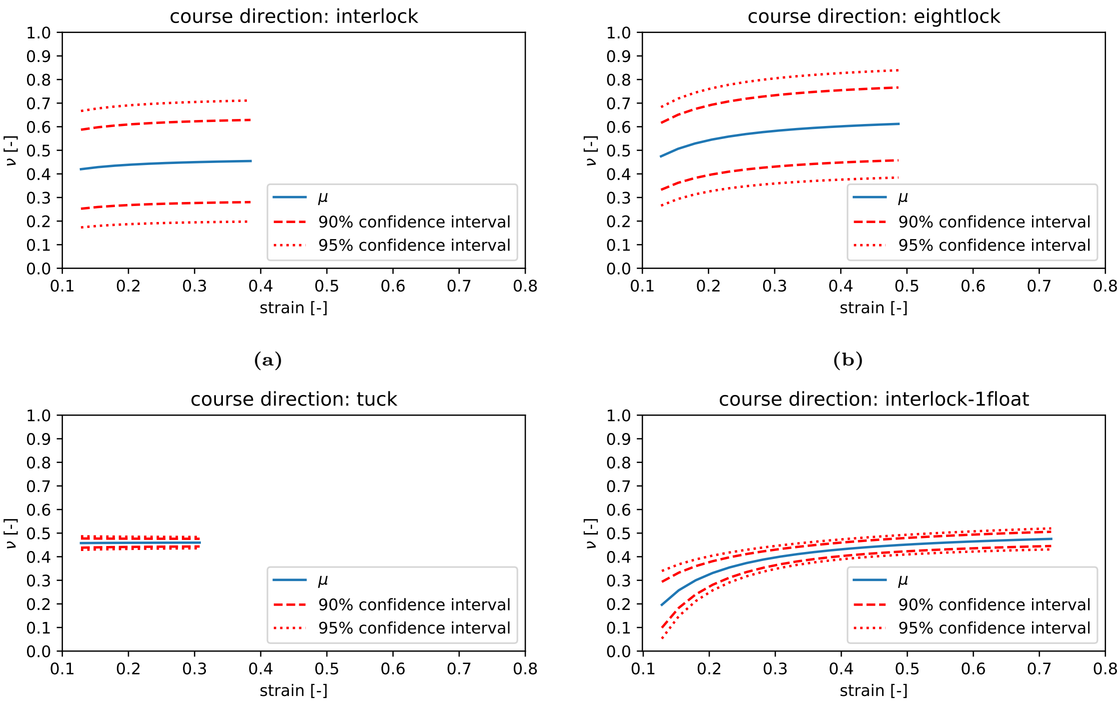

(a) (b) (c) (d)

Figure 8.4: Confidence intervals Poisson's ratios course direction

Comparison

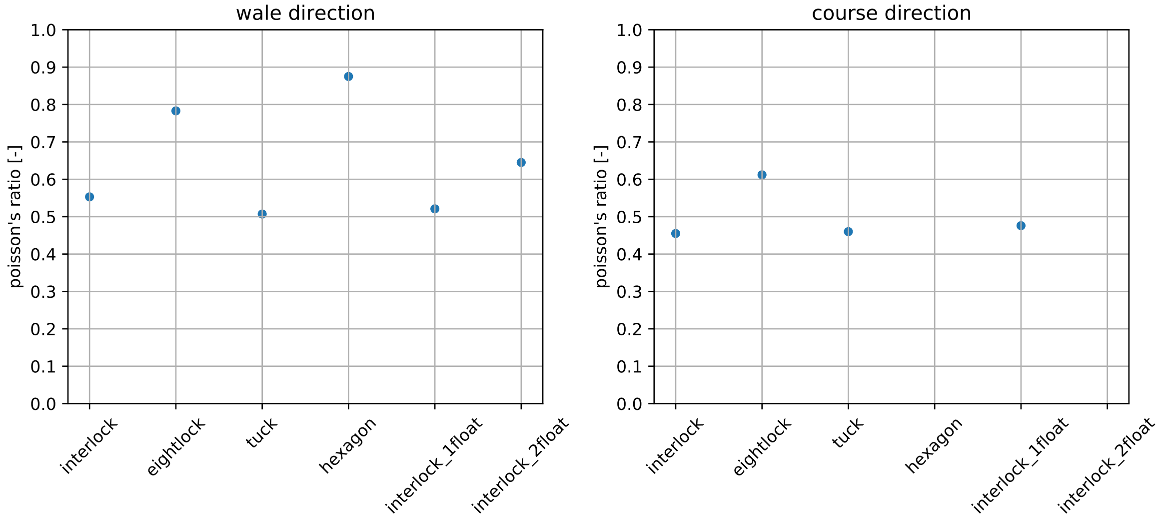

Figure 8.5: Comparison of Poisson's ratios at ε_{max}

When the results for the tests in wale and course direction are compared to each other, it can be concluded that the Poisson's ratio for every knitting pattern is lower in course direction. This is shown in Figure 8.5. This figure compares the Poisson's ratios for the different knitting patterns at the end of the tensile test. This does not mean that the values are compared at the same strain level because the clamps started to rotate at different amounts of strain.

Besides that, the Poisson's ratio of the fabrics is not constant but depends on the amount of strain that is applied to the fabric. When a large amount of strain is applied, the Poisson's ratio asymptotically approaches a boundary value. When the applied strain is low, the Poisson's ratio deviates a lot from this boundary value. This is caused by the geometric deformation of the fabric and is not necessarily representative of the behaviour of the knitting pattern itself. Therefore, this effect is not taken into account in the comparison.

8.1.3. Young's modulus

During the tensile tests, the load cells record the forces that are applied to the fabric. The response of the sensors can be plotted in a force-displacement diagram, see Figure 8.6 where the displacement of the clamps is converted into the strain of the fabric. The three graphs show the load recorded by both loadcells. To obtain the total force applied to the fabric, the average of the responses of the loadcells is taken. The force-displacement diagrams of all fabrics can be found in Appendix G.

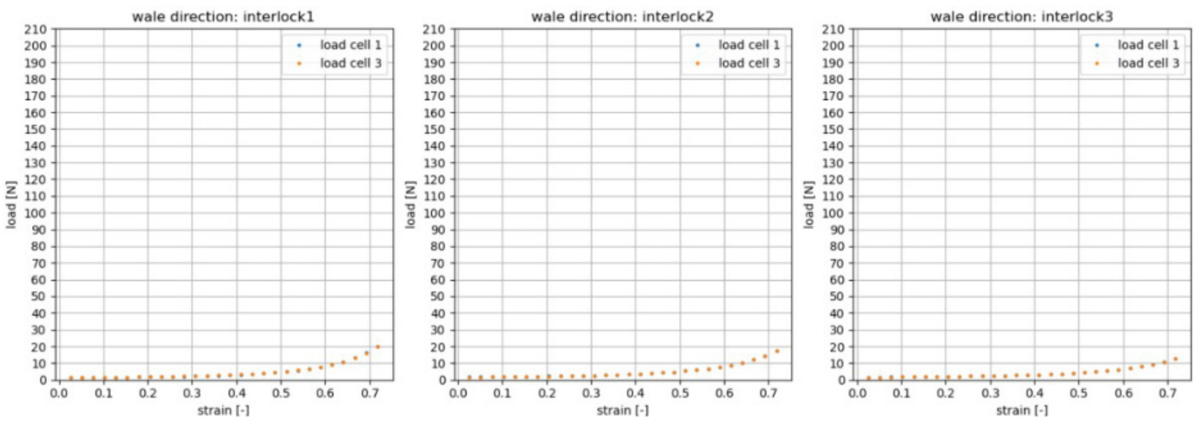

Figure 8.6: Force-strain diagrams interlock

To convert the force-strain diagram to a stress-strain diagram, the forces must be divided by the area of the fabric. The area of the fabric is likely not constant during testing, but this effect is difficult to measure. Therefore it is chosen to obtain the area of the fabric when it is in the most relaxed state and use that value to convert all forces to stresses. Appendix F shows an in-depth explanation of the area determination of the fabrics. The stress-strain diagrams for the fabrics made of the eightlock knitting pattern are shown in Figure 8.7.

The diagrams in Figure 8.7 show a non-linear relationship between stress and strain. Since the slope of the stress-strain curve represents the Young's modulus of the material, this property is not constant. For this research, it is decided to approximate the Young's modulus at the start (E1, crimp region (Zhu et al., 2011)) and end (E2, elastic region (Zhu et al., 2011)) of the stress-strain curves. Figure 8.8 shows the determination of the Young's modulus of the fabrics of the eightlock pattern. The first and last five datapoints are used to fit a linear relationship for the Young's moduli E1 and E2 respectively. Appendix H shows an overview of the graphs used to determine the Young's modulus of all fabrics.

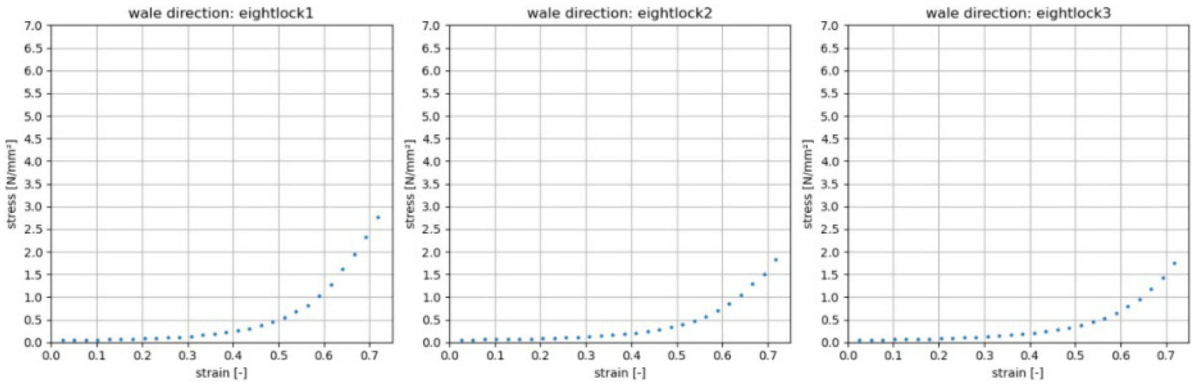

Figure 8.7: σ-ε diagrams eightlock

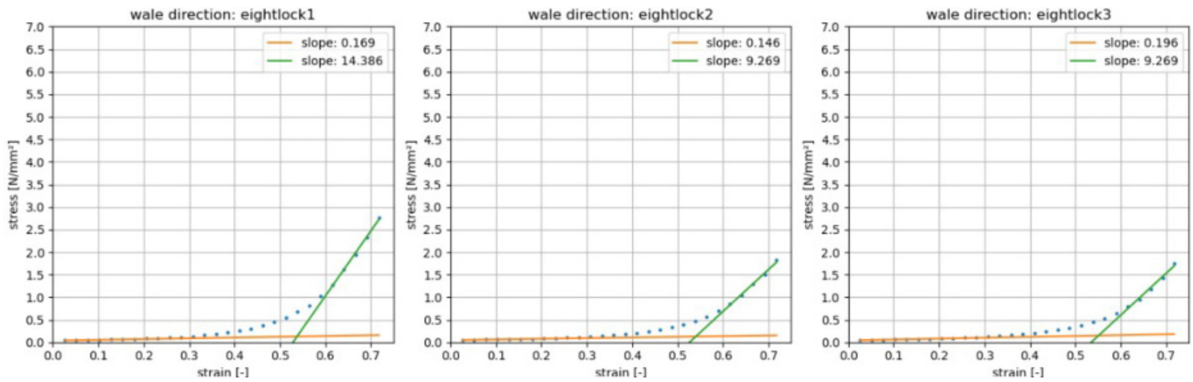

Figure 8.8: Young's modulus eightlock

Overview

Table 8.3 and Figure 8.9 show an overview of the Young's moduli for the different knitting patterns. In wale direction, large differences between the different knitting patterns are visible. E1 is rather small for all patterns, but E2 varies a lot. In course direction, the values for both E1 and E2 are small; all below 0.5 [N/mm²].

	Wale direction		Course direction	
Pattern name	E1 [N/mm²]	E2 [N/mm²]	E1 [N/mm²]	E2 [N/mm²]
interlock	0.063 ± 0.007	1.748 ± 0.470	0.097 ± 0.006	0.190 ± 0.011
eightlock	0.170 ± 0.020	10.98 ± 2.412	0.180 ± 0.012	0.437 ± 0.076
hexagon	0.715 ± 0.278	30.51 ± 7.150	-	-
tuck	0.077 ± 0.003	2.252 ± 0.556	0.119 ± 0.048	0.142 ± 0.023
interlock_1float	0.074 ± 0.021	0.956 ± 0.184	0.050 ± 0.004	0.237 ± 0.021
interlock_2float	0.081 ± 0.012	8.159 ± 1.569	-	-

Table 8.3: Overview Young's moduli

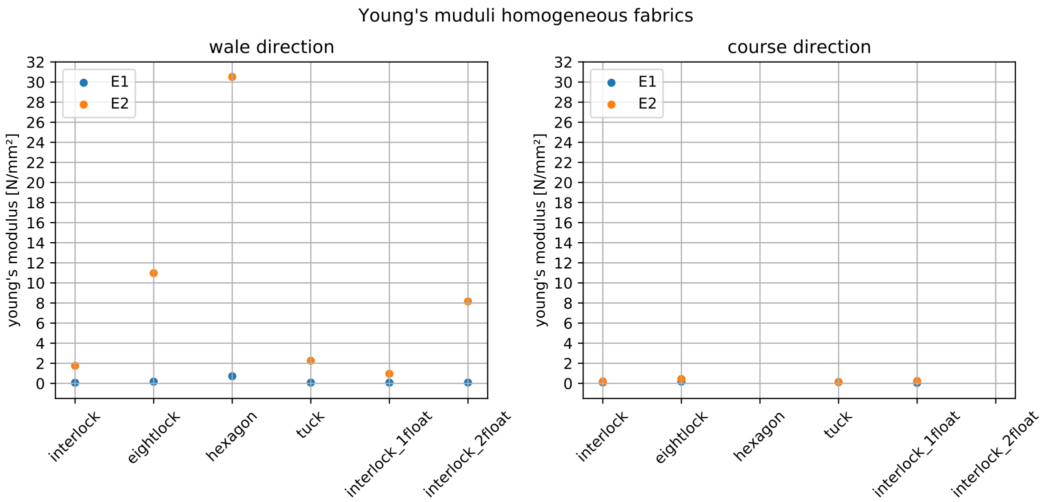

Figure 8.9: Overview Youngs's moduli

8.2. Non-homogeneous fabrics

As mentioned before, the non-homogeneous fabrics contain the interlock pattern as the primary knitting pattern. The secondary knitting pattern is tuck or eightlock. The tuck pattern is chosen because that pattern uses a different knitting operation. The tests on the homogeneous fabrics have shown that the interlock and tuck patterns behave quite similarly. Therefore, a combination of both patterns is expected to lead to similar results and the influence of the secondary pattern (tuck) will not be visible in the results of the tensile tests.

However, the test on the homogeneous fabrics of the interlock and eightlock pattern did show large differences. Therefore it is expected that the size of the circle of the secondary pattern (eightlock) will influence the outcome of the tensile tests.

8.2.1. Deformation curves

Similar to the homogeneous fabrics, the displacement of the buttons on the non-homogeneous fabrics is tracked by the Zeiss Correlate software. The buttons are placed on the interface of the two knitting patterns. This means that for a circle with a diameter of 25 pixels, the buttons are closer to each other than for a circle with a diameter of 75 pixels.

8.2.2. Poisson's ratio

Wale direction

Table 8.4 and Figure 8.10 show the results of the Poisson's ratio for the interlock_tuck fabrics. Since these fabrics are only tested once, a confidence interval is not plotted. A remarkable result is that the Poisson's ratio of the fabrics with the combined knitting patterns is a lot higher than the Poisson's ratios of the homogeneous interlock and tuck fabrics. This is visible in the graphical comparison of the Poisson's ratios in Figure 8.11.

Table 8.4: Overview characteristic values Poisson's ratio wale direction

	Interlock		Tuck		Ilock_tuck_d25		Ilock_tuck_d50		Ilock_tuck_d75	
	$\varepsilon = 0.13$	$\varepsilon = 0.72$	$\varepsilon = 0.13$	$\varepsilon = 0.72$	$\varepsilon = 0.13$	$\varepsilon = 0.72$	$\varepsilon = 0.13$	$\varepsilon = 0.72$	$\varepsilon = 0.13$	$\varepsilon = 0.72$
μ	0.589	0.553	0.316	0.507	0.697	0.679	0.717	0.717	0.623	0.699
σ_{90}	0.086	0.055	0.122	0.065	-	-	-	-	-	-
σ_{95}	0.127	0.081	0.180	0.096	-	-	-	-	-	-

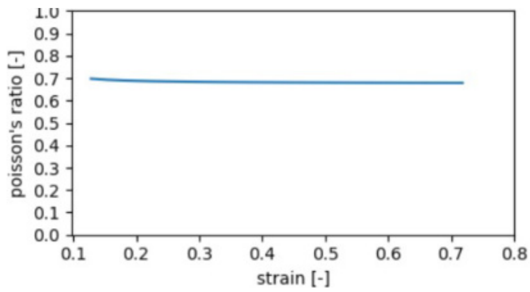

(a) interlock_tuck_d25

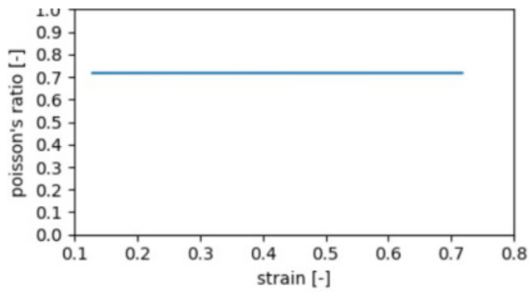

(b) interlock_tuck_d50

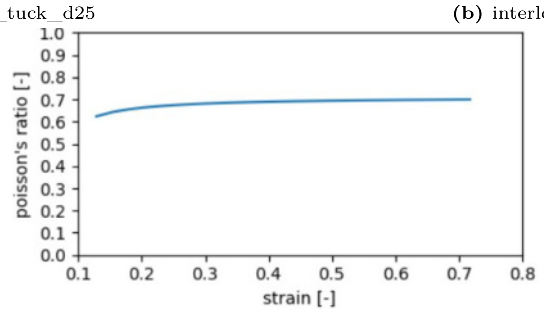

(c) interlock_tuck_d75

Figure 8.10: Poisson's ratios interlock_tuck

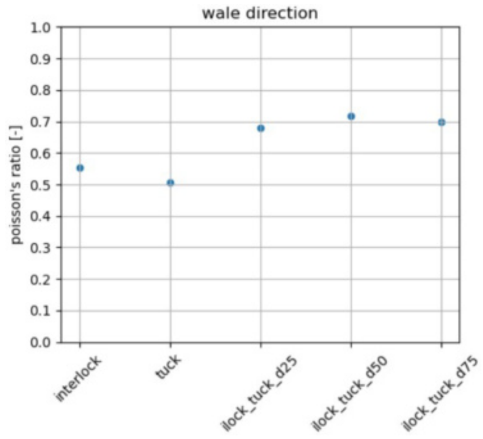

Figure 8.11: Overview Poisson's ratios

Table 8.5 and Figure 8.12 show the results of the Poisson's ratio for the interlock_eightlock fabrics. The visual comparison of the Poisson's ratios of the fabrics is shown in Figure 8.13. This figure shows that the Poisson's ratio of the knitted textile increases when the fabric contains a larger circle of the eightlock pattern.

Table 8.5: Overview characteristic values Poisson's ratio wale direction

	Interlock		Eightlock		Ilock_8lock_d25		Ilock_8lock_d50		Ilock_8lock_d75	
	$\varepsilon = 0.13$	$\varepsilon = 0.72$	$\varepsilon = 0.13$	$\varepsilon = 0.72$	$\varepsilon = 0.13$	$\varepsilon = 0.72$	$\varepsilon = 0.13$	$\varepsilon = 0.44$	$\varepsilon = 0.13$	$\varepsilon = 0.72$
μ	0.589	0.553	0.689	0.783	0.659	0.690	0.639	0.698	0.628	0.730
σ_{90}	0.086	0.055	0.064	0.011	0.112	0.041	0.033	0.023	0.030	0.020
σ_{95}	0.127	0.081	0.095	0.017	0.166	0.061	0.049	0.034	0.045	0.029

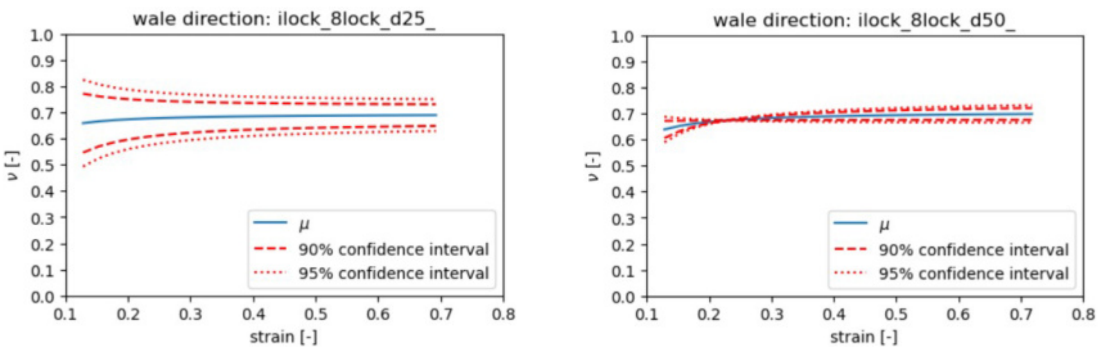

(a) (b)

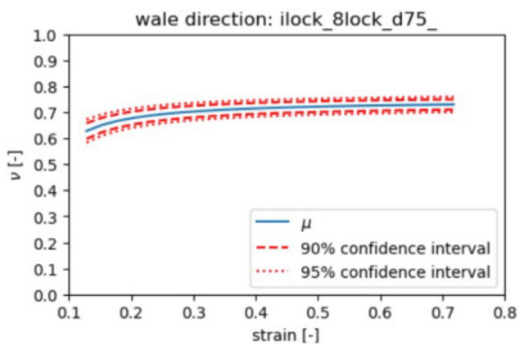

(c)

Figure 8.12: Poisson's ratios interlock_eightlock

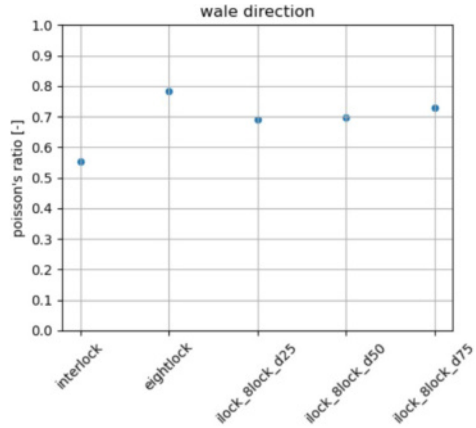

Figure 8.13: Overview Poisson's ratios

Course direction

Looking at the results of the interlock_tuck fabrics in course direction, a similar trend is visible as in the wale direction. The size of the circle with the secondary pattern seems to not influence the Poisson's ratio of the fabric. Besides that, the Poisson's ratio of the non-homogeneous fabrics is comparable to the ratios for the homogeneous fabrics.

Table 8.6: Overview characteristic values Poisson's ratio course direction

	Interlock		Tuck		Ilock_tuck_d25		Ilock_tuck_d50		Ilock_tuck_d75	
	$\varepsilon = 0.13$	$\varepsilon = 0.38$	$\varepsilon = 0.13$	$\varepsilon = 0.31$	$\varepsilon = 0.13$	$\varepsilon = 0.21$	$\varepsilon = 0.13$	$\varepsilon = 0.21$	$\varepsilon = 0.13$	$\varepsilon = 0.21$
μ	0.420	0.455	0.458	0.460	0.393	0.396	0.481	0.483	0.434	0.436
σ_{90}	0.167	0.174	0.019	0.016	-	-	-	-	-	-
σ_{95}	0.247	0.257	0.029	0.024	-	-	-		-	-

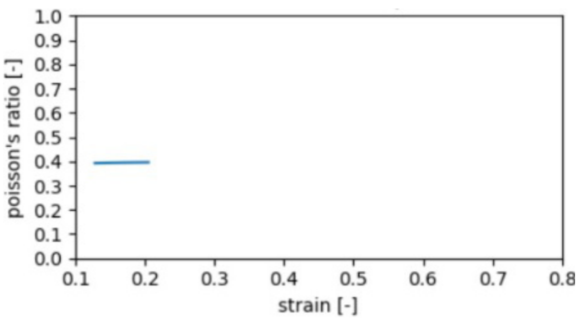

(a) interlock_tuck_d25

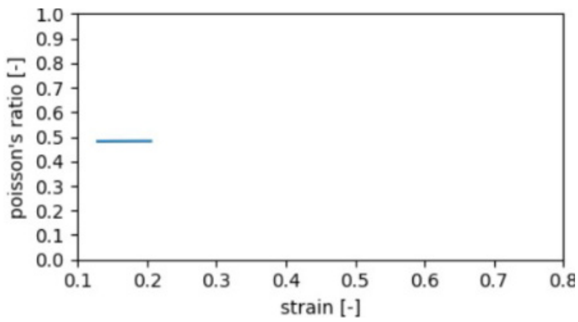

(b) interlock_tuck_d50

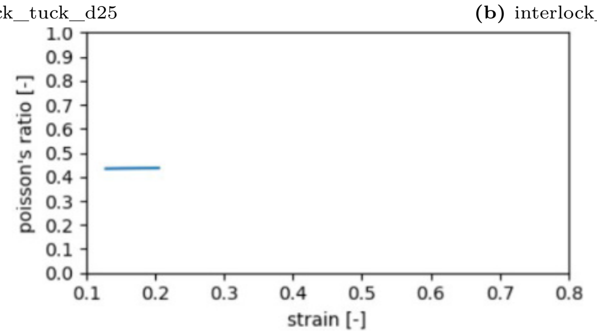

(c) interlock_tuck_d75

Figure 8.14: Poisson's ratios interlock_tuck

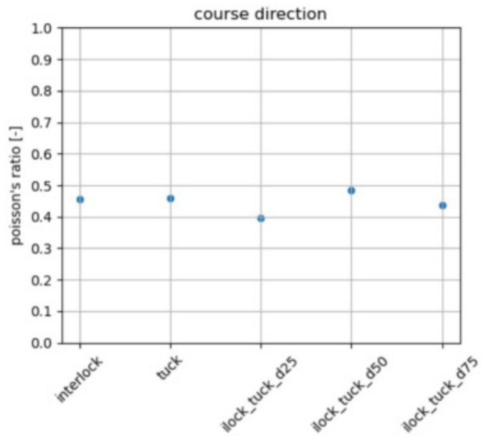

Figure 8.15: Overview Poisson's ratios

When the results of the non-homogeneous interlock_eightlock fabrics are compared to the homogeneous ones, a clear trend is visible (see Figure 8.17). The Poisson's ratio of the knitted textile increases when the diameter of the circle of the secondary knitting pattern becomes larger.

Table 8.7: Overview characteristic values Poisson's ratio course direction

	Interlock		Eightlock		Ilock_8lock_d25		Ilock_8lock_d50		Ilock_8lock_d75	
	$\varepsilon = 0.13$	$\varepsilon = 0.38$	$\varepsilon = 0.13$	$\varepsilon = 0.31$	$\varepsilon = 0.13$	$\varepsilon = 0.26$	$\varepsilon = 0.13$	$\varepsilon = 0.36$	$\varepsilon = 0.13$	$\varepsilon = 0.38$
μ	0.420	0.455	0.475	0.612	0.515	0.547	0.550	0.613	0.581	0.669
σ_{90}	0.167	0.174	0.142	0.154	0.020	0.020	0.023	0.036	0.067	0.080
σ_{95}	0.247	0.257	0.209	0.227	0.029	0.030	0.034	0.053	0.099	0.118

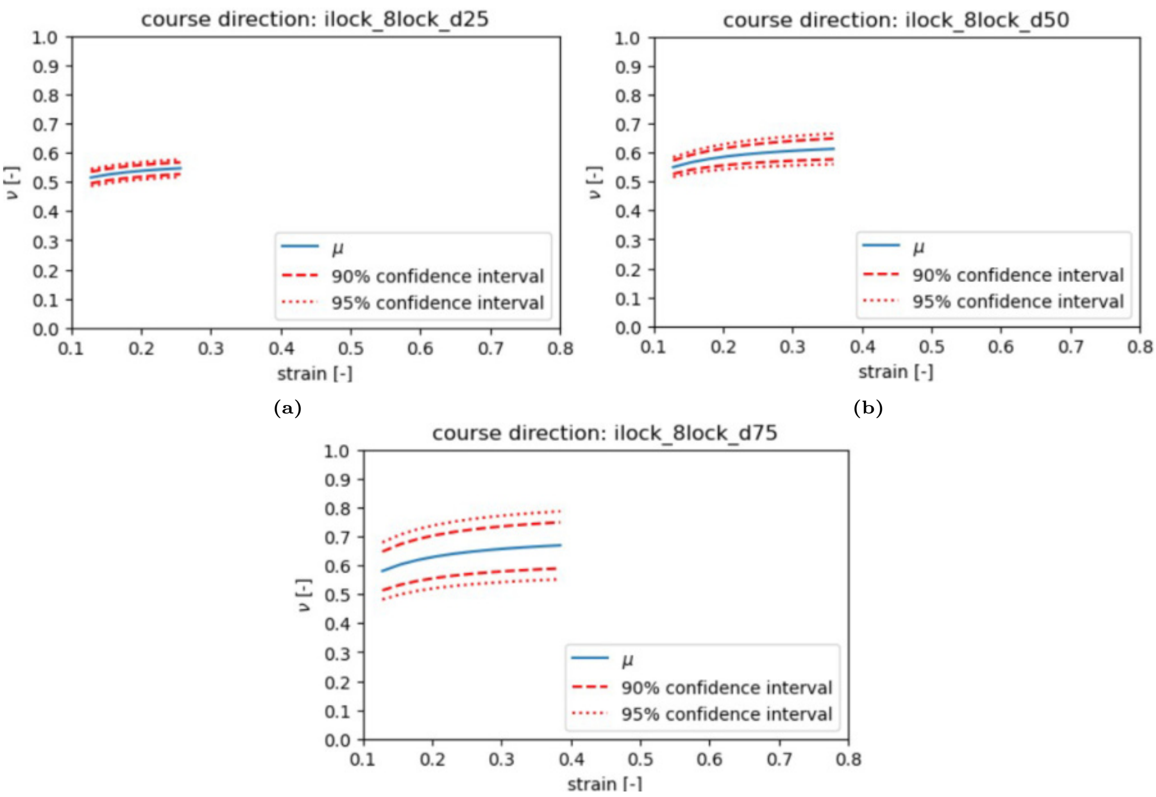

(a) (b) (c)

Figure 8.16: Poisson's ratios interlock_eightlock

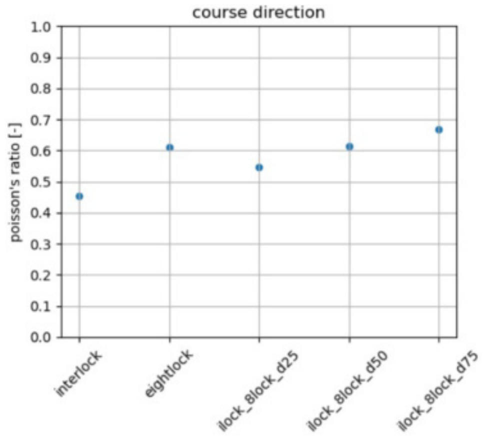

Figure 8.17: Overview Poisson's ratios

Overview
When comparing the Poisson's ratios in wale and course direction for the fabrics containing the interlock and tuck pattern, the ratios are larger in wale direction for all of the fabrics. This is in line with the expected orthotropic behaviour of knitted textiles.

Besides that, Figure 8.18 shows an interesting detail. For both wale and course direction, the fabric containing a circle with a diameter of 50 pixels shows a slightly larger Poisson's ratio than the fabrics with a circle with a 25 or 75 pixel diameter. This effect can not be explained by the small number of tests that has been performed in this research.

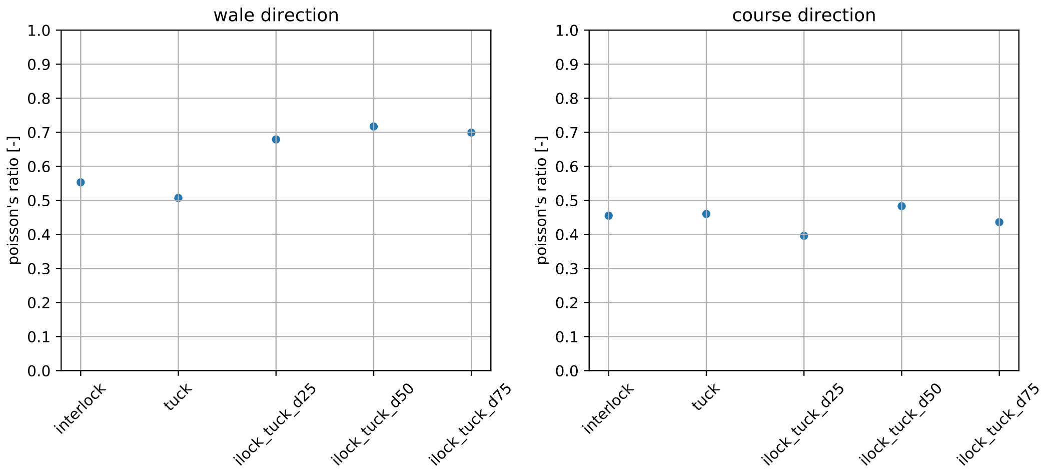

Figure 8.18: Overview Poisson's ratios

A comparison of the Poisson's ratios of the interlock_eightlock fabrics is shown in Figure 8.19. This figure shows that in both directions, the trend of the Poisson's ratios for the non-homogeneous fabrics is similar. When the amount of eightlock is increased, the Poisson's ratio increases likewise. However, in course direction the value for the Poisson's ratio of the fabric with the largest circle exceeds the value for the homogeneous eightlock fabric.

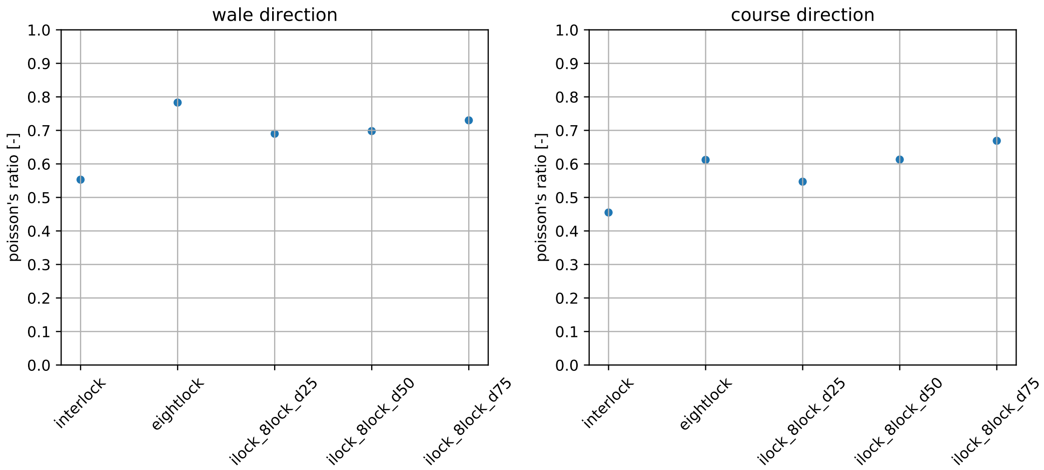

Figure 8.19: Overview Poisson's ratios

8.2.3. Young's modulus

Table 8.8 shows the measured Young's moduli for the non-homogeneous fabrics. A graphical comparison is shown in Figure 8.20 and 8.21. When looking at the Young's moduli of the combined fabrics in both wale and course direction, both the interlock_tuck and interlock_eightlock fabrics show the same trend; the Young's modulus increases when the area covered by the secondary knitting pattern increases.

	Wale direction		Course direction	
Pattern name	E1 [N/mm²]	E2 [N/mm²]	E1 [N/mm²]	E2 [N/mm²]
ilock_tuck_d25 *	0.059	1.444	0.121	0.144
ilock_tuck_d50 *	0.080	1.623	0.106	0.133
ilock_tuck_d75 *	0.064	2.468	0.110	0.123
ilock_8lock_d25	0.074 ± 0.007	3.250 ± 0.647	0.102 ± 0.014	0.204 ± 0.029
ilock_8lock_d50	0.080 ± 0.010	4.378 ± 0.377	0.102 ± 0.014	0.432 ± 0.053
ilock_8lock_d75	0.088 ± 0.011	6.637 ± 0.941	0.102 ± 0.013	0.545 ± 0.067

Table 8.8: Overview Young's moduli (* only tested once)

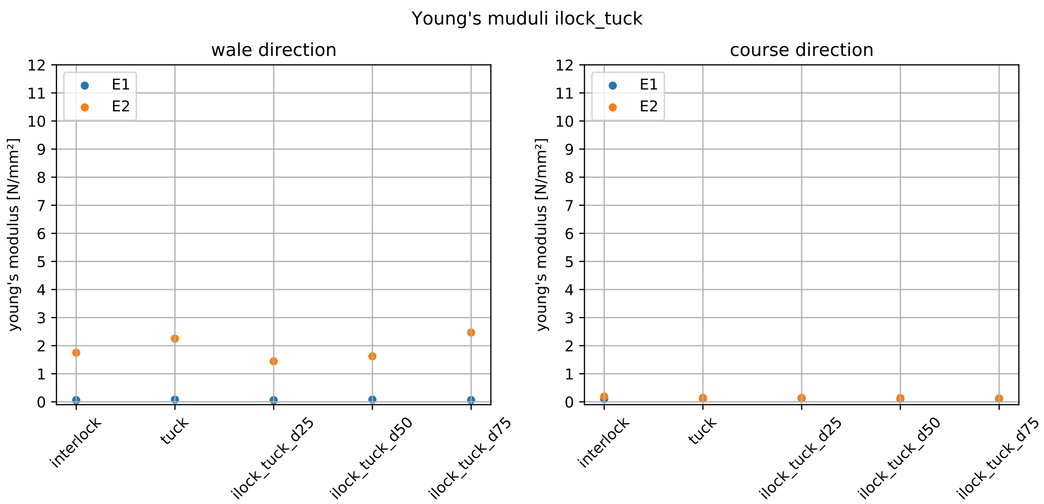

Figure 8.20: Overview Youngs's moduli

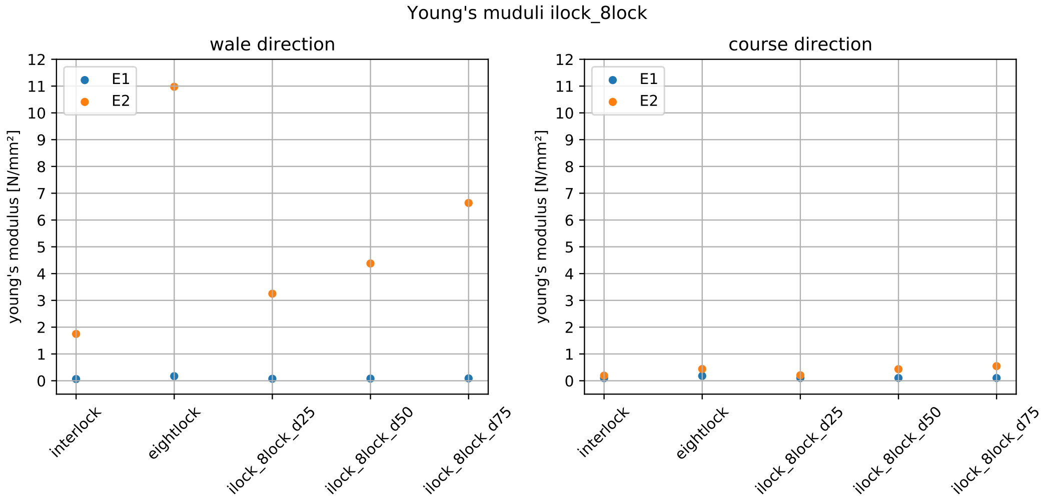

Figure 8.21: Overview Youngs's moduli

Part IV

Reflection

9
Discussion

This chapter provides a critical analysis of the results presented in chapter 8. Section 9.1 discusses the results and section 9.2 focuses on the limitations of this research. Subsection 9.2.1 goes into depth about the limitations of the setup itself, while subsection 9.2.2 elaborates on the properties of the fabrics. Subsection 9.2.3 discusses inconsistencies related to the results.

9.1. Results

9.1.1. Homogeneous fabrics

Poisson's ratio

The Poisson's ratio for homogeneous solids is always between -1 and 0.5 (see section 2.2). It is known that these boundaries are not valid for woven fabrics due to their non-homogeneous structure. The results presented in chapter 8 show that the boundaries are also not valid for knitted textiles. The measured values for the Poisson's ratio of the tested fabrics in wale direction all exceed the boundary value. In course direction, only the Poisson's ratio of the eightlock pattern is larger than 0.5.

When the measured Poisson's ratios for the homogeneous fabrics are compared (Figure 9.1), the fabrics containing the interlock, tuck and interlock_1float pattern show a comparable value in both wale and course direction. However, there is a large difference between the Poisson's ratio of the interlock and eightlock patterns. The interlock pattern has a Poisson's ratio of 0.553 and 0.455 while the eightlock pattern has a ratio of 0.783 and 0.612 in wale and course direction respectively. This difference is interesting since both knitting patterns are composed of the same knitting operations but in a different configuration.

The larger Poisson's ratio for the eightlock pattern can be explained by the ribbed structure of the fabric. As mentioned in section 5.1 the eightlock fabric is ribbed because two similar knitting operations are performed after each other. This creates small zones in which the two layers of the fabric are not connected. Therefore the fabric experiences less resistance and can deform more freely compared to a fabric containing the interlock pattern.

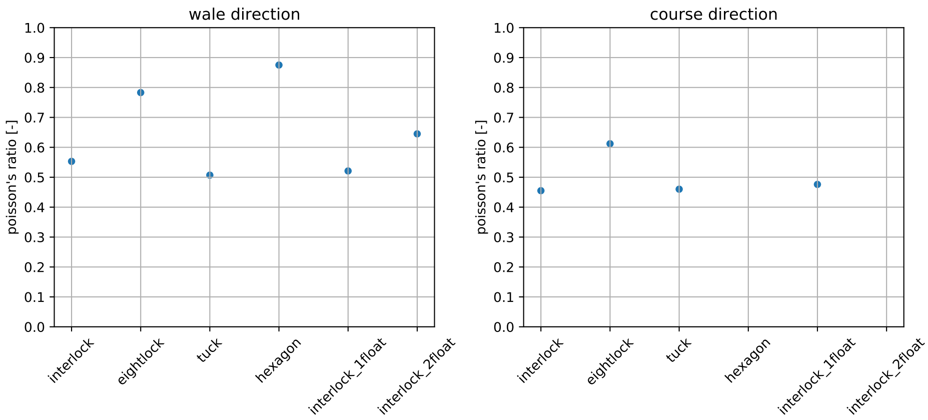

Figure 9.1: Comparison of Poisson's ratios at ε_{max}

Young's modulus

As mentioned in section 2.2, the stress-strain diagram of fabrics consists of four regions. During the tests performed in this research, the fabrics are tested up to a point within the elastic region. In this region, the Young's modulus represents the stiffness of the fabric's knitting pattern and the geometric deformation does not influence this property. The Young's modulus in the elastic region is shown as E2 in Figure 9.2.

The hexagon pattern is in wale direction far stiffer than the other knitting patterns considered in this research. This is caused by the locking in place of the hexagons of yarn when the fabric is tensioned. This locking mechanism ensures that the yarns can not deform freely and this causes the applied forces to increase rapidly (see Appendix G).

Furthermore, the eightlock pattern has a Young's modulus in wale direction that is more than six times as large as the Young's modulus of the interlock pattern. This is due to the ribbed structure of the eightlock pattern. This structure reinforces the fabric which causes it to be stiffer than the interlock pattern. However, this reinforcing principle did not show up when the fabrics containing the tuck pattern were tested. A tuck stitch creates bracings between the two layers of the double-layered fabric but Figure 9.2 shows that this does not increase the stiffness of the fabric.

When the fabrics were tested in course direction, the test had to be stopped earlier because the clamps started to rotate. Due to this, the fabrics had not reached their stiffening point yet and the stress-strain diagram only shows the crimp region. Therefore, the measured values for the Young's modulus are not representative of the behaviour of the knitting patterns because they are highly influenced by the geometric deformation of the yarns since the elastic region is not reached yet. This explains the fact that the measured values are all small compared to the values in wale direction.

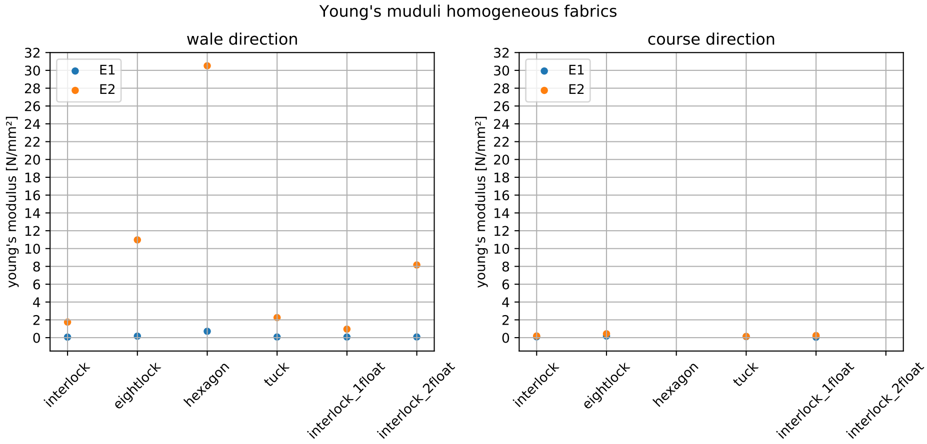

Figure 9.2: Overview Youngs's moduli

9.1.2. Non-homogeneous fabrics

Poisson's ratio

Combining different knitting patterns is expected to influence the mechanical properties of the fabrics. For the Poisson's ratio this is shown in Figure 9.3. It was expected that the Poisson's ratio would be affected by the size of the circle containing the secondary knitting pattern. For the interlock_eightlock fabrics it indeed is the case that the Poisson's ratio linearly increases when the size of the circle is increased (see Figure 9.3b).

However, for the interlock_tuck fabrics this is not the case. The Poisson's ratio for the interlock pattern is larger than for the tuck pattern. It was therefore expected that the Poisson's ratio would decrease if the size of the circle containing the tuck pattern was increased. But this turned out to not be the case. The Poisson's ratio of the combined fabrics is significantly larger than for both the homogeneous patterns it is composed of. Furthermore, both in wale and course direction, the Poisson's ratio of the fabric with the medium-sized circle is the largest. Both phenomena are likely caused by the interaction between the primary and secondary knitting patterns.

For the interlock_eightlock fabrics, the interaction between the different knitting patterns also plays a role. The tests in course direction have shown that the Poisson's ratio increases to a value higher than that of either individual knitting pattern.

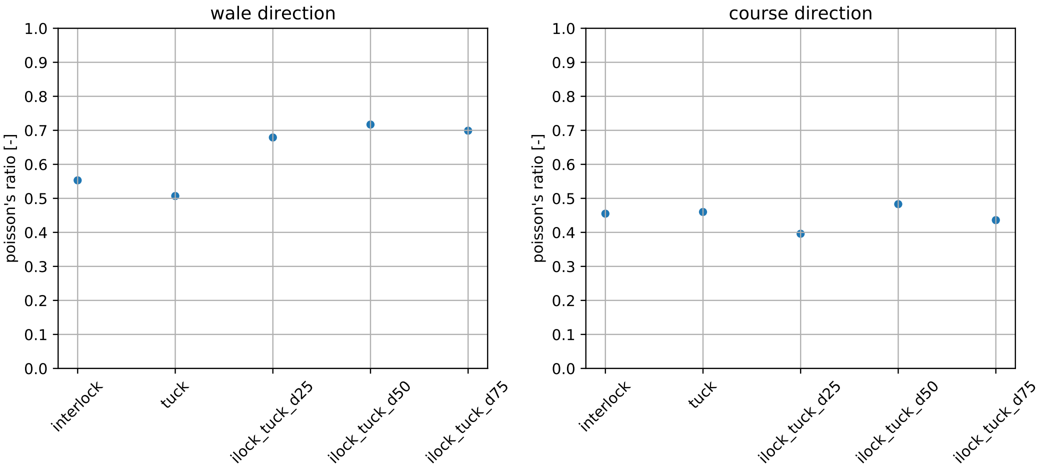

(a) interlock_tuck

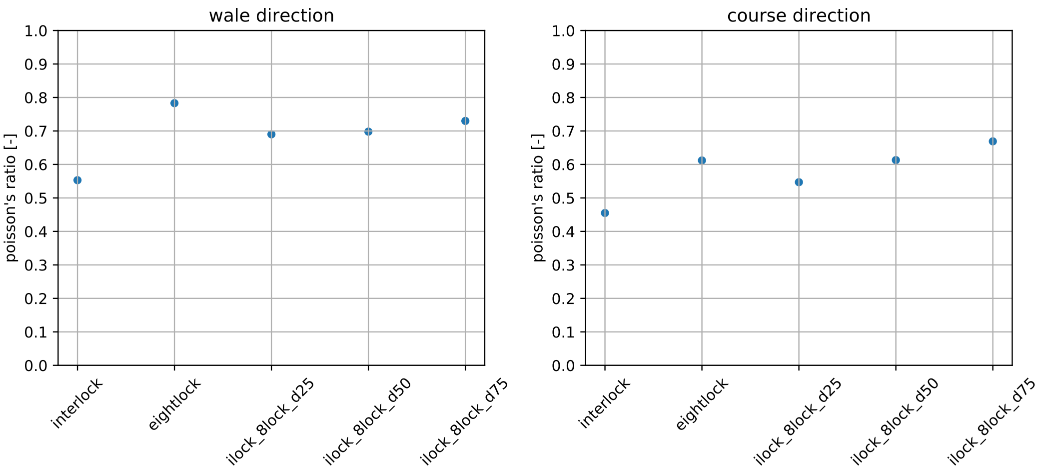

(b) interlock_eightlock

Figure 9.3: Overview Poisson's ratios

Young's modulus

When the knitting patterns are combined, it is expected that the size of the circle influences the properties of the fabrics. This indeed is the case, see Figure 9.4. Both for the interlock_tuck and the interlock_eightlock fabrics, the secondary knitting pattern has a larger Young's modulus in wale direction. When the stiffer secondary knitting pattern covers a larger area of the fabric, the Young's modulus increases.

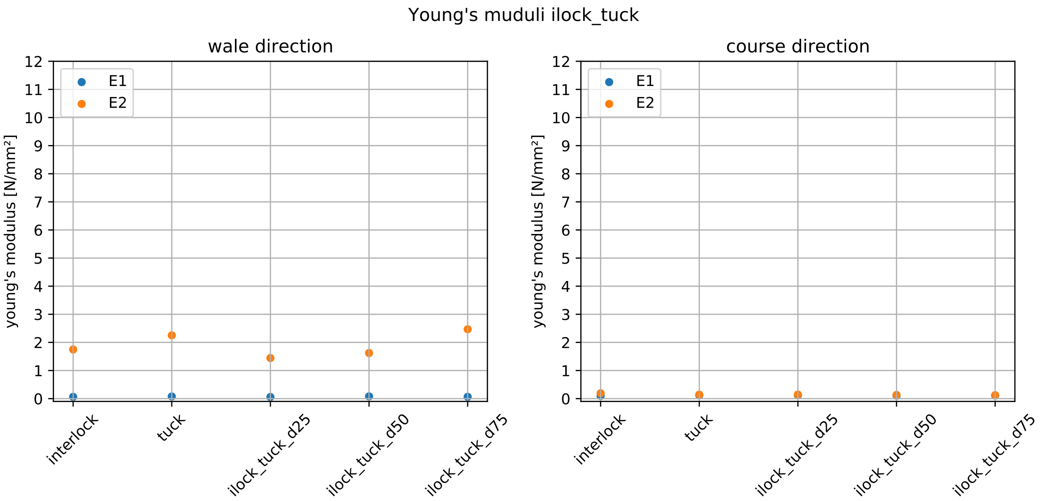

(a) interlock_tuck

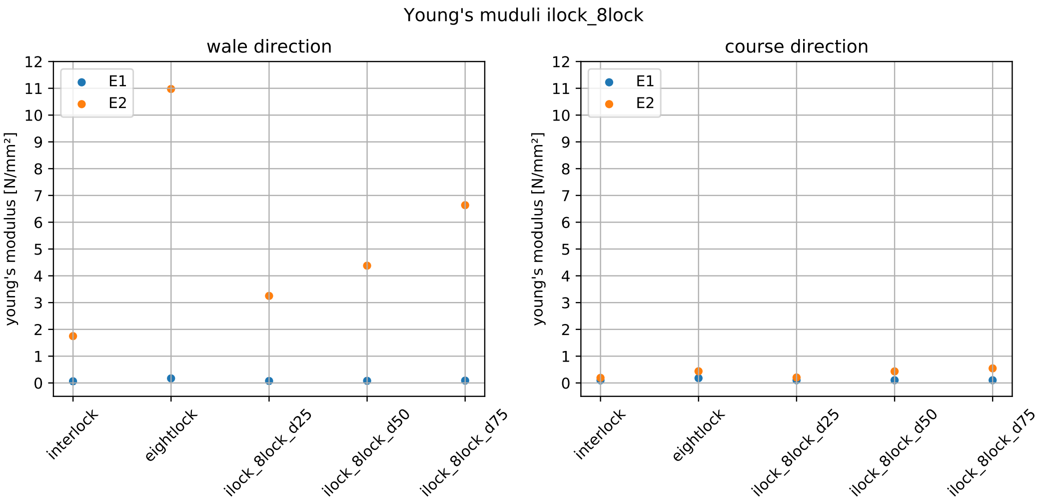

(b) interlock_eightlock

Figure 9.4: Overview Youngs's moduli

9.2. Limitations

9.2.1. Setup

The main drawback of the test setup used during this research is that the clamps can rotate. This feature is useful when asymmetric fabrics are tested, but not when performing uniaxial tests on symmetrical knitted fabrics. Because the clamps can rotate freely, any fabric asymmetricalities will influence the test results. The asymmetricalities can for example be caused by the start and the closing of the fabrics. This was the case for almost all fabrics tested in course direction.

Another reason that causes the clamps to rotate can be the way the fabrics are placed in the clamps. The rods that are clamped have to be inserted in the channels of the fabrics. When the rods are clamped, the fabric has to be centered as much as possible. However, small deviations from this position can already cause a lot of rotation of the clamps when the applied strain becomes large.

9.2.2. Fabrics

The start and closing not only cause the clamps to rotate, but they also influence the test results. When they both are stiffer than the fabric itself, the measured loads represent the stiffness of the start and closing and not the fabric itself. Besides that, when the applied strain is large, the start and closing get fully tensioned, but the main part of the fabric will start to wrinkle. This effect shows that the fabric is not properly tensioned.

Another point of attention is the starting size of the fabrics. During this research, the size of the fabrics is calibrated to all the same size. In this way, the different knitting operations are not one-on-one interchanged. On the contrary, the setup size would be a limitation if the fabrics were all made with the same amount of pixels in the bitmap file. Because the size of the fabrics varies, they can not all be tested to the same amount of strain. This makes a good comparison of the results very difficult.

9.2.3. Results

A couple of inconsistencies can be noticed when looking at the results. First, not all fabrics are tensioned to the same amount of strain. This is the case especially when testing the fabrics in course direction. This is caused by the rotating clamps due to the stiffness of the closing. Because the fabrics are not tested to the same amount of strain, the comparison of the Poisson's ratio and Young's modulus is not fully representative of the comparison of the properties of the knitting patterns itself.

Furthermore, the stiffening point is not reached for all fabrics. This means that the value for E2 is not reached for every fabric even though in Table 8.3 and 8.8 an overview of this property is presented. Because the stiffening point is not reached, the Young's modulus of the fabrics would increase if more strain was applied. This is not possible to do with the closing that is used during this research.

10 Conclusion

This thesis has given insight into the mechanical properties of knitted fabrics, with a particular focus on the Poisson's ratio and Young's modulus in both wale and course direction. This research has demonstrated that the knitting pattern has a significant influence on these properties.

In addition to these findings, this study has shown that non-homogeneous fabrics containing two different knitting patterns can show unexpected behaviour compared to the homogeneous fabrics from which they are composed. This is likely caused by the interaction between the two knitting patterns. However, more research is required to fully explain this effect.

10.1. Application

The determined properties can be used as an input parameter when knitted textiles are modelled. This can both be used while performing a form-finding process and while modelling the influence of concrete pressure on the knitted textile when it is used as a formwork. Besides that, the determined properties can be used to perform a structural analysis on a tensioned knitted membrane under various load combinations.

Furthermore, the results of this thesis can be used when a knitting pattern has to be selected for a certain application. Depending on the purpose of the knitted textile, a choice of the knitting pattern can be made based on the Young's modulus of the fabric.

The results of the tests on the non-homogeneous fabrics have shown that combining different knitting patterns influences the properties of the fabric. The patterns can be combined based on aesthetics as well as on the desired local stiffness of the fabric. For certain applications, it could be desired that the fabric is stiffer in certain locations; this can be achieved by using a different knitting pattern. However, when a combination of knitting patterns is used it has to be kept in mind that this will influence the behaviour of the fabric as a whole. Due to the interaction between the knitting patterns, the properties are not linear related to the properties of the fabrics containing a single knitting pattern.

10.2. Recommendations for future work

Since there is not yet a lot of research performed on the mechanical behaviour of knitted fabrics, multiple recommendations for future work are listed below.

- Exploring the possibilities of using a different type of closing.
  In section 6.2 multiple considerations for a closing are presented, but the final choice is still not optimal.
- Studying the influence of the shape of the secondary knitting pattern when non-homogeneous fabrics are tested.
  In this thesis, only a circular shape of the secondary knitting pattern is considered. Other shapes of the secondary pattern could have a different influence on the properties of the fabrics.
- Studying the interaction between the primary and secondary knitting patterns.
  The results presented in section 8.2 show that the interaction between the primary and secondary

knitting pattern can result in a stiffer fabric than the corresponding homogeneous fabrics. More research has to be performed to conclude whether this effect plays a role in other combinations of knitting patterns.

- Studying the behaviour of knitted fabrics when different materials or combinations of different materials are used during the fabrication process.
  This thesis is only limited to the use of Diolen polyester yarns. Different results are expected when different materials are used or when different materials are combined.
- Making prototypes of membrane structures using the properties found in this research.
  Making prototypes is a useful method to see how the material behaves on a bigger scale than in the material tests.
- Modelling and analysing the behaviour of a knitted membrane and comparing the results to physical models.
  Verifying digital models with physical models is essential to ensure that the results produced by the digital model are correct.

References

Boston University. (2021). *Confidence intervals for sample size less than 30*. Retrieved May 17, 2024, from https://sphweb.bumc.bu.edu/otlt/MPH-Modules/PH717-QuantCore/PH717-Module6-RandomError/PH717-Module6-RandomError11.html

Brnada, S., Šomođi, Ž., & Kovačević, S. (2019). A new method for determination of poisson's ratio of woven fabric at higher stresses. *Journal of Engineered Fibers and Fabrics*, *14*, 1–13. https://doi.org/10.1177/1558925019856225

Carneiro, V. H., & Puga, H. (2018). Temperature variability of poisson's ratio and its influence on the complex modulus determined by dynamic mechanical analysis. *Technologies*, *81*(6). https://doi.org/10.3390/technologies6030081

Cerbu, C., Xu, D., Wang, H., & Roșca, I. C. The use of digital image correlation in determining the mechanical properties of materials [012007]. In: *399*. IOP Conf. Series: Materials Science and Engineering. 012007. 2018.

Chauhan, R., & Ghosh, S. (2023). Knitted fabric production.

Dabiryan, H., & Jeddi, A. A. (2012). Analysis of warp-knitted fabric structure part iv: Modeling the initial poisson's ratio inelastic deformation region. *The Journal of The Textile Institute*, *103*(12), 1352–1360. https://doi.org/10.1080/00405000.2012.685269

Echenagucia, T. M., Pigram, D., Liew, A., Mele, T. V., & Block, P. (2019). A cable-net and fabric formwork system for the construction of concrete shells: Design, fabrication and construction of a full scale prototype. *Structures*, (18), 72–82. https://doi.org/10.1016/j.istruc.2018.10.004

Fletcher, H. M., & Roberts, S. H. (1954). The relationship of the geometry of plain knit cotton fabric to its dimensional change and elastic properties. *Textile Research Journal*, *24*(8), 729–737. https://doi.org/10.1177/004051755402400806

García de Soto, B., Agustí-Juanc, I., Hunheviczd, J., Jossd, S., Graserd, K., Habertc, G., & Adeyc, B. T. (2018). Productivity of digital fabrication in construction: Cost and time analysis of a robotically built wall. *Automation in Construction*, (92), 297–311. https://doi.org/10.1016/j.autcon.2018.04.004

Gercek, H. (2006). Poisson's ratio values for rocks. *International Journal of Rock Mechanics & Mining Sciences*, *44*, 1–13. https://doi.org/10.1016/j.ijrmms.2006.04.011

Gosling, P., Bridgens, B., Albrecht, A., Alpermann, H., Angeleri, A., Barnes, M., Bartle, N., Canobbio, R., Dieringer, F., Gellin, S., Lewis, W., Mageau, N., Mahadevan, R., Marion, J., Marsden, P., Milligan, E., Phang, Y., Sahlin, K., Stimpfle, B., ... Uhlemann, J. (2013). Analysis and design of membrane structures: Results of a round robin exercise. *Engineering Structures*, 313–328. https://doi.org/10.1016/j.engstruct.2012.10.008

Heslop, A. (2010). *Basic theories of tensile fabric architecture*. Retrieved August 8, 2024, from https://www.architen.com/articles/basic-theories-of-tensile-membrane-architecture/

IQSdirectory. (n.d.). Retrieved March 4, 2024, from https://www.iqsdirectory.com/articles/load-cell/strain-gauge.html

ISO 4921:2000. (2000). *Knitting - basic concepts - vocabulary* (tech. rep.). International Organization for Standardization.

ISO 8388:1998. (1998). *Knitted fabrics - types - vocabulary* (tech. rep.). International Organization for Standardization.

Jadhav, A. A., Vaskar, T., & Pillai, P. V. (Eds.). (2023). *Biaxial tensile tests to study mechanical behaviour of thin soft materials.*

Jinyun, Z., Yi, L., Lam, J., & Xuyong, C. (2010). The poisson ratio and modulus of elastic knitted fabrics. *Textile Research Journal*, *80*(18). https://doi.org/10.1177/0040517510371864

Kariouh, A. (2023). *Flexibly formed concrete* [Master's thesis, TU Delft].

Lloyd, D. W., & Hearle, J. W. S. (1977). An examination of a 'wide-jaw' test for the determination of fabric poisson ratios. *Journal of the Textile Institute*, (9).

LSAA. (2010). *Membrane structures.* Retrieved August 15, 2024, from https://lsaa.org/images/pdf_files/Forms_Brochures/Marketing_booklet_2010.pdf

Mizutani, M., & Ando, K. (2015). Influence of a wide range of moisture contents on the poisson's ratio of wood. *Journal of Wood Science*, 81–85. https://doi.org/10.1007/s10086-014-1438-7

OKorder. (n.d.). *What is the weight of steel formwork?* Retrieved January 18, 2024, from https://ask.okorder.com/questions/what-is-the-weight-of-steel-formwork_1246072.html

Osman, N., & Mohamed, R. (2020). Negative poisson's ratio based on weft knitted fabric with different loop length. *International Journal of Engineering and Information Systems*, *4*, 21–26.

Popescu, M. (2019). *Knitcrete - stay-in-place knitted formworks for complex concrete structures* [Doctoral dissertation, ETH Zurich].

Popescu, M., Rippmann, M., Liew, A., Reiter, L., Flatt, R. J., van Mele, T., & Block, P. (2021). Structural design, digital fabrication and construction of the cable-net and knitted formwork of the knitcandela concrete shell. *Structures*, (31), 1287–1299. https://doi.org/10.1016/j.istruc.2020.02.013

Poplavko, Y. M. (2019). Mechanical properties of solids.

Studio Light and Shade. (2018). https://www.istockphoto.com/nl/foto/wit-en-blauw-winter-gebreide-achtergrond-gm936335546-256131755?phrase=knitted+fabric&searchscope=image%2Cfilm

Tiwari, S. K., Fei, P. T. C., & McLaren, J. D. A pilot study: Evaluating the influence of knitting patterns and densities on fabric properties for sports applications. In: In *Procedia engineering. 60.* 2013, 373–377.

Weeger, O., Sakhaei, A. H., Tan, Y. Y., Quek, Y. H., Lee, T. L., Yeung, S.-K., Kaijima, S., & Dunn, M. L. (2018). Nonlinear multi-scale modelling, simulation and validation of 3d knitted textiles. *Applied composite materials*, *25*, 797–810. https://doi.org/10.1007/s10443-018-9702-4

Wilson, J. (2001). Handbook of textile design. Woodhead Publishing Limited.

Yu, L., & Pan, B. (2014). In-plane displacement and strain measurements using a camera phone and digital image correlation. *Optical Engineering*, *53*(5). https://doi.org/10.1117/1.OE.53.5.054107

Zhang, P. (2010). Advanced industrial control technology.

Zhu, D., Mobasher, B., & Rajan, S. D. (2011). Dynamic tensile testing of kevlar 49 fabrics. *Journal of Materials in Civil Engineering*, *23*, 230–239. https://doi.org/10.1061/(ASCE)MT.1943-5533.0000156

A

Arduino code to control motors

This appendix shows the Arduino code used by the Teensy to be able to control the motors.

```
#include "Arduino.h"
#include <AccelStepper.h>
#include <Encoder.h>

AccelStepper Axis1(1, 2, 1);     // axis 1; pin 2 = step, pin 1 = direction
Encoder Enc1(21, 22);            // encoder 1
AccelStepper Axis2(1, 8, 7);     // axis 2
Encoder Enc2(3, 4);              // encoder 2
AccelStepper Axis3(1, 14, 13);   // axis 3
Encoder Enc3(9, 10);             // encoder 3
AccelStepper Axis4(1, 20, 19);   // axis 4
Encoder Enc4(15, 16);            // encoder 4

#define MM 25
#define PPR 1000
#define MAXTRAVEL 200.0

bool isReferenced = false;
bool hasOvertravelled = false;

int mode = 0;

enum modes {
  POSITION_MODE = 1
};

float encoderPosition() {
  return -Enc1.read() / PPR;
}

void setup() {

  Serial.begin(115200);

  Axis1.setMaxSpeed(1000);
  Axis1.setAcceleration(10000);
  Axis1.setPinsInverted(true, false, true);

  Axis2.setMaxSpeed(1000);
  Axis2.setAcceleration(10000);
  Axis2.setPinsInverted(true, false, true);

  Axis3.setMaxSpeed(1000);
  Axis3.setAcceleration(10000);
  Axis3.setPinsInverted(true, false, true);

  Axis4.setMaxSpeed(1000);
  Axis4.setAcceleration(10000);
  Axis4.setPinsInverted(true, false, true);
```

```

  Serial.println("StepperControl");
  Serial.println("Send '?' for help\n");
}

void loop() {
  char buf[20];
  int writePos = 0;
  while (Serial.available() > 0) {

    char c = Serial.read();
    if (c == '\n' || c == '\r') {
      writePos = 0;
      Serial.print('\n');

      char* p = &buf[1];
      float d = atof(p);

      switch (buf[0]) {
        case '?':
          Serial.print("i,j,k,l[pos]\t- incremental move (ex. i20 for positive 20mm move, i-20 for negative move)\n");
          Serial.print("a[pos]\t- absolute move\n");
          Serial.print("p\t- get the current position\n");
          Serial.print("e\t- get the current encoder position\n");
          Serial.print("z\t- set the encoder position to zero\n");
          Serial.print("u[pos]\t- incremental move of axis 1 and 3\n");
          Serial.print("b[pos]\t- incremental move of all axis");
          break;
        case 'a':
          mode = POSITION_MODE;

          if (isReferenced) {
            if (d <= MAXTRAVEL && d >= 0.0) {

              float curPos = encoderPosition();
              float dx = d - curPos;

              Axis1.move(dx * MM);
              Serial.print("Moving to ");
              Serial.print(d);
              Serial.println(" mm");
            } else {
              Serial.println("ERROR: This move is invalid (negative absolute position or exceeds MAXTRAVEL)");
            }
          } else {
            Serial.println("ERROR: Axis is not homed");
          }
          break;

        case 'e':
          Serial.println("Current encoder position: ");
          Serial.print(encoderPosition());
          Serial.println(" mm");
          break;

// control axis 1
        case 'i':
          mode = POSITION_MODE;

          if (d <= MAXTRAVEL) {
            {
              Axis1.move(d * MM);
              Serial.print("Moving axis 1 by ");
              Serial.print(d);
              Serial.println(" mm");
            }
          } else {
            Serial.println("ERROR: This move exceeds MAXTRAVEL");
          }
```

```
          break;

// control axis 2
        case 'j':
          mode = POSITION_MODE;

          if (d <= MAXTRAVEL) {
            {
              Axis2.move(d * MM);
              Serial.print("Moving axis 2 by ");
              Serial.print(d);
              Serial.println(" mm");
            }
          } else {
            Serial.println("ERROR: This move exceeds MAXTRAVEL");
          }
          break;

// control axis 3
        case 'k':
          mode = POSITION_MODE;

          if (d <= MAXTRAVEL) {
            {
              Axis3.move(d * MM);
              Serial.print("Moving axis 3 by ");
              Serial.print(d);
              Serial.println(" mm");
            }
          } else {
            Serial.println("ERROR: This move exceeds MAXTRAVEL");
          }
          break;

// control axis 4
        case 'l':
          mode = POSITION_MODE;

          if (d <= MAXTRAVEL) {
            {
              Axis4.move(d * MM);
              Serial.print("Moving axis 4 by ");
              Serial.print(d);
              Serial.println(" mm");
            }
          } else {
            Serial.println("ERROR: This move exceeds MAXTRAVEL");
          }
          break;

// control axis 1 and 3 simultaneously for uniaxial test
        case 'u':
          mode = POSITION_MODE;

          if (d <= MAXTRAVEL) {
            {
              Axis1.move(d * MM);
              Axis3.move(d * MM);
              Serial.print("Moving by ");
              Serial.print(d);
              Serial.println(" mm");
            }
          } else {
            Serial.println("ERROR: This move exceeds MAXTRAVEL");
          }
          break;

// control all axis simultaneously for biaxial test
        case 'b':
          mode = POSITION_MODE;

```

```
          if (d <= MAXTRAVEL) {
            {
              Axis1.move(d * MM);
              Axis2.move(d * MM);
              Axis3.move(d * MM);
              Axis4.move(d * MM);
              Serial.print("Moving by ");
              Serial.print(d);
              Serial.println(" mm");
            }
          } else {
            Serial.println("ERROR: This move exceeds MAXTRAVEL");
          }
          break;

        case 'p':
          Serial.print("Current position: ");
          Serial.print(Axis1.currentPosition() / MM);
          Serial.println(" mm");
          break;

        case 'z':
          Serial.println("Setting encoder position to zero");
          Enc1.write(0);
          isReferenced = true;
          break;

        default:
          Serial.println("ERROR:\tUndefined command");
          break;
      }
    } else {
      buf[writePos] = c;
      writePos++;
      Serial.print(c);
    }
  }

  switch (mode) {
    case POSITION_MODE:

      Axis1.run();
      Axis2.run();
      Axis3.run();
      Axis4.run();
      break;
  }
}
```

B

Python code to control test setup

This appendix shows the Python code that is used to control the test setup.

```python
import logging
import os
import time
from datetime import datetime
from loadcell_to_force import *
from serial import Serial
from colorama import Fore


STEP = 5
AXIS_LENGTH = 140

PORT_T = "COM5"
BAUDRATE_T = 115200
PORT_DA = "COM6"
BAUDRATE_DA = 57600

HERE = os.path.dirname(__file__)
DTSTRING_FORMAT = "%Y%m%d"

def make_folder_if_not_exists(folder_path: str) -> str:
    if not os.path.exists(folder_path):
        os.makedirs(folder_path)
    return folder_path

def get_dt_string() -> str:
    return datetime.now().strftime(DTSTRING_FORMAT)

def open_serial_connection(port: str, baudrate: int) -> Serial:
    try:
        return Serial(port, baudrate, timeout=1)
    except Exception as e:
        print(f"Error␣opening␣serial␣port:␣{e}")
        return None

def send_command(ser: Serial, command: str) -> None:
    ser.write(command.encode())
    time.sleep(0.2)

def read_response(ser: Serial) -> str:
    time.sleep(0.5)
    response = ser.read(ser.in_waiting)
    return response.decode()

def loads_array_to_text(array_of_loads):
    for i, load in enumerate(array_of_loads):
        print(f"Load␣cell␣{i+1}:␣{load:.3f}␣[N]")

def main():
```

```
    ser_teensy = open_serial_connection(PORT_T, BAUDRATE_T)
    ser_da = open_serial_connection(PORT_DA, BAUDRATE_DA)
    if not (ser_teensy and ser_da):
        return

    # Homing loop
    print("Home␣the␣axis")
    while True:
        print(read_response(ser_teensy))
        command = input("Enter␣command␣(Send␣'?'␣for␣help␣|␣'exit'␣to␣quit):␣")
        if command == "exit":
            break
        if command[0] != "u":
            print("Inaccessible␣commands␣during␣homing,␣try␣incremental␣uniaxial␣move␣command")
        else:
            send_command(ser_teensy, command + "\n")

    # zeroing all load cells and encoders
    z_list = ["z0", "z1", "z2", "z3"]
    for z in z_list:
        send_command(ser_teensy, f"{z}\n")
        send_command(ser_teensy, "e\n")
        send_command(ser_da, f"{z}\n")
    print("load␣cells␣and␣encoders␣are␣set␣to␣zero")

    # Loop
    x = 0
    iterations = 1
    test_nr = 1
    pattern_name = input('Enter␣pattern␣name:␣')
    channel_location = input('Enter␣channel␣position␣(top_bottom␣or␣sides):')

    file_path = os.path.join(HERE, 'load_data', channel_location, f"{pattern_name}_{get_dt_string()}_{test_nr}_data.csv")
    while os.path.exists(file_path):
        test_nr +=1
        print('\n', Fore.RED + f'The␣load␣file␣already␣exists!␣Test_nr␣is␣changed␣to␣{test_nr}\n')
        file_path = os.path.join(HERE, 'load_data', channel_location, f"{pattern_name}_{get_dt_string()}_{test_nr}_data.csv")
    else:
        print('\n', Fore.GREEN + 'The␣file␣does␣not␣exist.␣Continue␣with␣test␣\n')
        print(Fore.RED + "Don't␣forget␣to␣place␣measurement␣tape")
        with open(file_path, "a") as datafile:
            while x < AXIS_LENGTH:
                cont = input('continue?␣(y␣or␣no):')
                if cont == 'y':
                    print(f'iteration␣{iterations}')
                    send_command(ser_teensy, f"u{STEP}.00\n")
                    send_command(ser_teensy, "e\n")
                    response_t = read_response(ser_teensy)
                    send_command(ser_da, "l")
                    if iterations == 1:
                        response_da = read_response(ser_da)[52:-2]
                    else:
                        response_da = read_response(ser_da)[:-2]
                    numbers = response_da.split(';')
                    floats = np.asarray(numbers, dtype=float)
                    loads = loadcell_to_force(floats)
                    loads_array_to_text(loads)
                    for load in loads:
                        if load > 150:
                            print(Fore.RED + 'Loads␣are␣too␣large.␣Interupt␣test')

                    # write loads to logfile
                    if x == 0:
                        logline = f"encoder,␣load␣cell␣1,␣load␣cell␣2,␣load␣cell␣3,␣load␣cell␣4␣\n"
                        datafile.write(logline)
                    pos = response_t.split("\n")[-2].split("␣mm")[0]
```

```
                    logline = f"{pos}, {loads[0]}, {loads[1]}, {loads[2]}, {loads[3]}\n"
                    datafile.write(logline)

                    time.sleep(1.0)

                    x += STEP
                    print(f'displacement = {x}\n')
                    iterations += 1
                else:
                    break

    print(Fore.BLACK + 'finished')

    ser_teensy.close()
    ser_da.close()

if __name__ == "__main__":
    main()
```

The code below is used to convert the loadcell output to a force. To do this, the loadcells have to be calibrated. This is done by recording the response of the four loadcells when a known force is applied. For each loadcell, three of these measurements have been done which results in enough data points to fit a linear relationship.

```
import numpy as np

def loadcell_to_force(loadcell_data, g=9.81):
    """Input loadcell_output as array of four values (the output values of the loadcells)

    Output:
    Force values measured by the four load cells in Newton (with g = 9.81)"""

    if len(loadcell_data) != 4:
        raise Exception('Input should contain four values')

    else:
        load = [2.090, 4.095, 8.105]
        sensor1 = [90.4, 176.8, 349.3]
        sensor2 = [87.5, 171.6, 339.9]
        sensor3 = [92.5, 181.1, 357.8]
        sensor4 = [90.1, 176.4, 349.8]
        sensor_data = [sensor1, sensor2, sensor3, sensor4]

        coefficients = []

        for count, data in enumerate(sensor_data):
            a, b = np.polyfit(load, data, 1)
            coefficients.append([a, b])

        N_list = []
        for i, coef in enumerate(coefficients):
            a = coef[0]
            b = coef[1]
            kg = (loadcell_data[i] - b) / a
            N = kg * g

            N_list.append(N)

    return N_list
```

C

Zeiss correlate software

This appendix explains how the pictures taken during the tensile tests can be used to determine the displacement of the buttons.

Define scale

When the images are imported into the software, first the correct scale of the pictures has to be defined. This has to be done because the software is able to determine the displacement of points in pixels. The amount of pixels can be converted into a distance with the right scale. For the determination of the scale, the measurement tape is needed. Figure C.1 shows that two points on the measurement tape are used, and the software automatically calculates the distance between the points in pixels.

The points which are used to define the scale are ideally not placed close to each other. This is the case to minimise the error when clicking on the points.

Figure C.1: Scale definition

Define point components

To let the software identify the stickers that are placed on the buttons, the minimum radius of the points has to be defined. The stickers that are used on the buttons have a radius of 0.8 mm. To make sure the software recognises the stickers, the minimum radius is set a bit smaller, see Figure C.2.

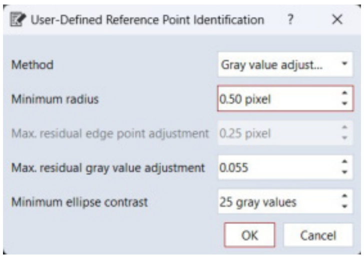

Figure C.2: Settings for radius of points

The points are recognised based on the contrast of the point itself compared to their surrounding area. As can be seen in Figure C.3 many more points are recognised than only the stickers that are placed on the buttons. This is caused by shadows that are visible in the images. The black tape is placed on top of the clamps to minimise the amount of shadows and thus the amount of points that gets recognised.

Not all points shown in Figure C.3 are tracked by the software. To determine which points are tracked, the points have to be selected. For every fabric, this is done in the configuration shown in Figure C.4.

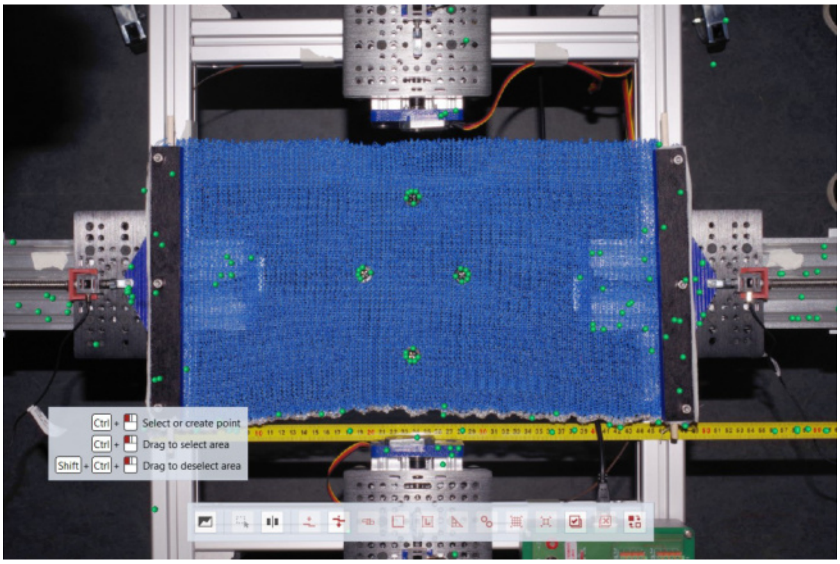

Figure C.3: Define point component

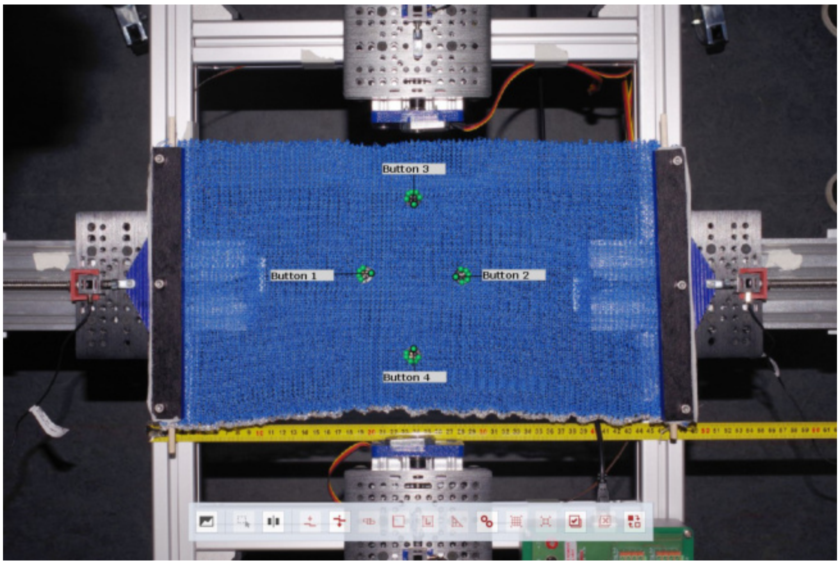

Figure C.4: Location of buttons

Displacements

When the software has recognised the buttons, the displacement can be shown with vectors. Since buttons 1 and 3 mainly move horizontally and buttons 2 and 4 vertically, it is chosen to track only the x- and y-displacement respectively. This is also shown in Figure C.5.

Because the software determines the location of the buttons based on contrast, the buttons are not recognised correctly in every frame. This can be caused by the reflection of light on the buttons. Figure C.6 shows for example that button 1 is not recognised in this image. Button 4 on the contrary is recognised, but not at the right location. This will result in a large peak in the displacement diagram.

Figure C.7 shows the displacement diagram as shown by the Zeiss Correlate software. This diagram shows that some buttons are not recognised in every image. This results in missing data points and therefore the graph is not continuous. The diagram should be interpolated to account for the missing data points.

Besides that, the diagram shows sudden jumps in the displacement of certain points. At these points, the buttons are recognised at a different location than where they are supposed to be recognised. These outliers should be removed before the data is used for post-processing purposes.

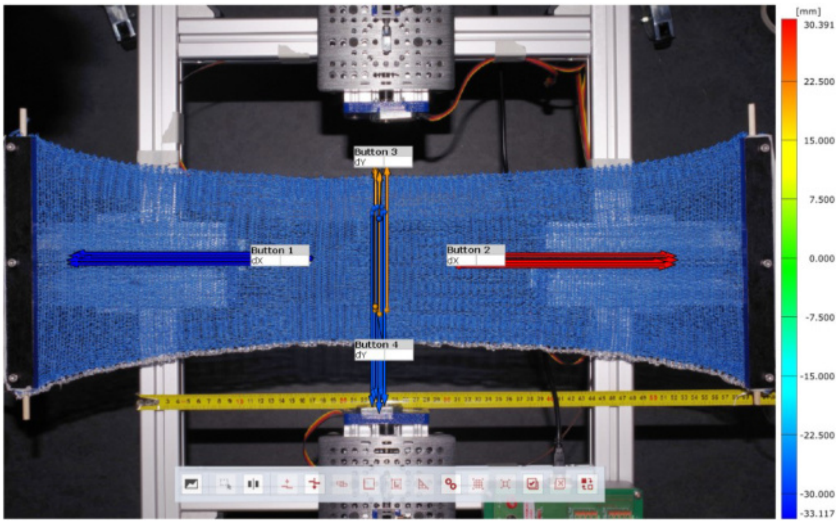

Figure C.5: Button displacement

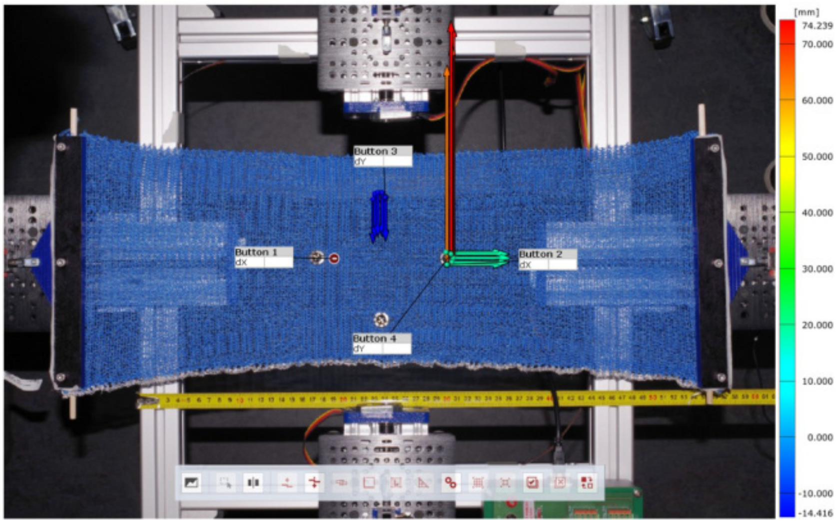

Figure C.6: Displacement irregularities

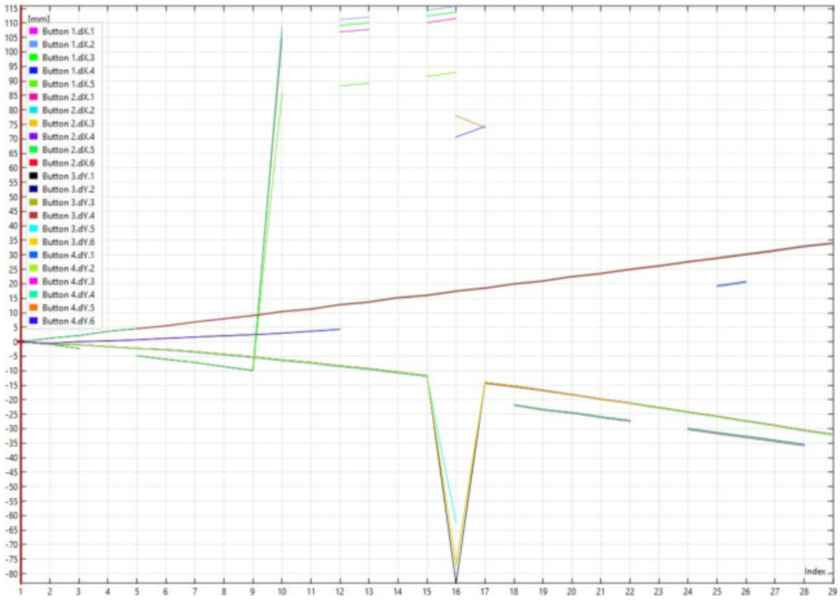

Figure C.7: Displacement diagram

D

Displacement diagrams

D.1. Homogeneous fabrics

	Wale direction		Course direction	
Pattern name	Distance button 1-2 [mm]	Distance button 3-4 [mm]	Distance button 1-2 [mm]	Distance button 3-4 [mm]
interlock1	386.4	176.6	71.60	160.3
interlock2	84.10	171.0	72.80	124.3
interlock3	90.00	173.1	73.20	111.7
eightlock1	390.0	177.5	80.70	119.7
eightlock2	81.13	180.9	81.28	133.0
eightlock3	71.81	176.7	81.00	135.5
hexagon1	71.44	208.8	-	-
hexagon2	71.73	205.2	-	-
hexagon3	92.07	210.2	-	-
tuck1	394.5	202.3	83.02	77.90
tuck2	85.31	192.4	82.00	70.02
tuck3	86.00	199.3	79.80	79.62
interlock_1float1	393.8	110.0	75.36	202.8
interlock_1float2	69.54	98.21	86.91	140.1
interlock_1float3	77.73	103.7	77.80	138.7
interlock_2float1	396.2	71.63	-	-
interlock_2float2	72.63	62.30	-	-
interlock_2float3	82.51	63.41	-	-

Table D.1: Distances

Wale direction

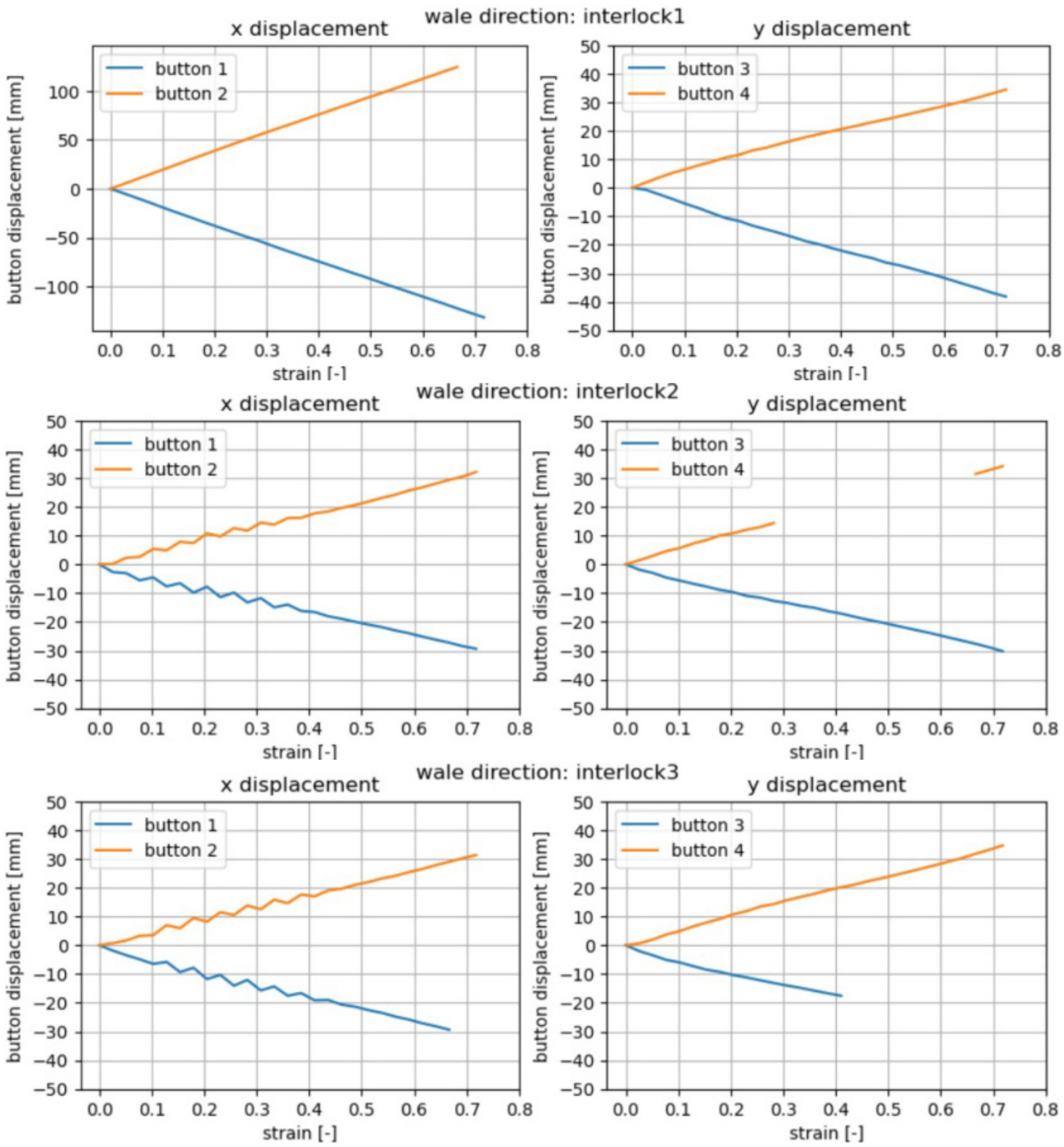

Figure D.1: Interlock (note: diagrams interlock1 are different scale)

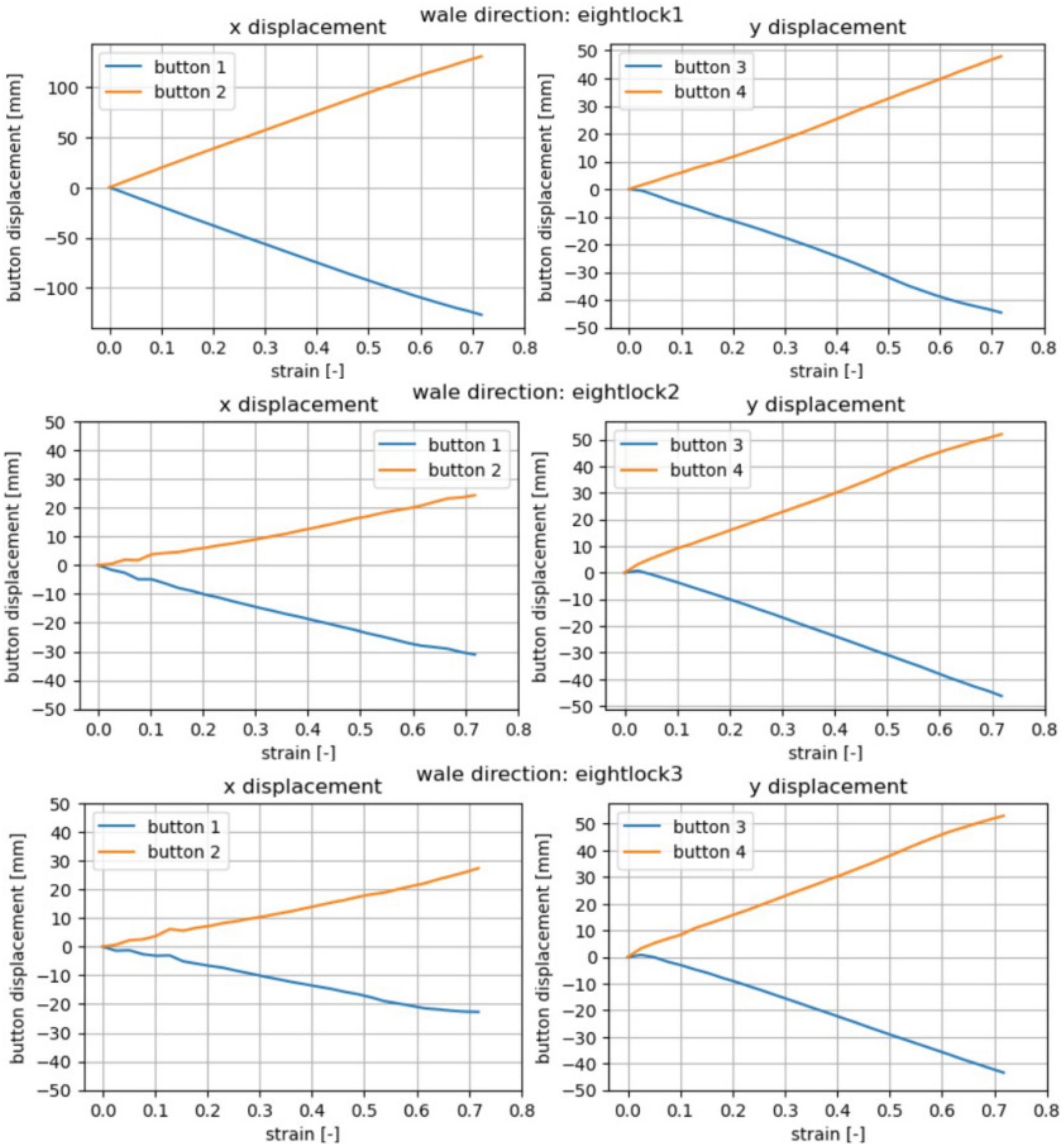

Figure D.2: Eightlock (note: diagrams eightlock1 are different scale)

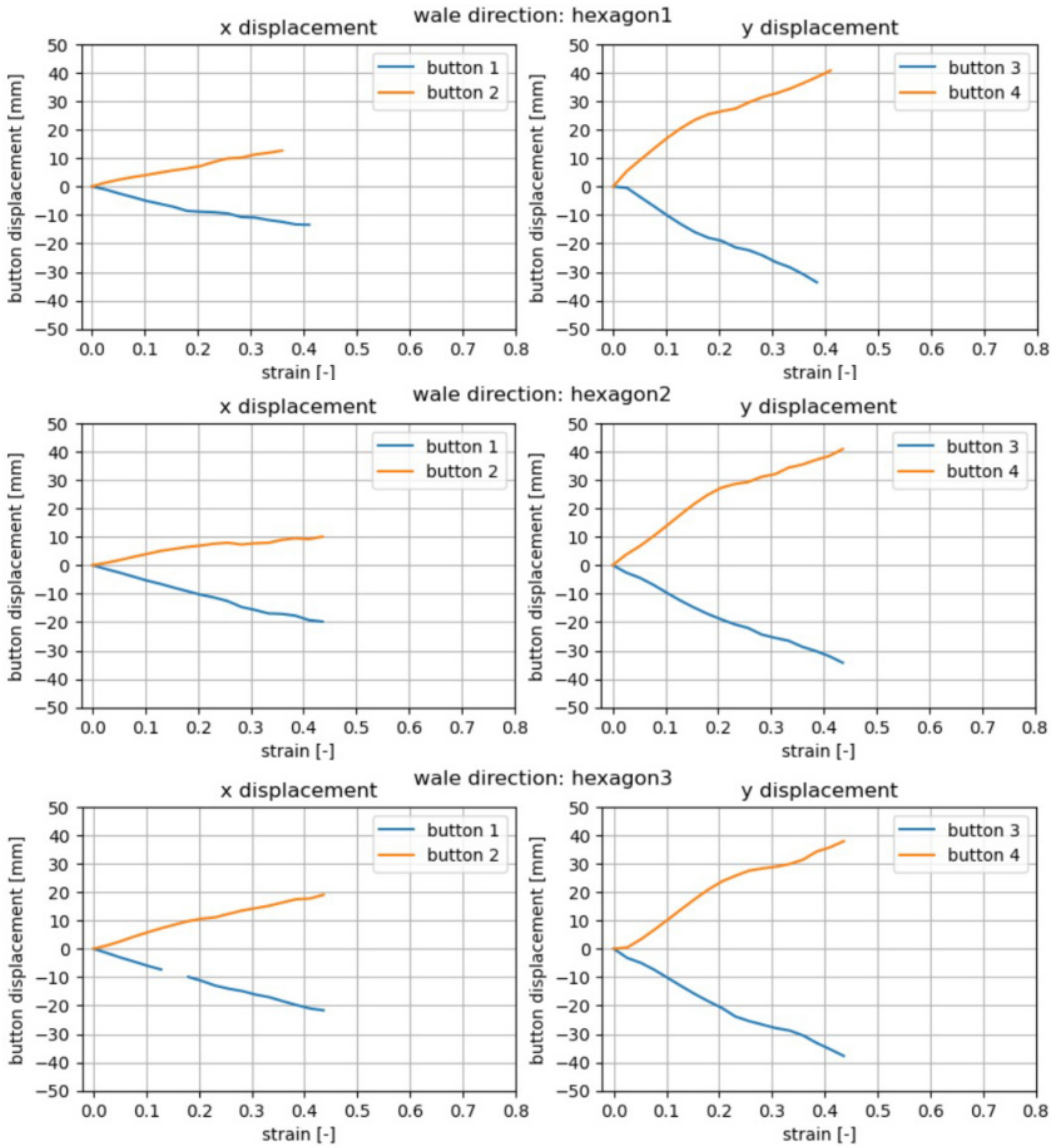

Figure D.3: Hexagon

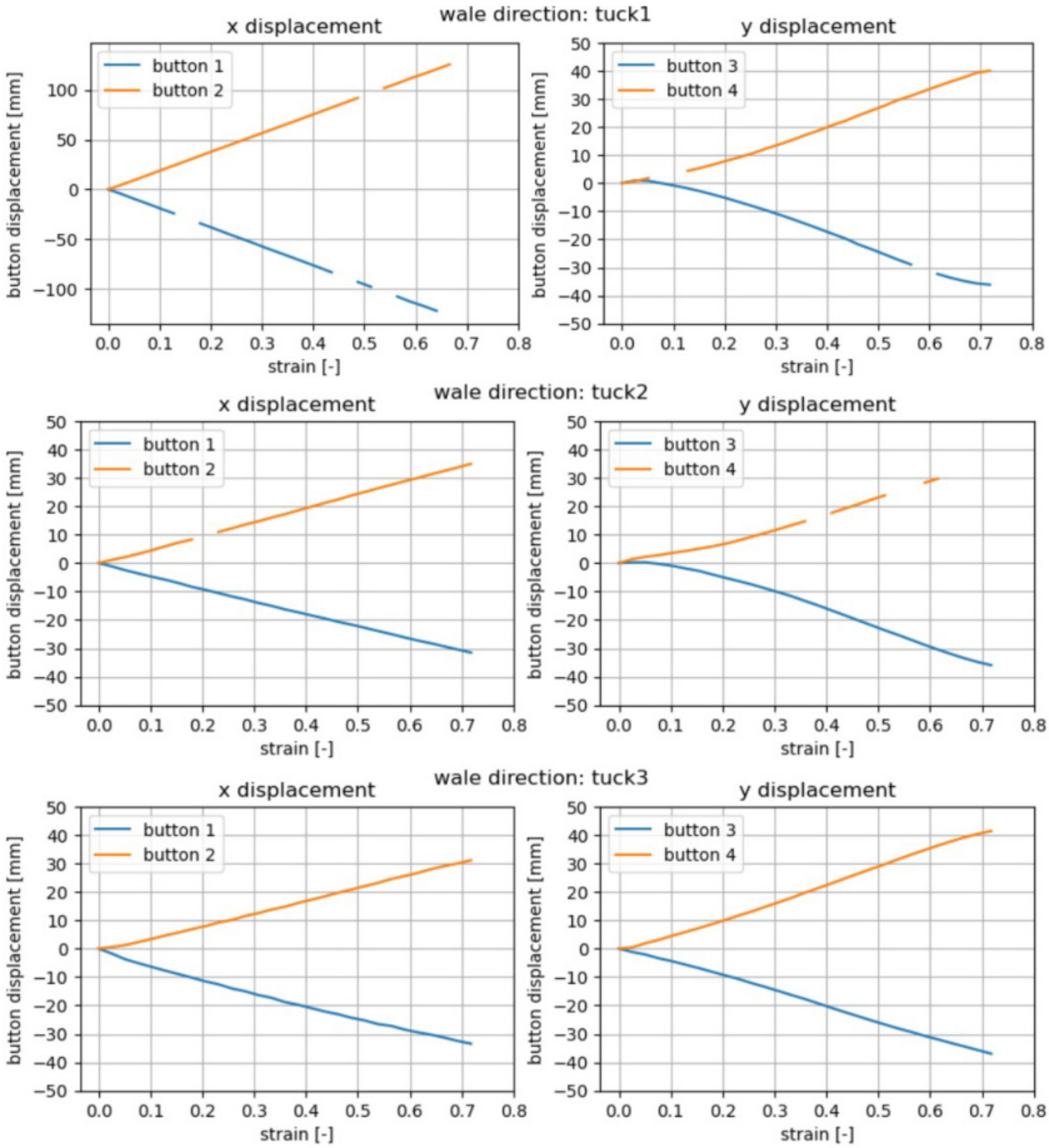

Figure D.4: Tuck (note: diagrams tuck1 are different scale)

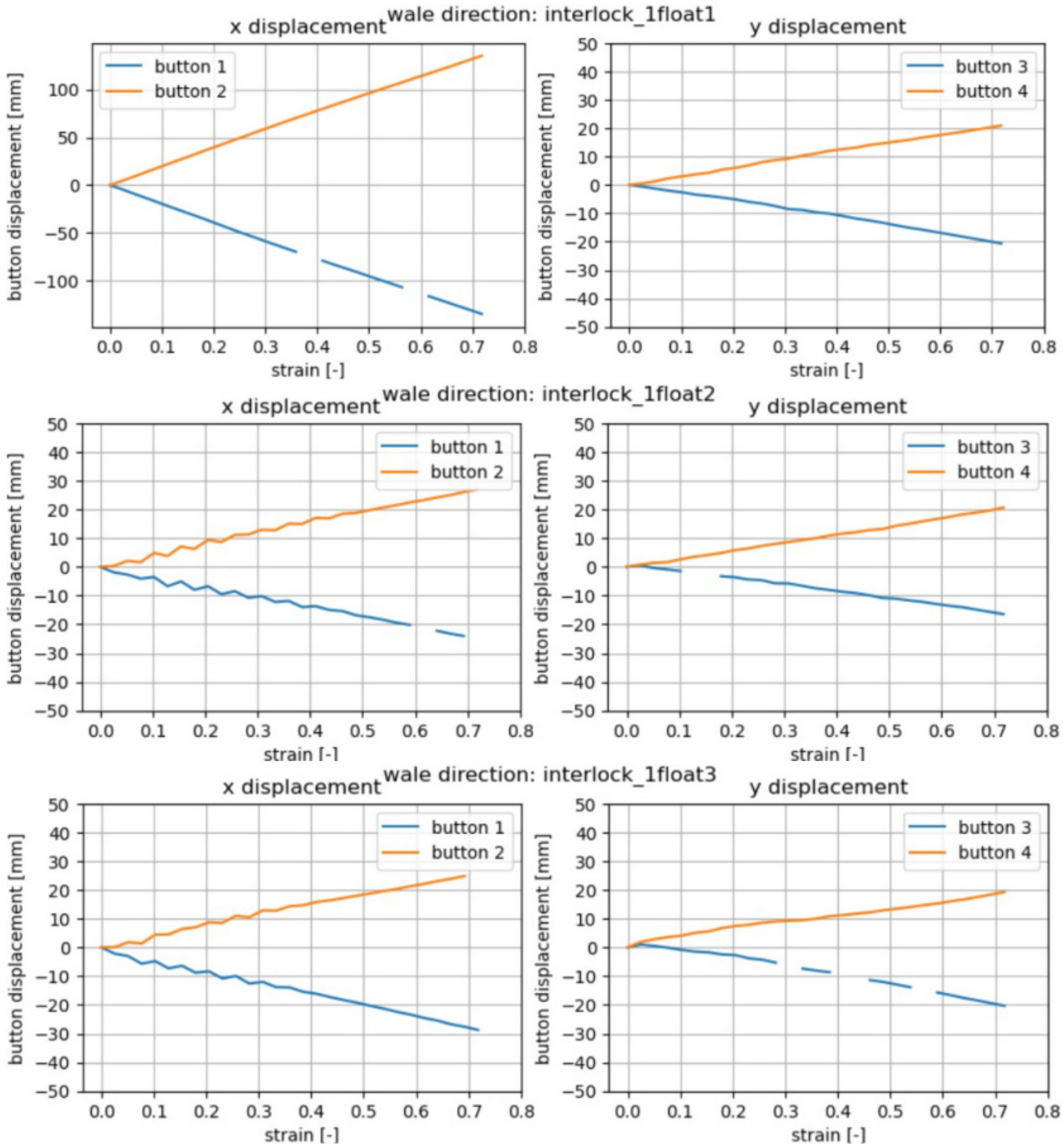

Figure D.5: Interlock_1float (note: diagrams interlock_1float1 are different scale)

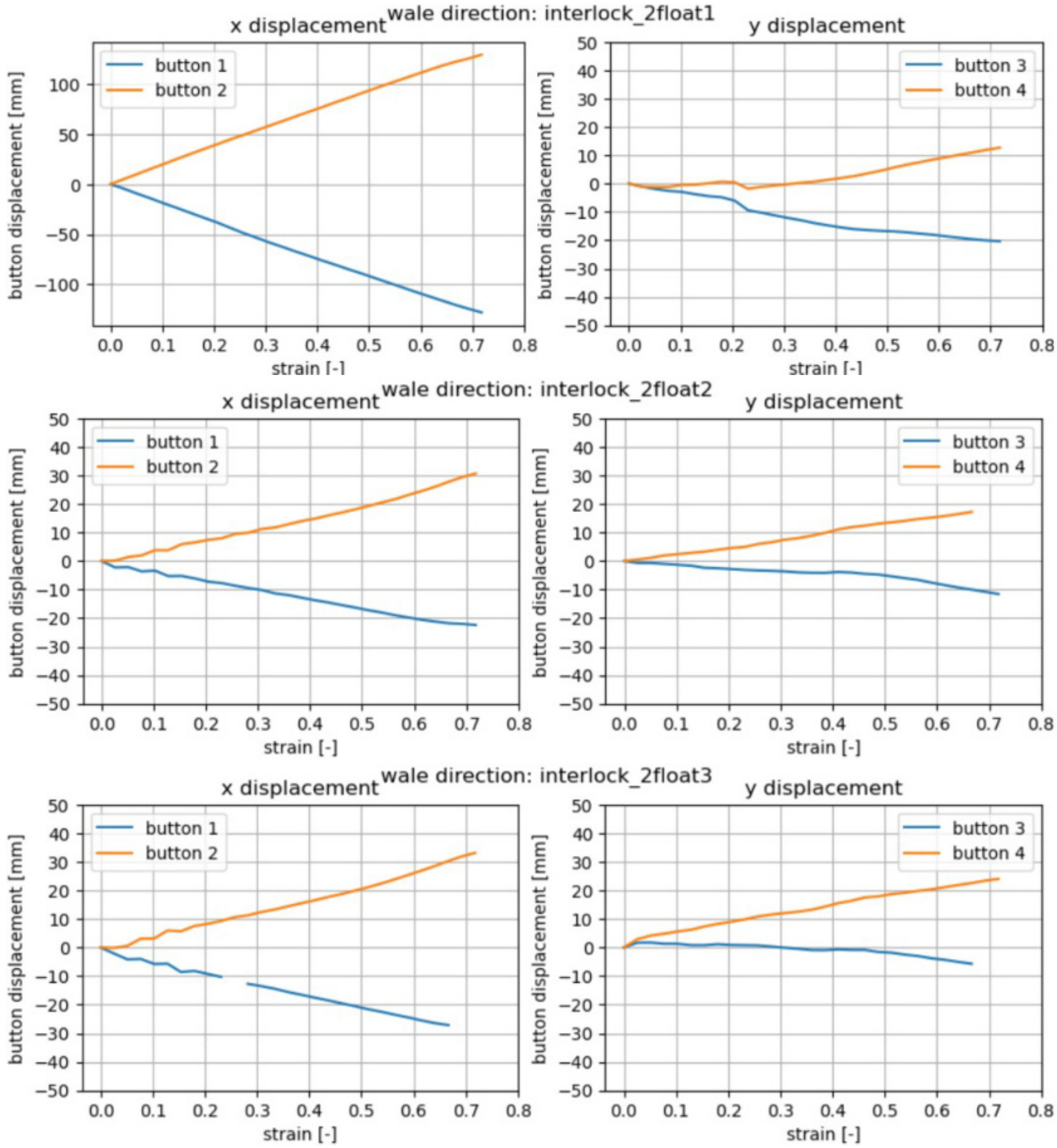

Figure D.6: Interlock_2float (note: diagrams interlock_2float1 are different scale)

Course direction

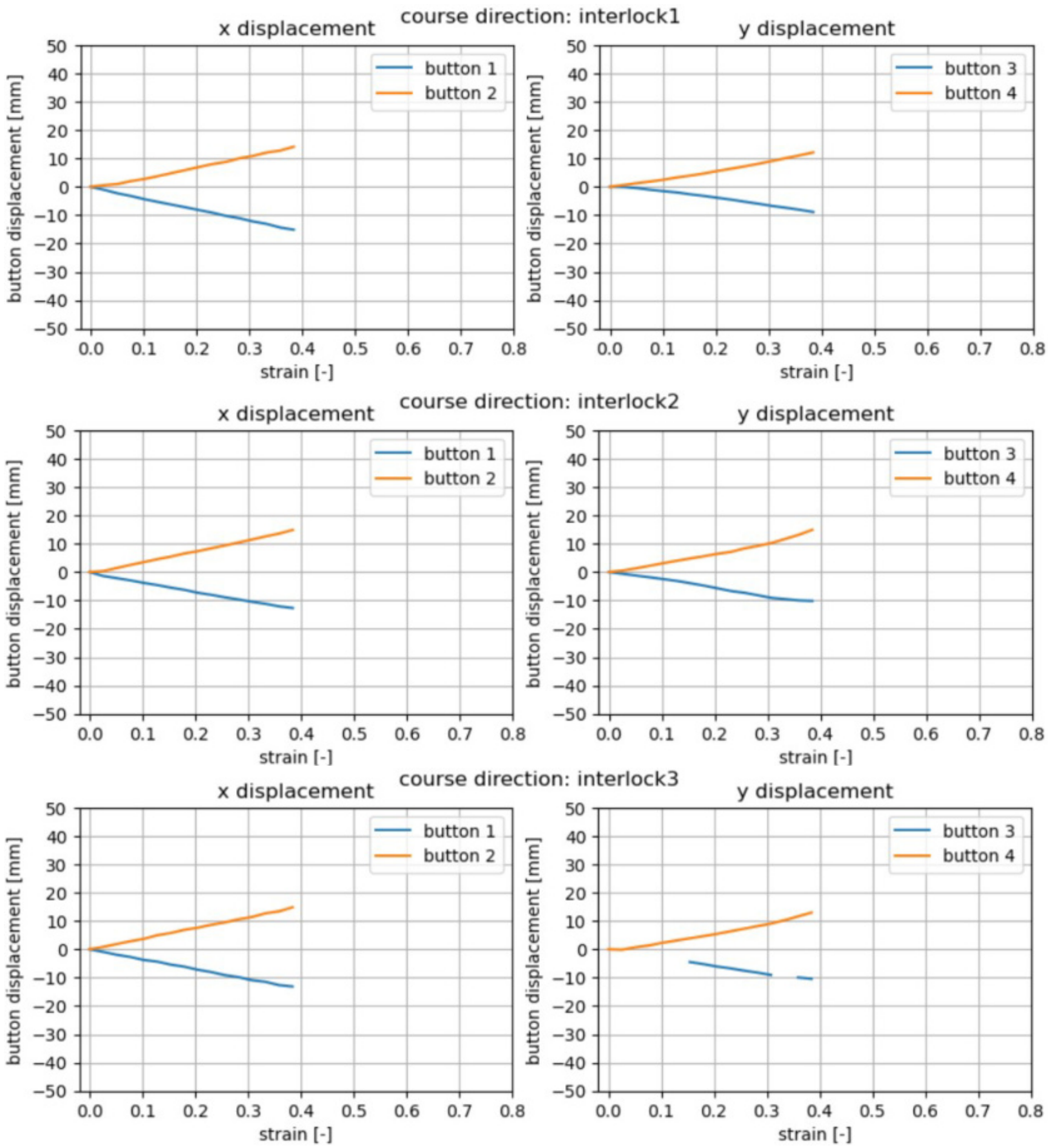

Figure D.7: Interlock

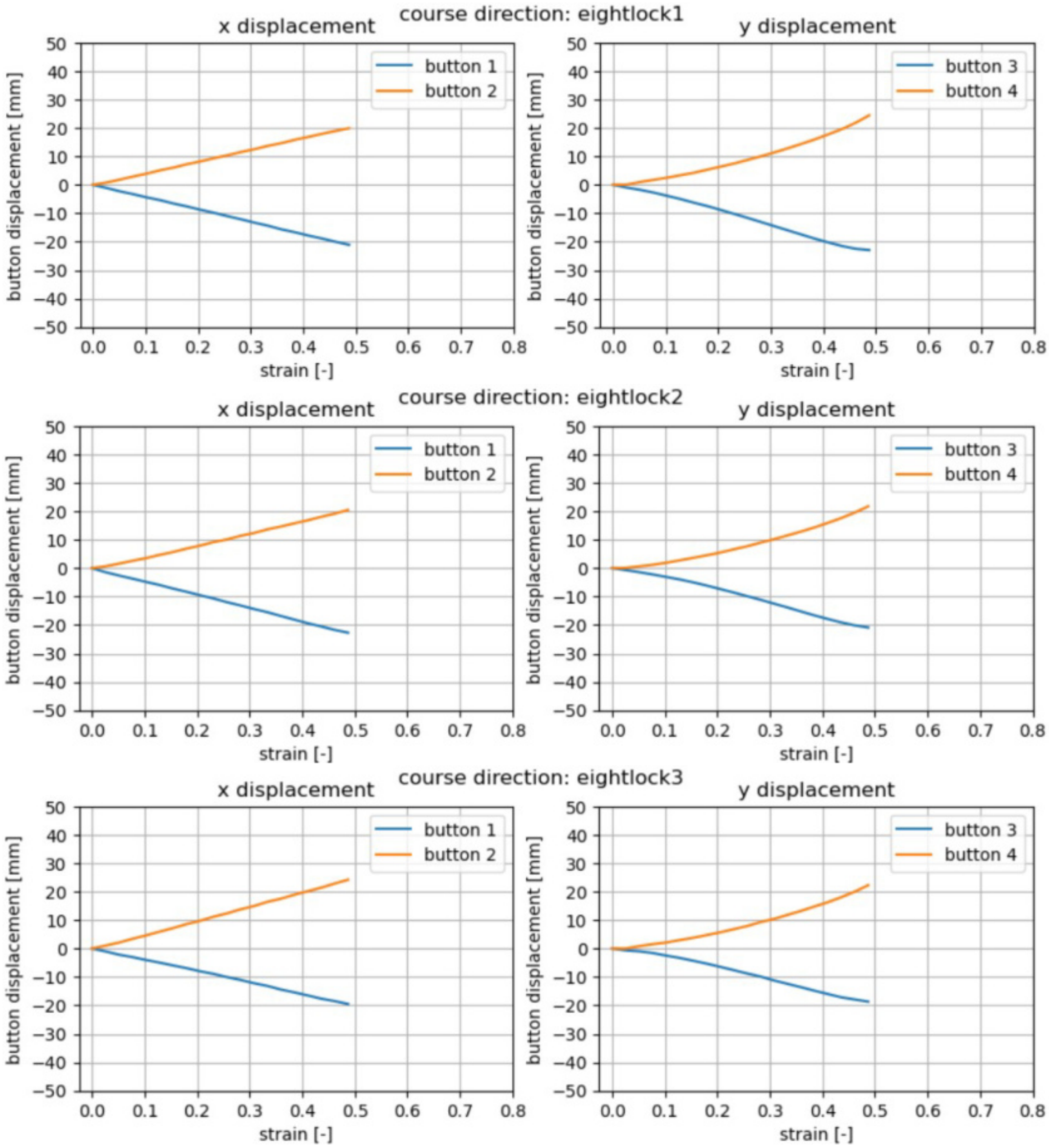

Figure D.8: Eightlock

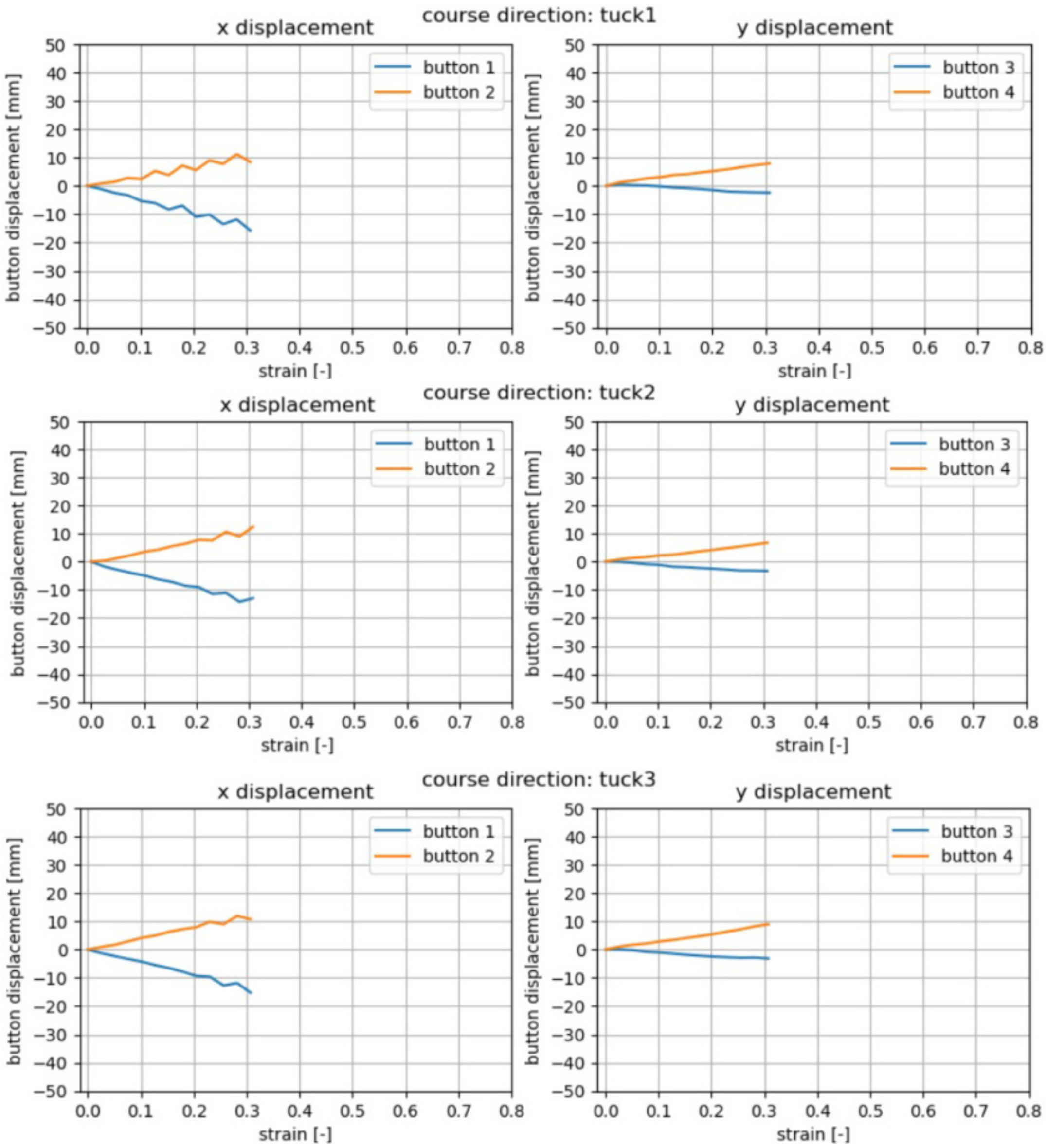

Figure D.9: Tuck

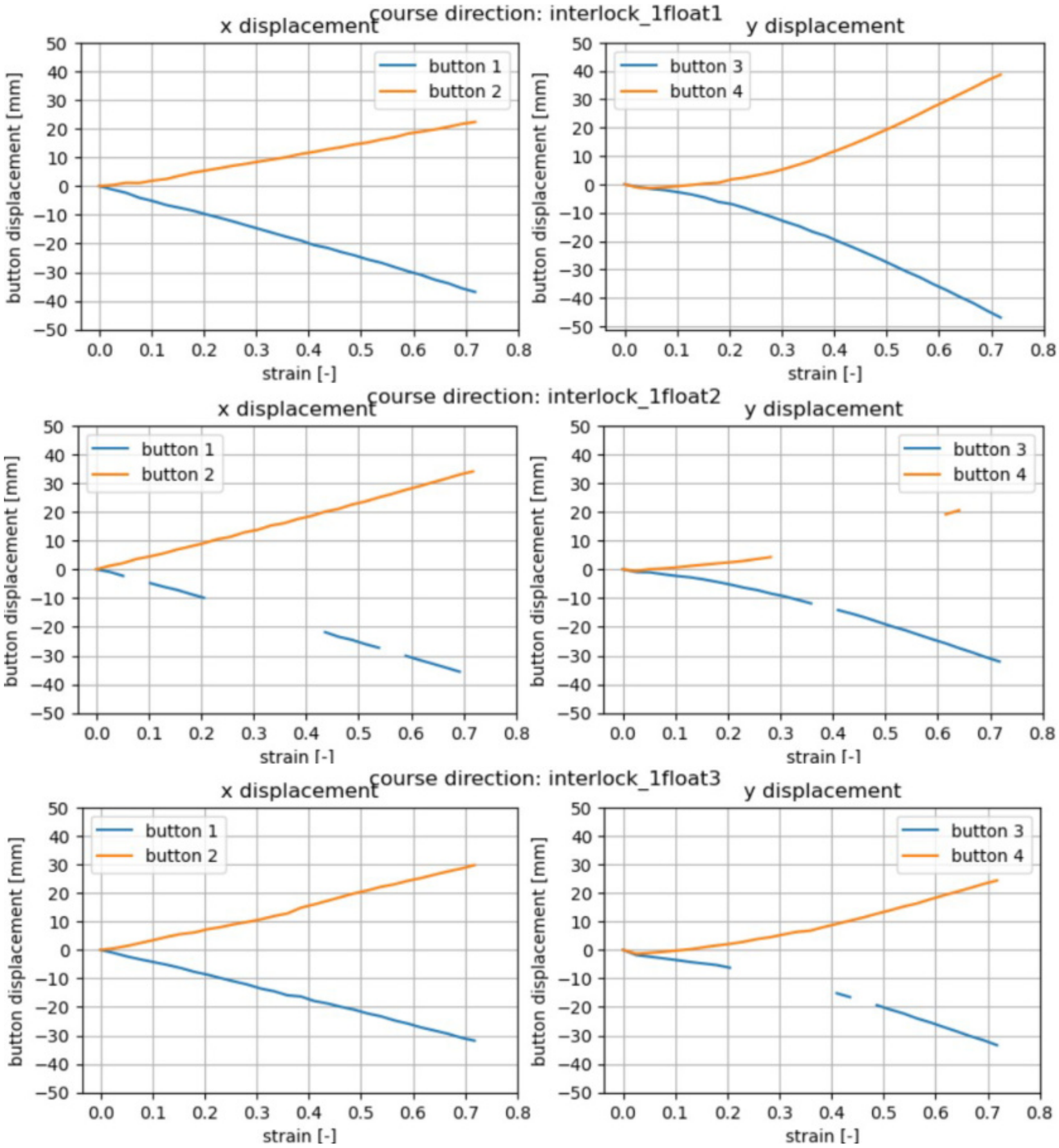

Figure D.10: Interlock_1float

D.2. Non-homogeneous fabrics

	Wale direction		Course direction	
Pattern name	Distance button 1-2 [mm]	Distance button 3-4 [mm]	Distance button 1-2 [mm]	Distance button 3-4 [mm]
ilock_tuck_d25_1	61.71	81.6	110.9	36
ilock_tuck_d50_1	109.9	138.5	213	73.7
ilock_tuck_d75_1	159.7	160.7	306.6	97.8
ilock_8lock_d25_1	69.2	58.89	92.31	47.7
ilock_8lock_d25_2	66.3	58.27	86	50.31
ilock_8lock_d25_3	64.32	57.84	85.21	48.51
ilock_8lock_d50_1	126.9	133.4	184.1	90.94
ilock_8lock_d50_2	123.9	124.1	180	86.03
ilock_8lock_d50_3	112	125.2	179.2	89.71
ilock_8lock_d75_1	178.6	178.6	280.1	136.6
ilock_8lock_d75_2	176	175.7	278.5	133.3
ilock_8lock_d75_3	181.1	173.8	281.4	132.4

Table D.2: Distances

Wale direction

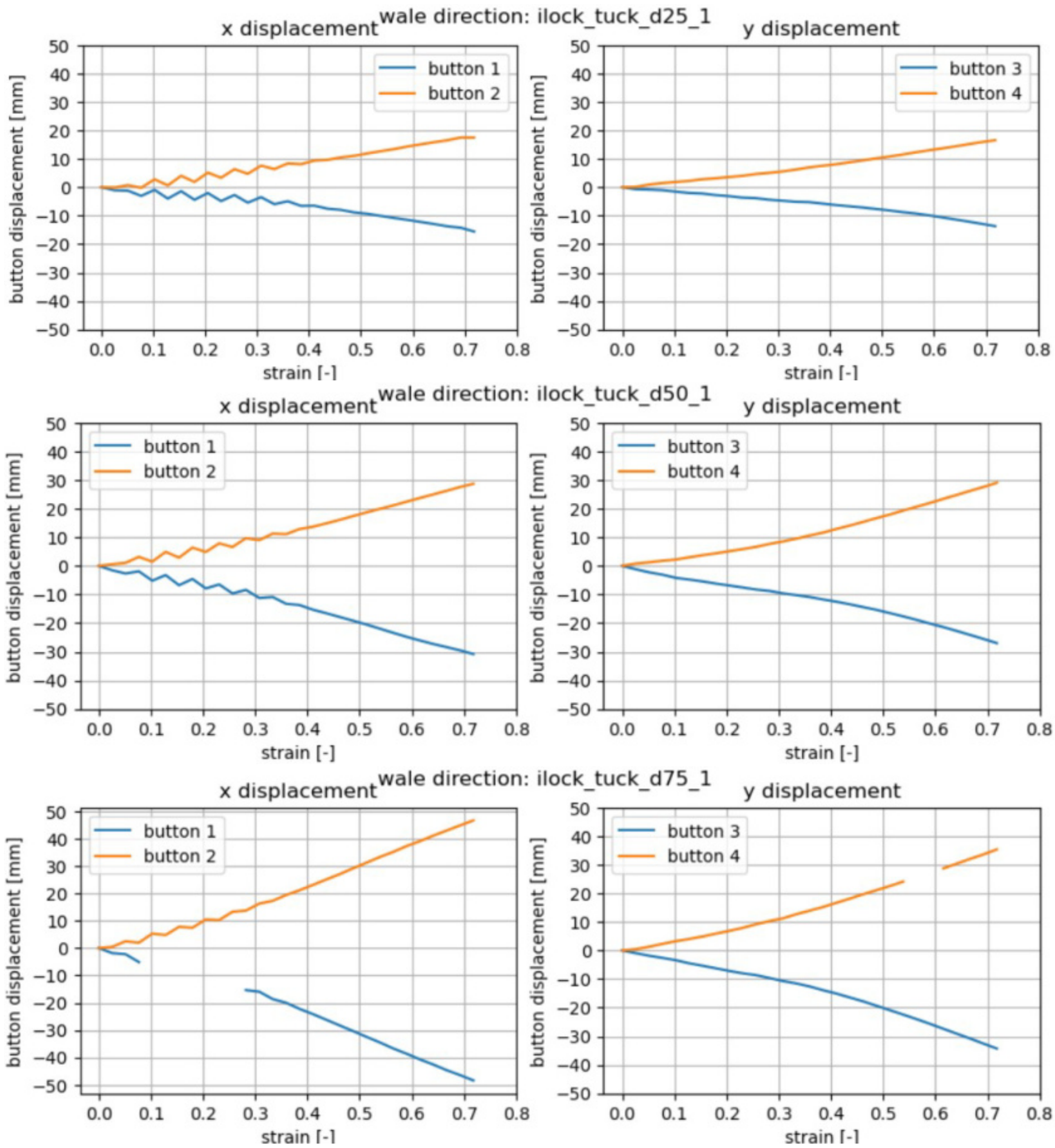

Figure D.11: Interlock_tuck (note: every fabric only tested once)

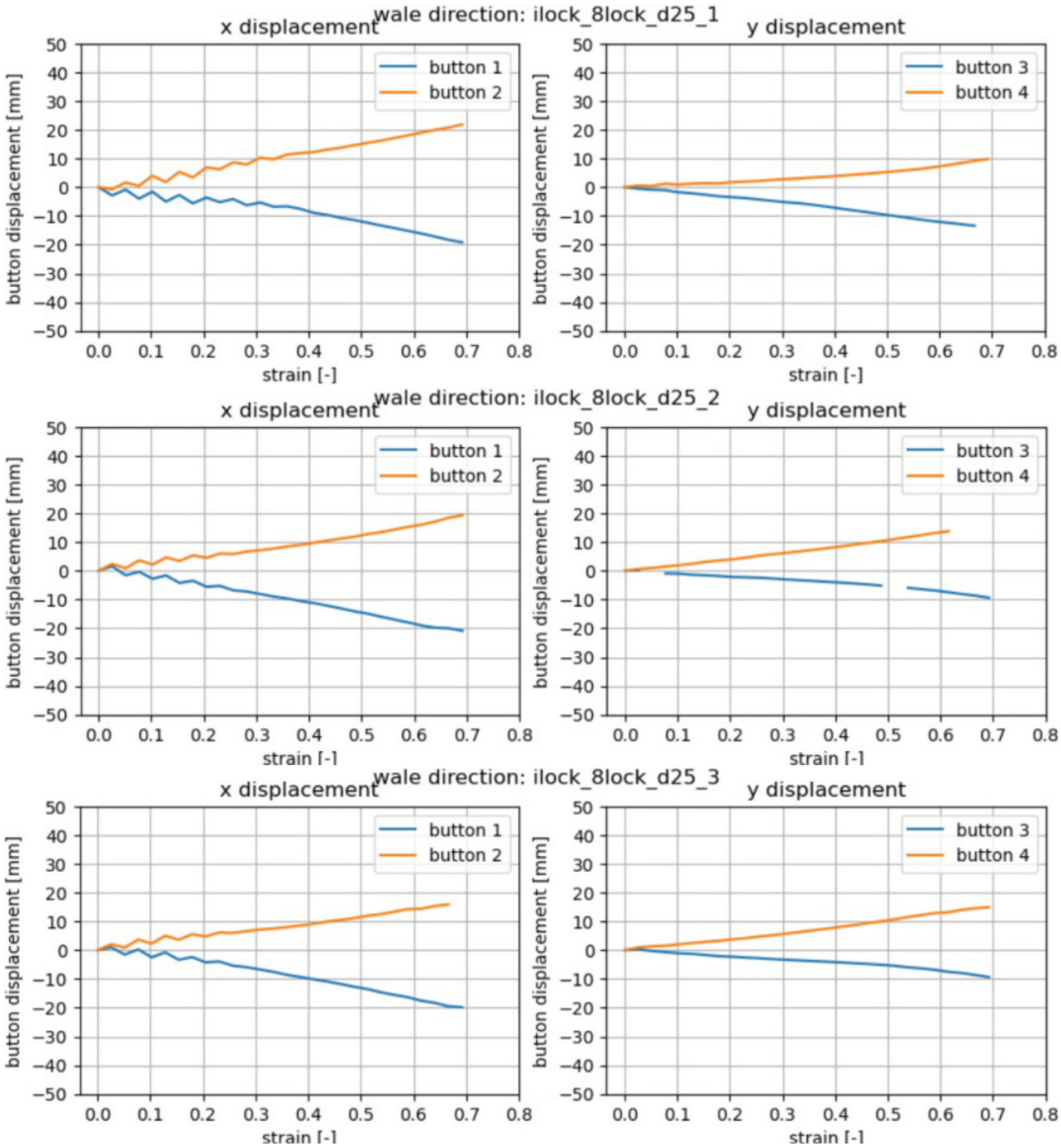

Figure D.12: Interlock_eightlock_d25

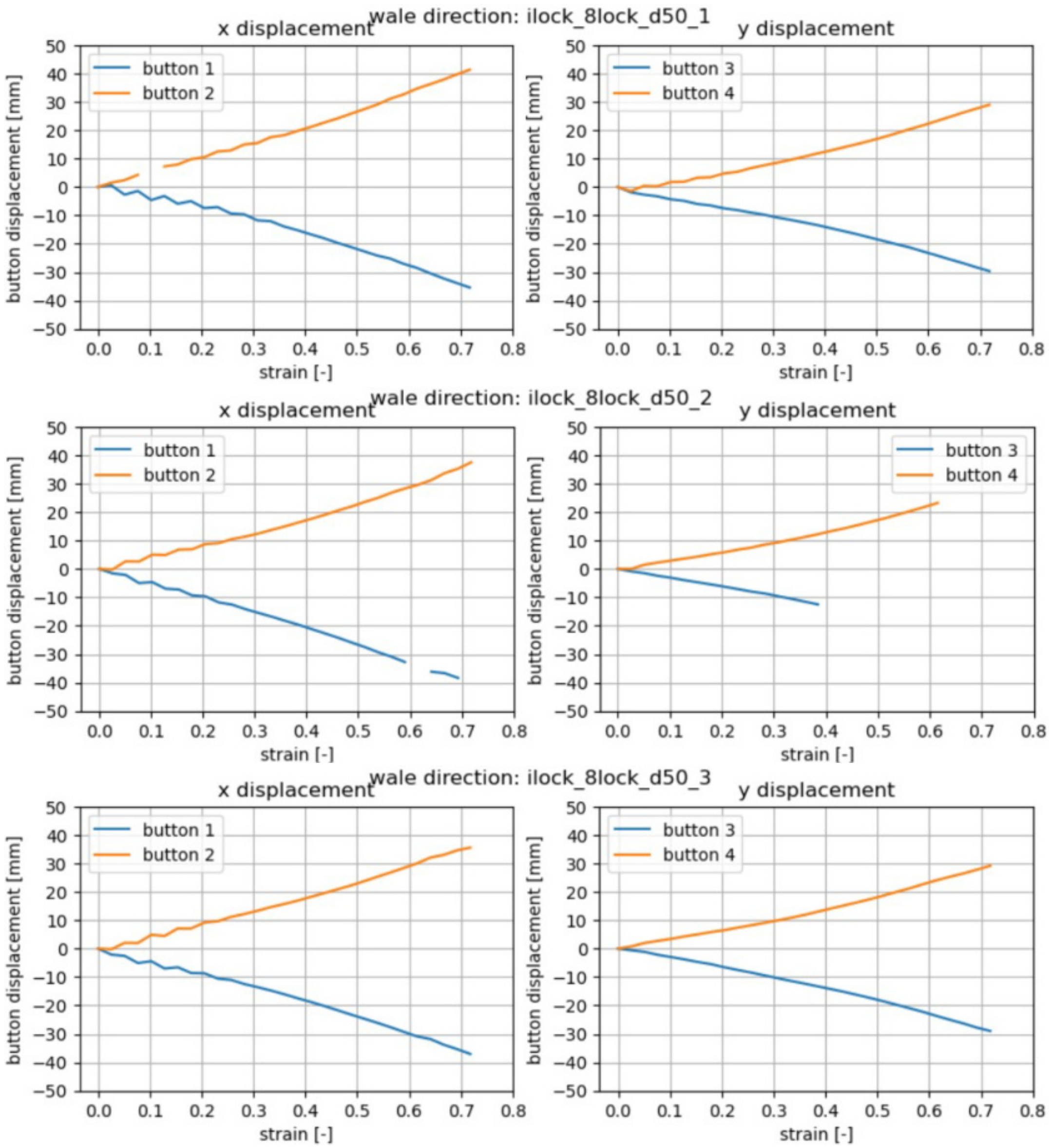

Figure D.13: Interlock_eightlock_d50

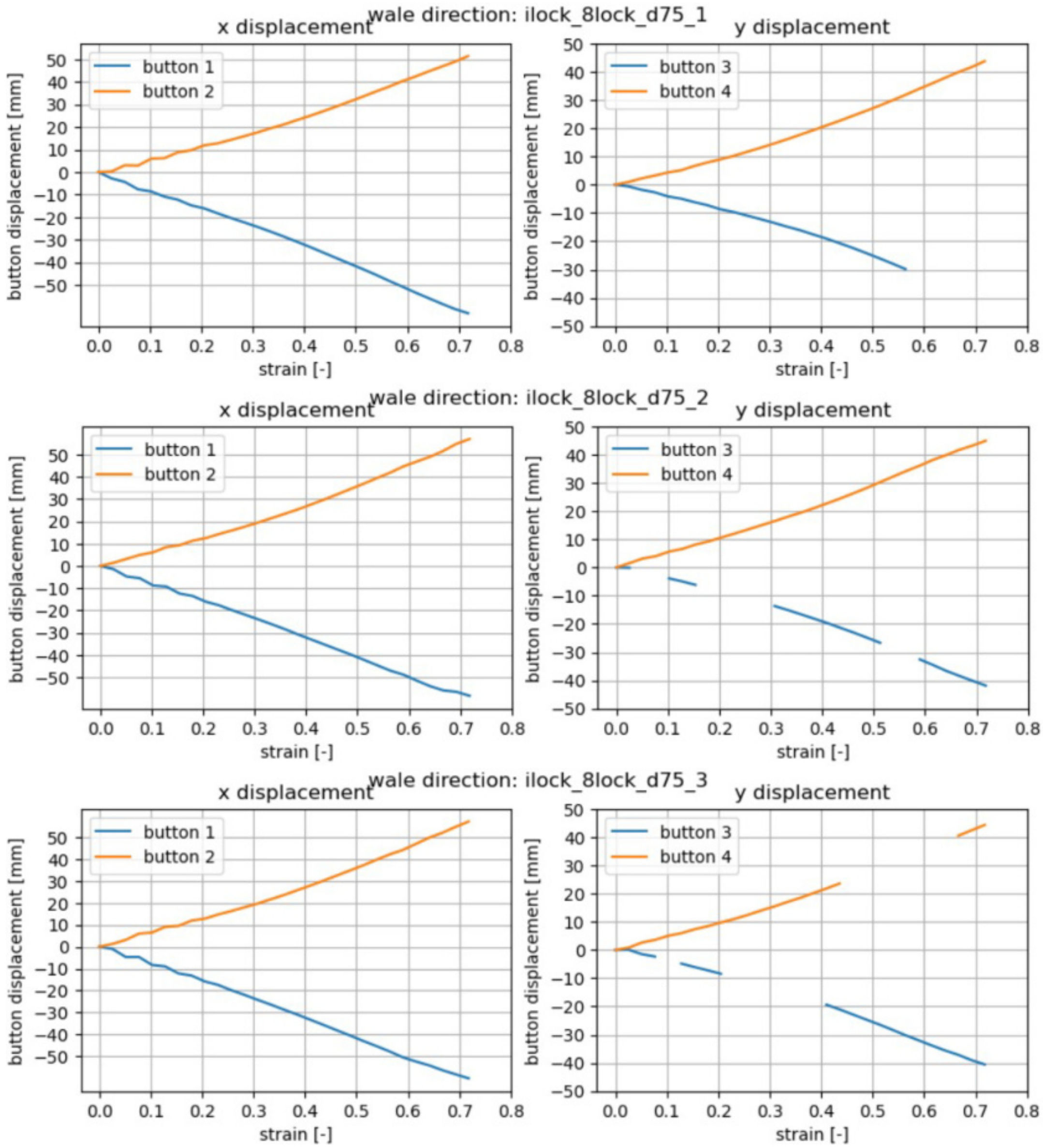

Figure D.14: Interlock_eightlock_d75

Course direction

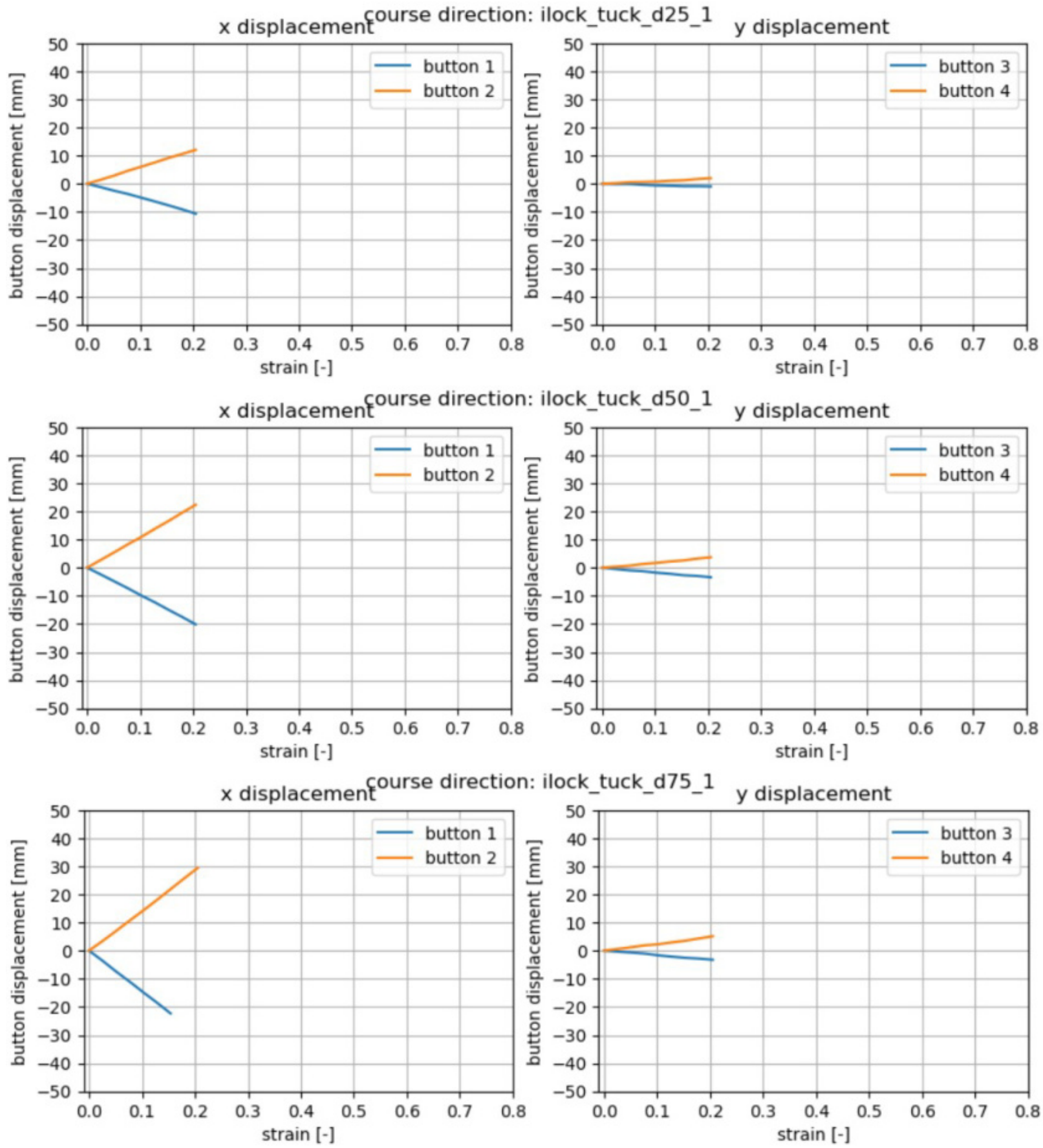

Figure D.15: Interlock_tuck (note: every fabric only tested once)

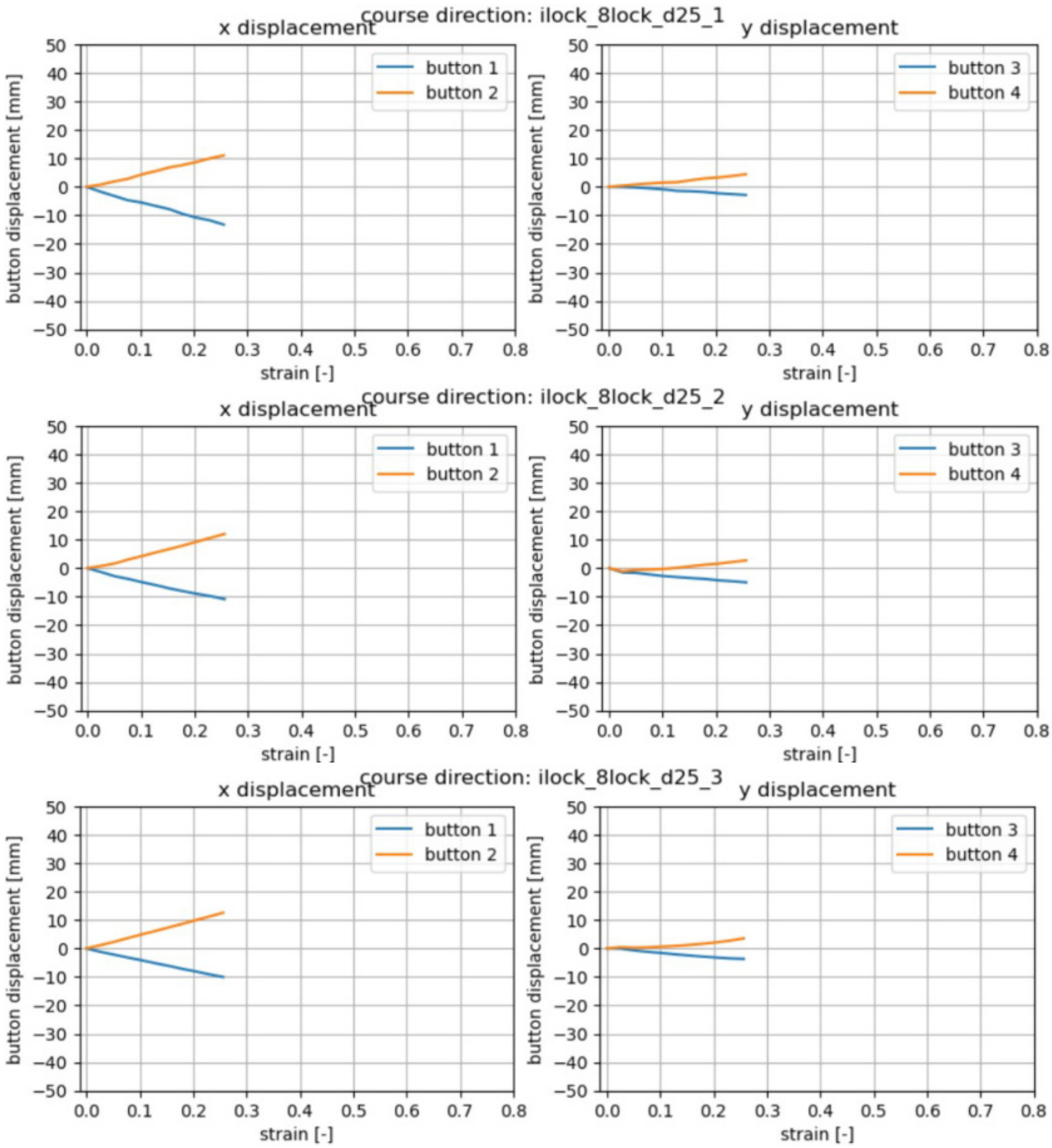

Figure D.16: Interlock_eightlock_d25

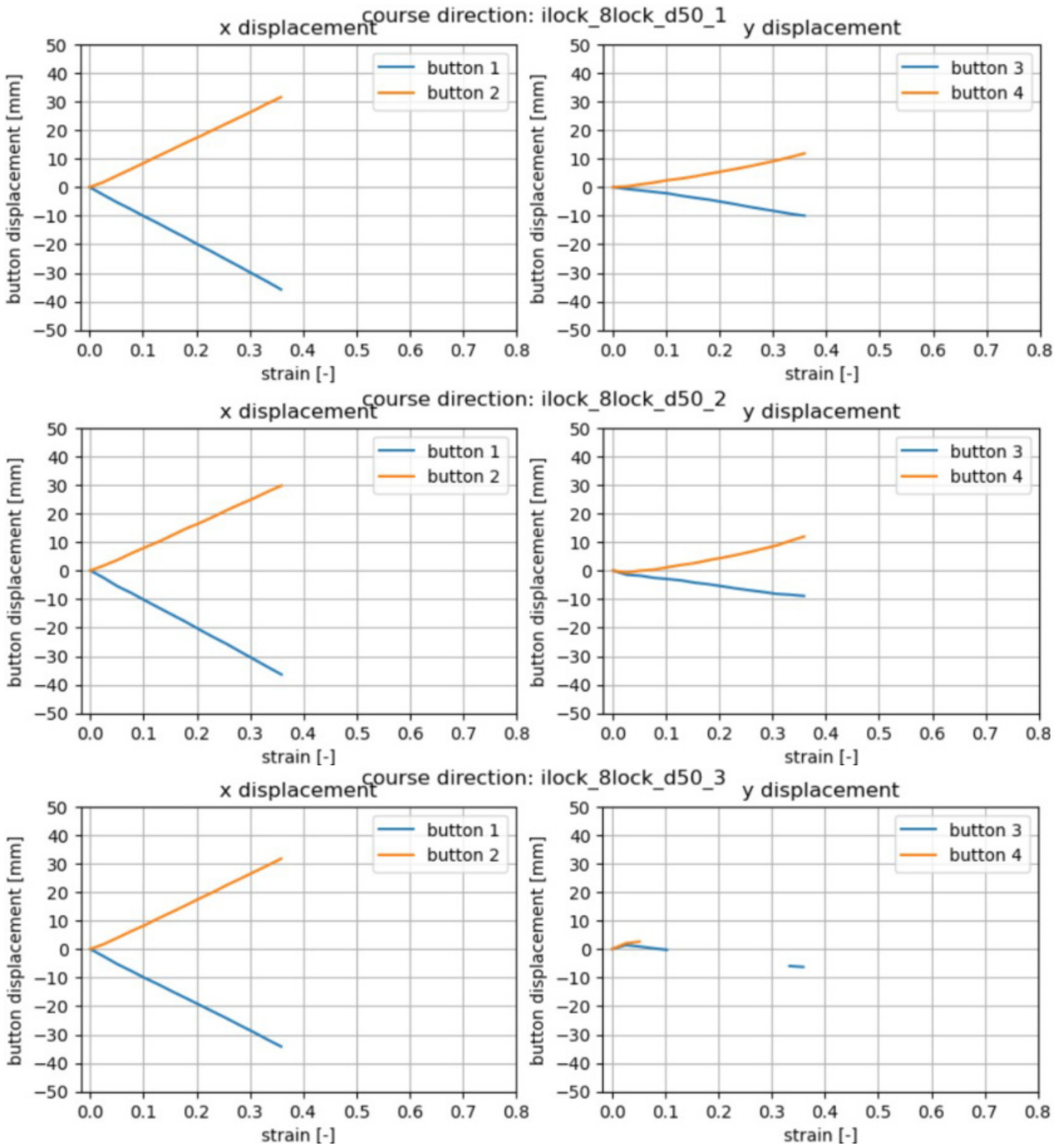

Figure D.17: Interlock_eightlock_d50

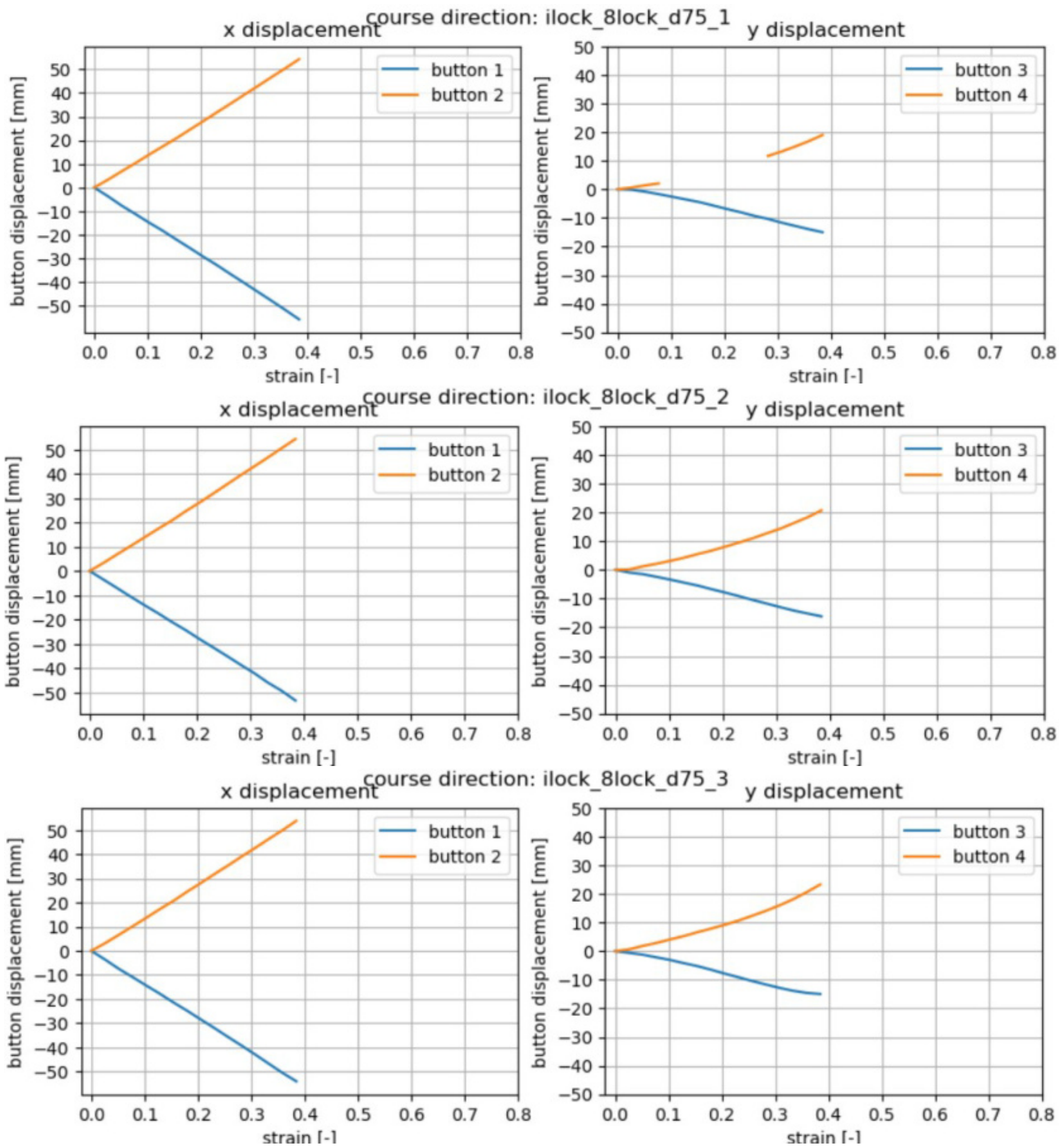

Figure D.18: Interlock_eightlock_d75

E

Poisson's ratios

E.1. Homogeneous fabrics

Wale direction

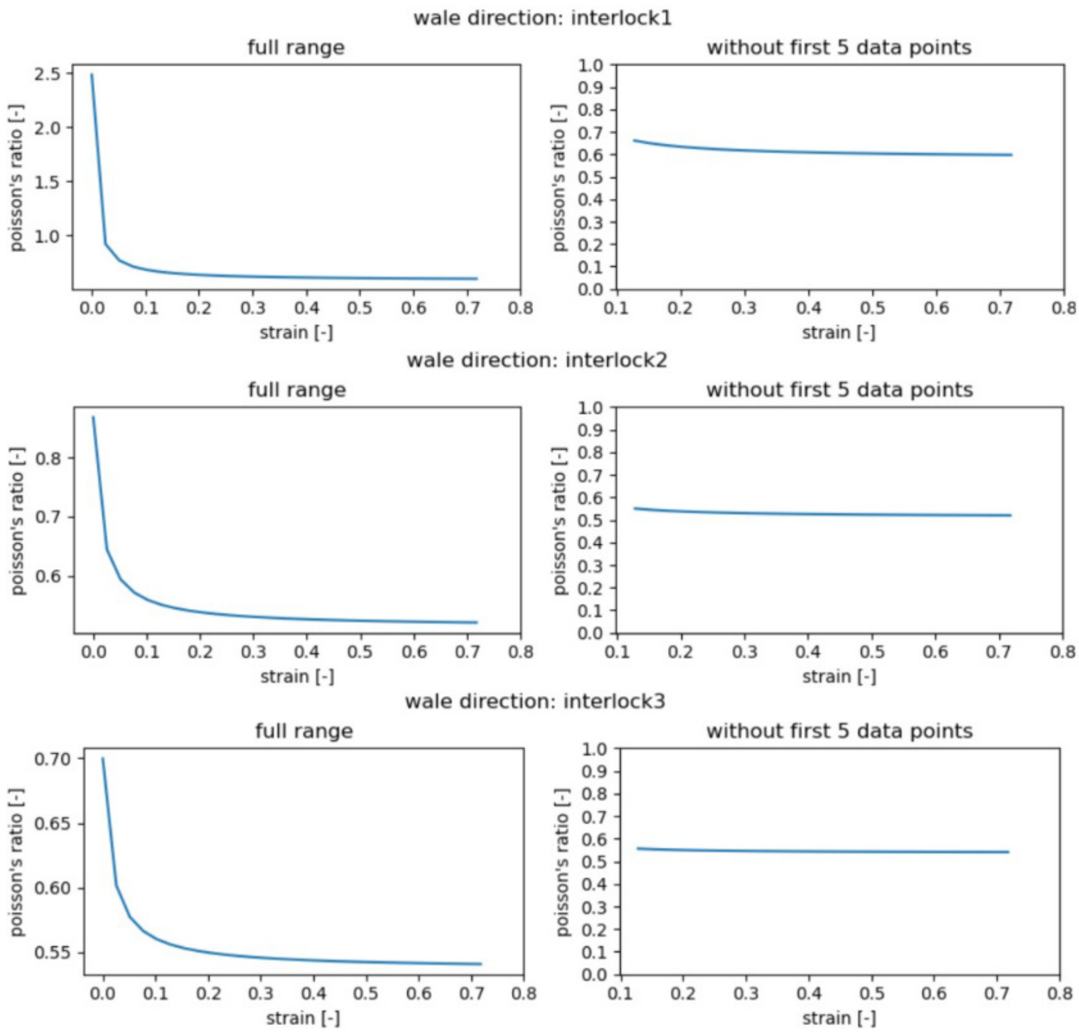

Figure E.1: Interlock

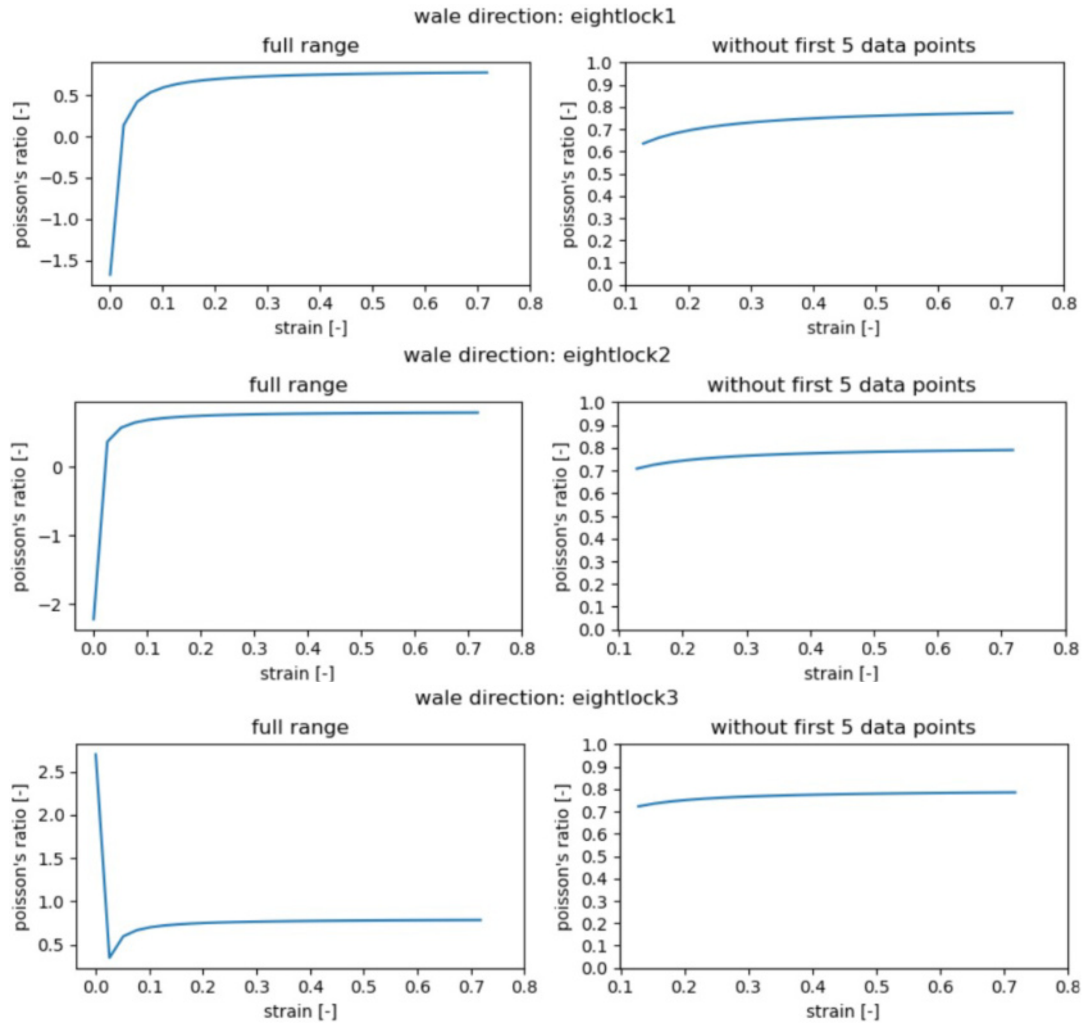

Figure E.2: Eightlock

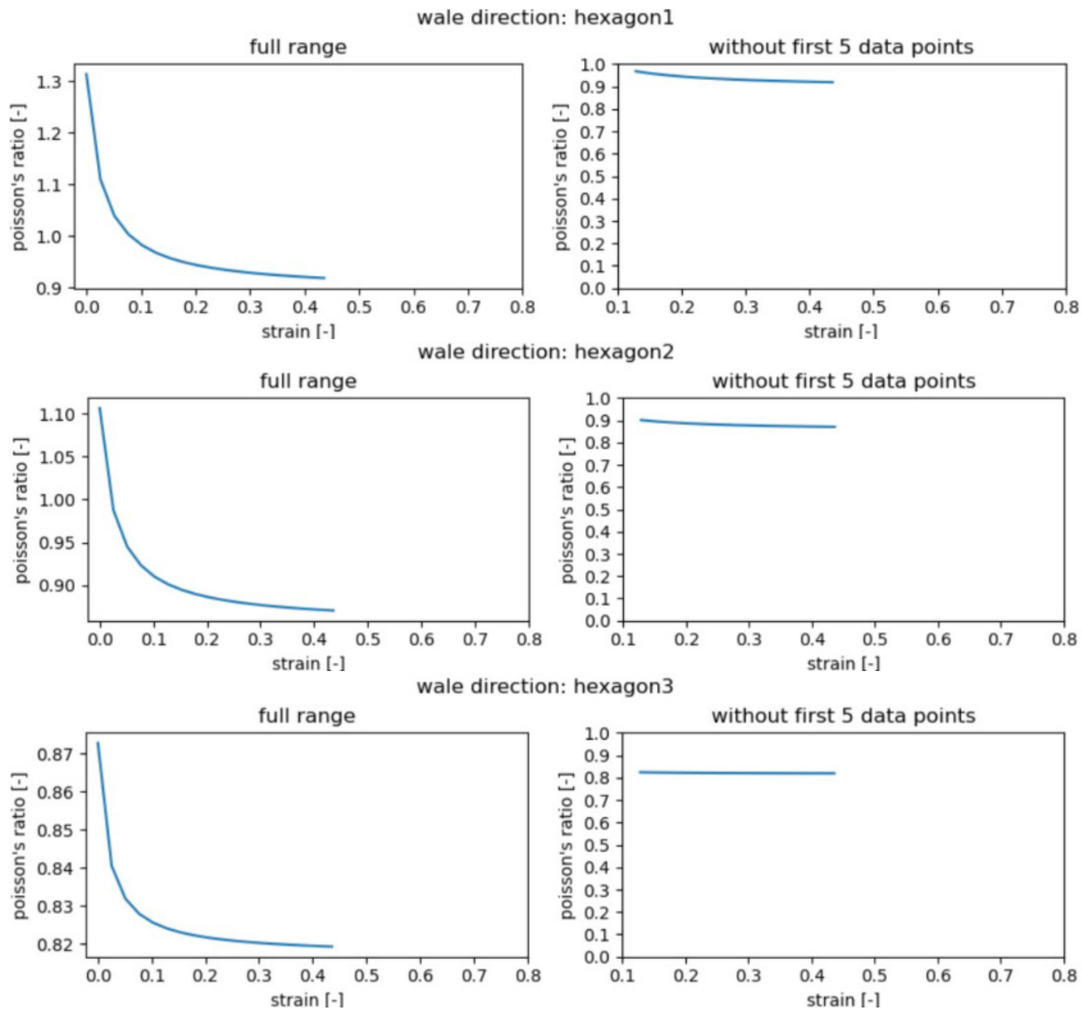

Figure E.3: Hexagon

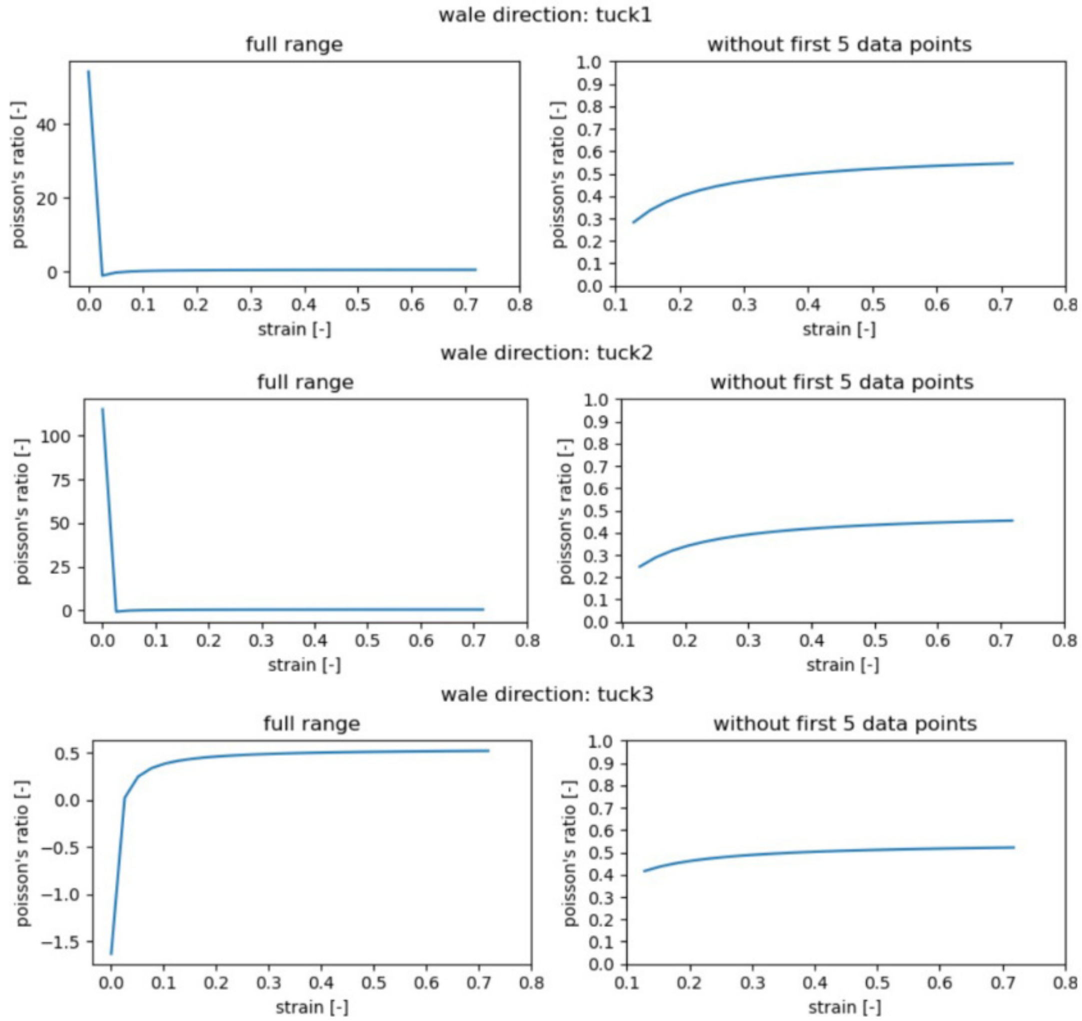

Figure E.4: Tuck

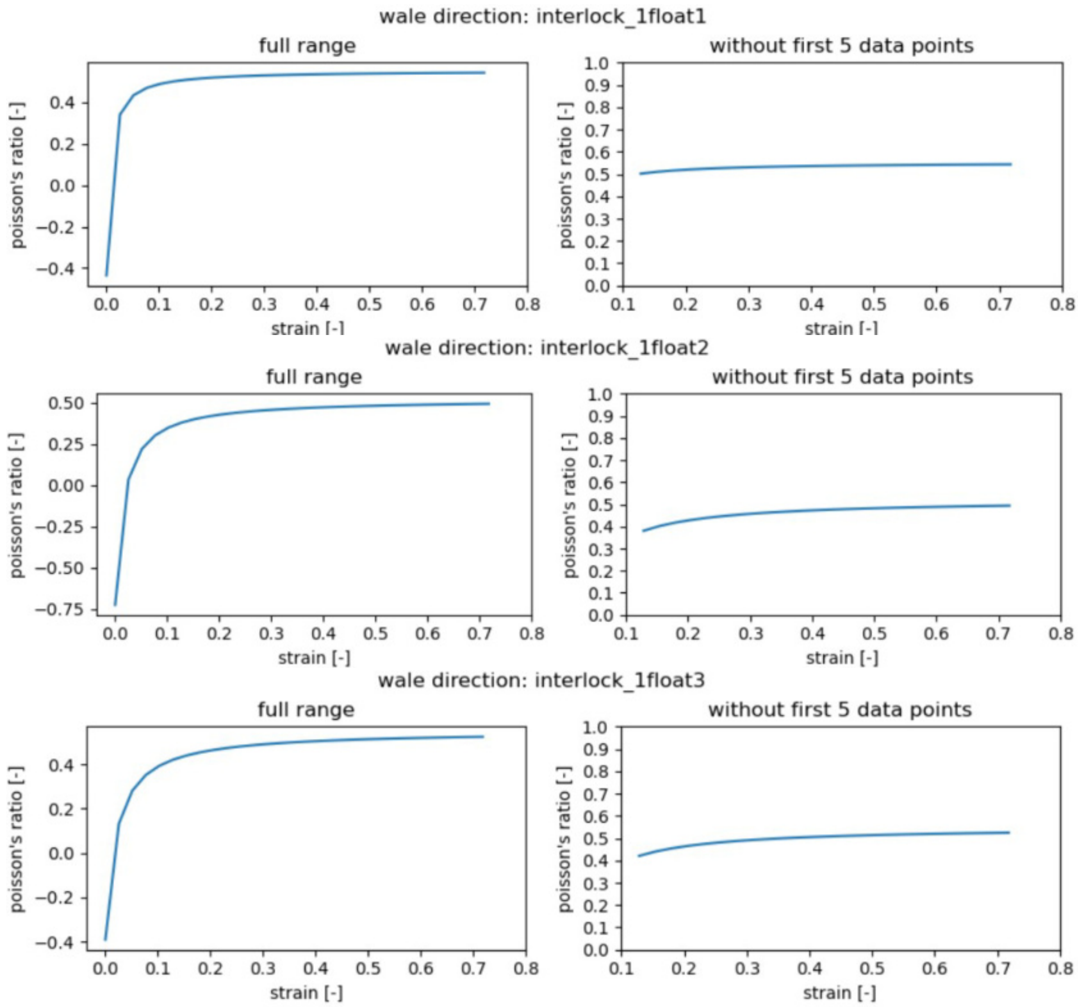

Figure E.5: Interlock_1float

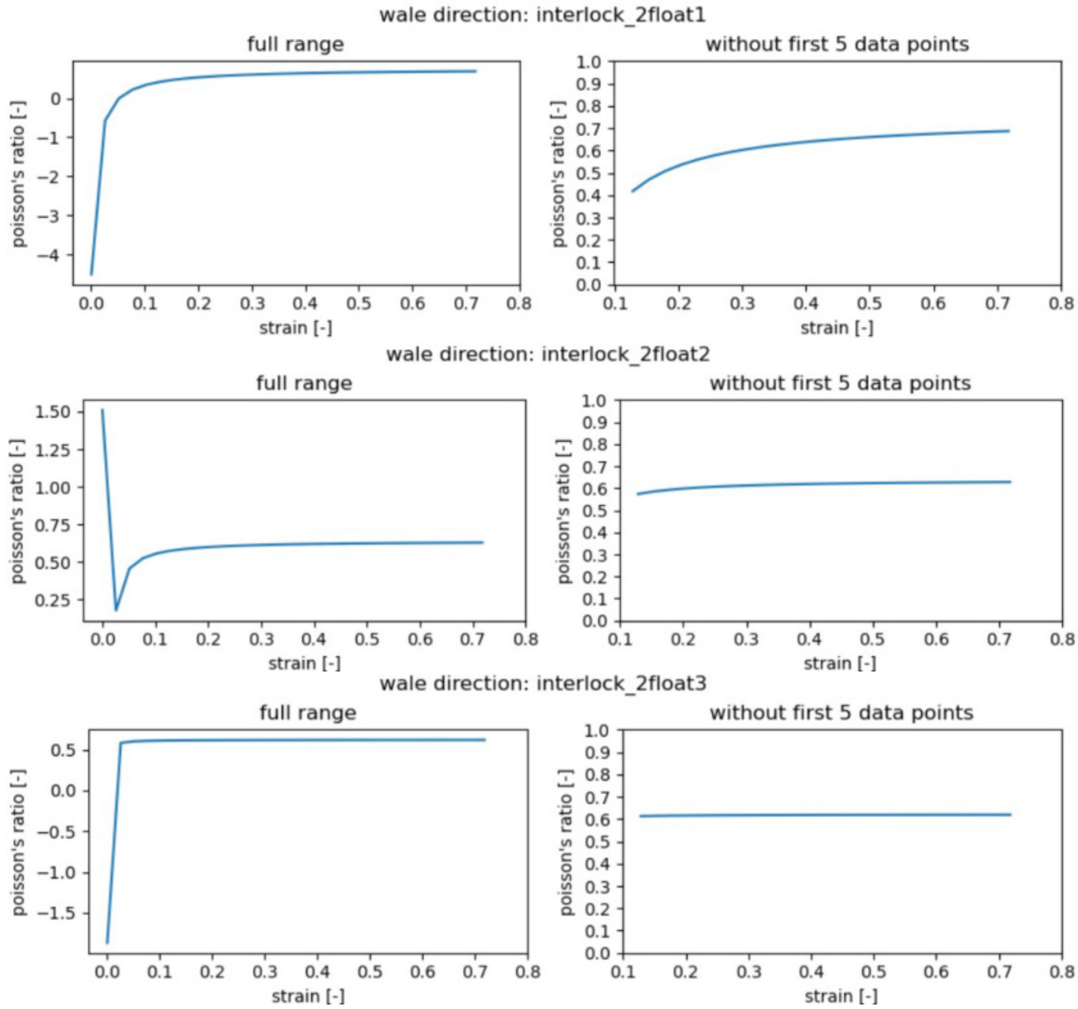

Figure E.6: Interlock_2float

Course direction

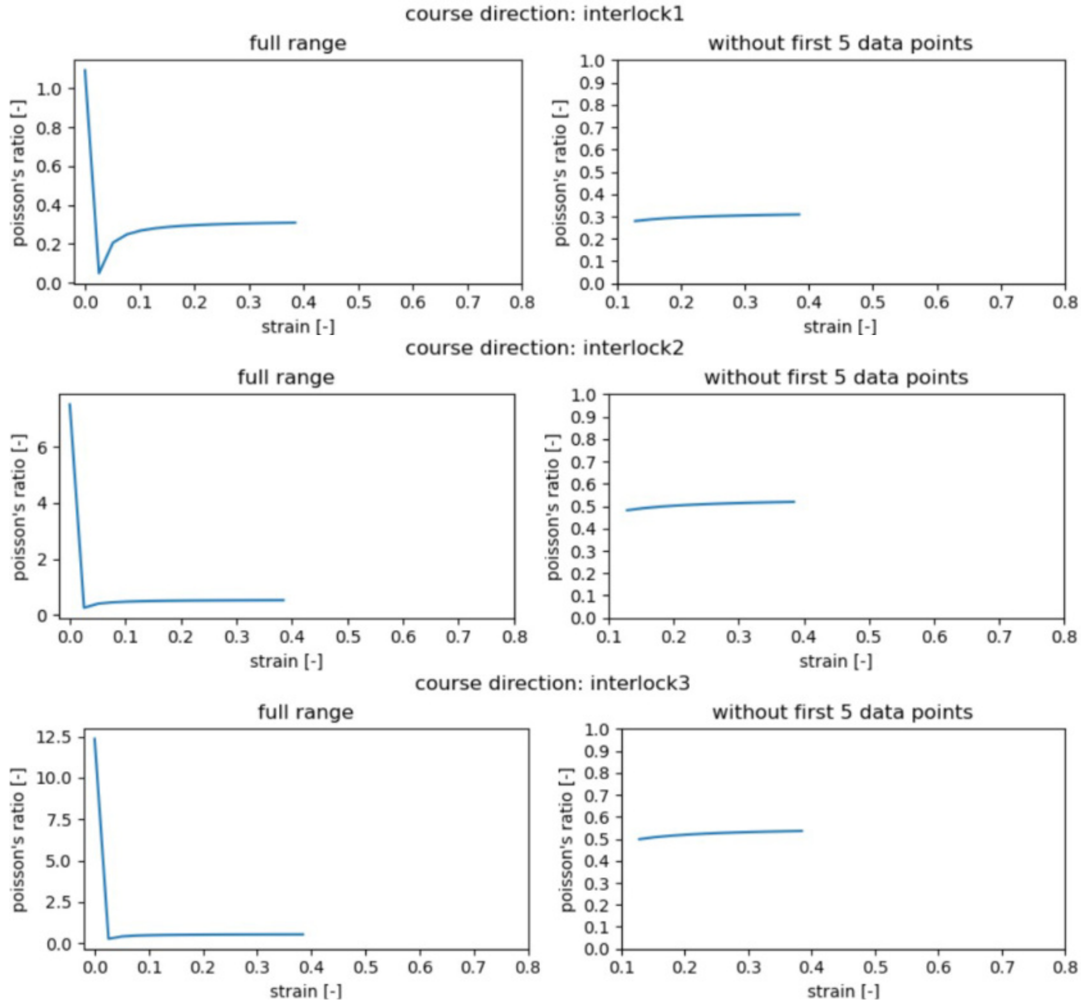

Figure E.7: Interlock

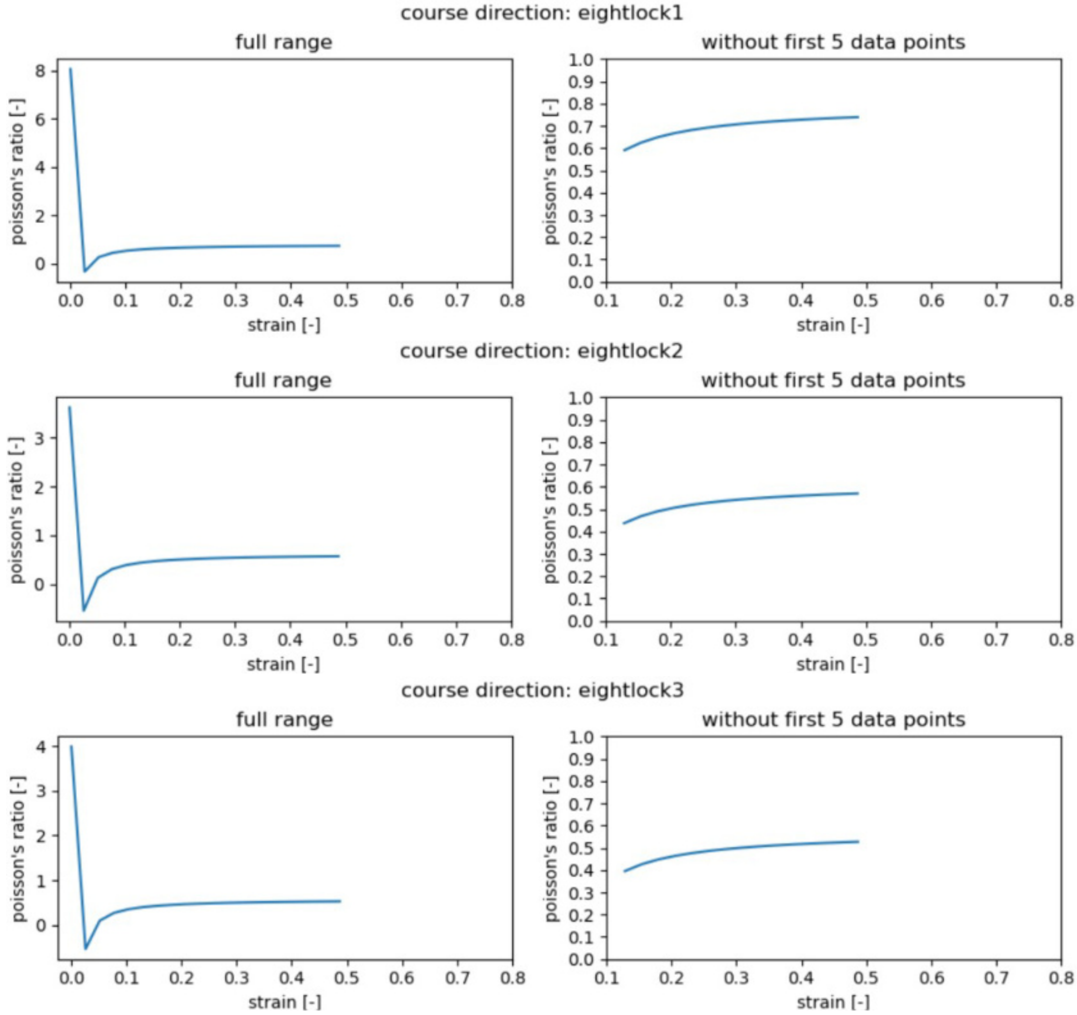

Figure E.8: Eightlock

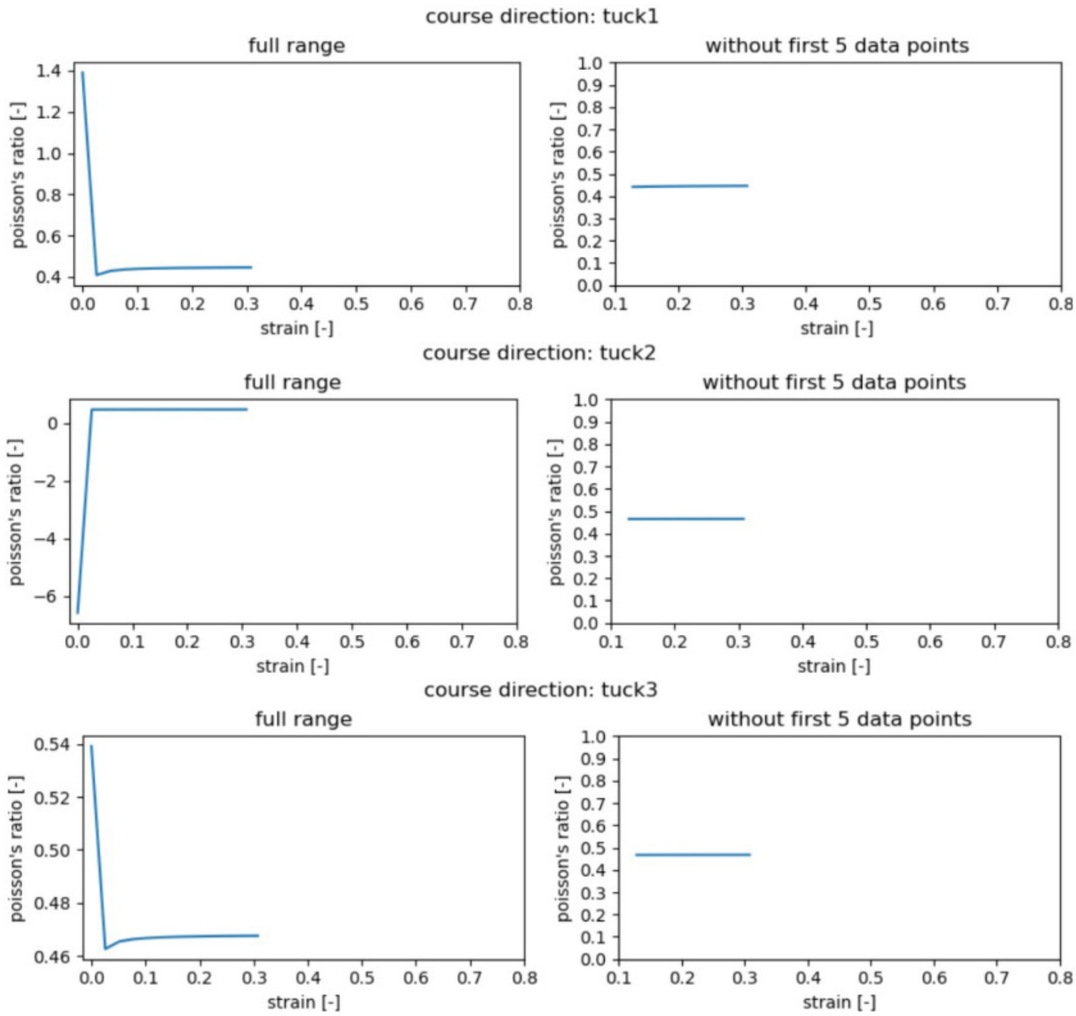

Figure E.9: Tuck

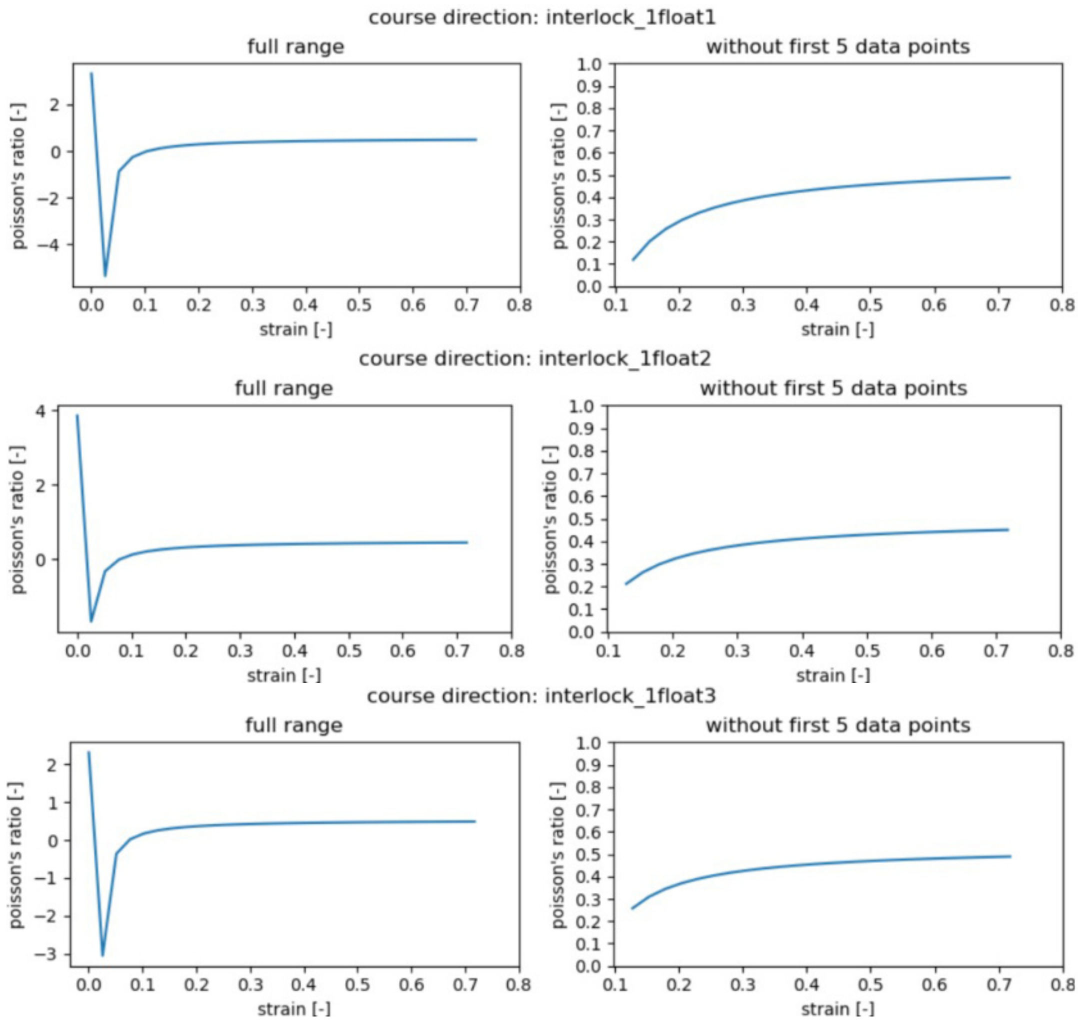

Figure E.10: Interlock_1float

E.2. Non-homogeneous fabrics

Wale direction

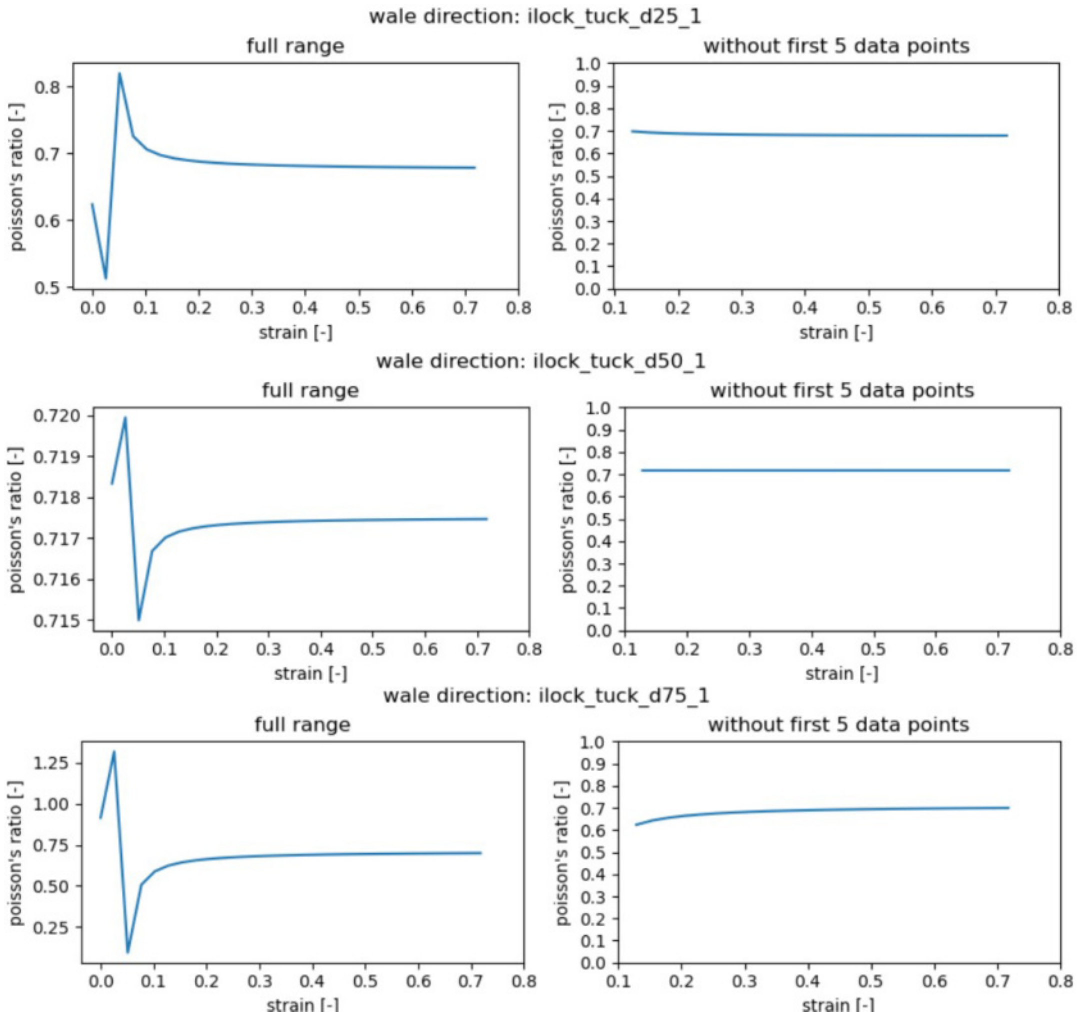

Figure E.11: Interlock_tuck

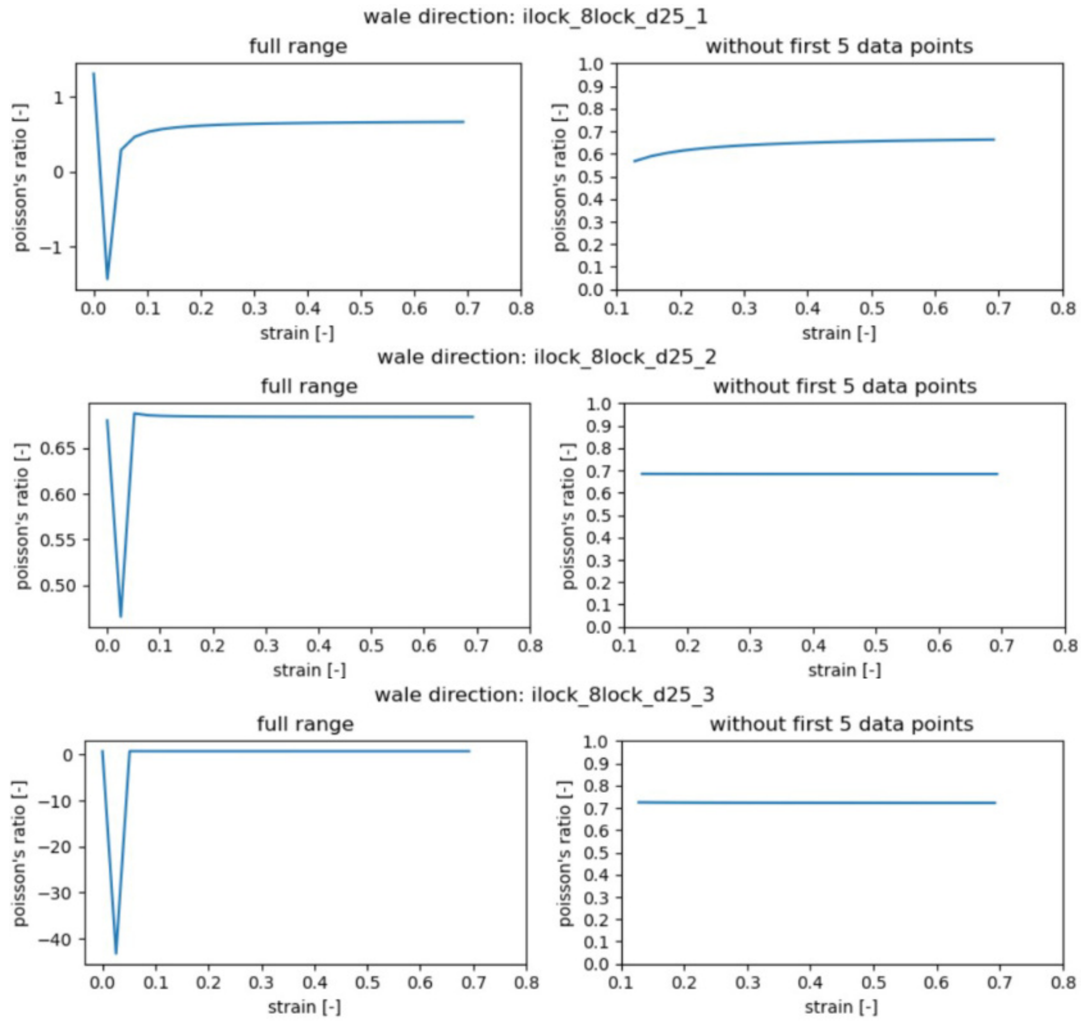

Figure E.12: Interlock_eightlock_d25

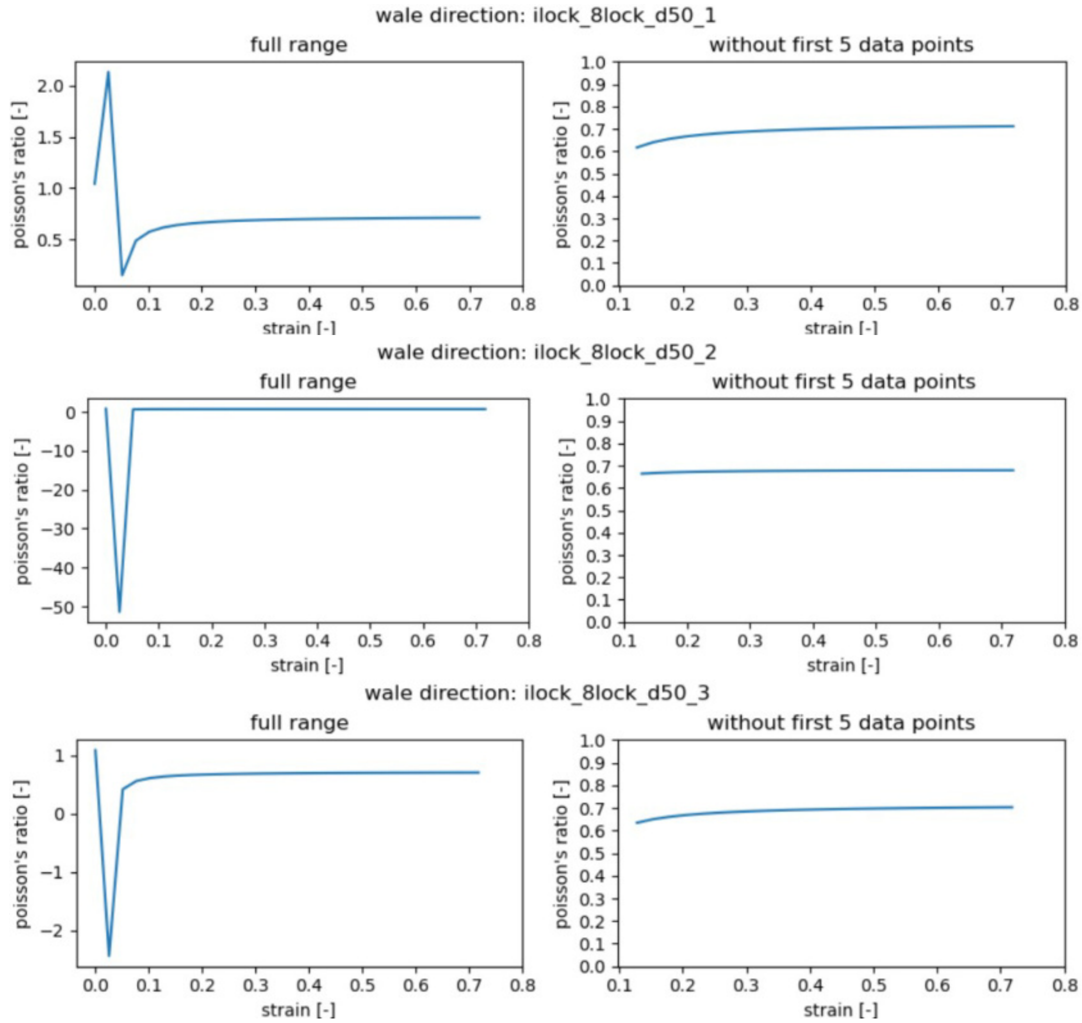

Figure E.13: Interlock_eightlock_d50

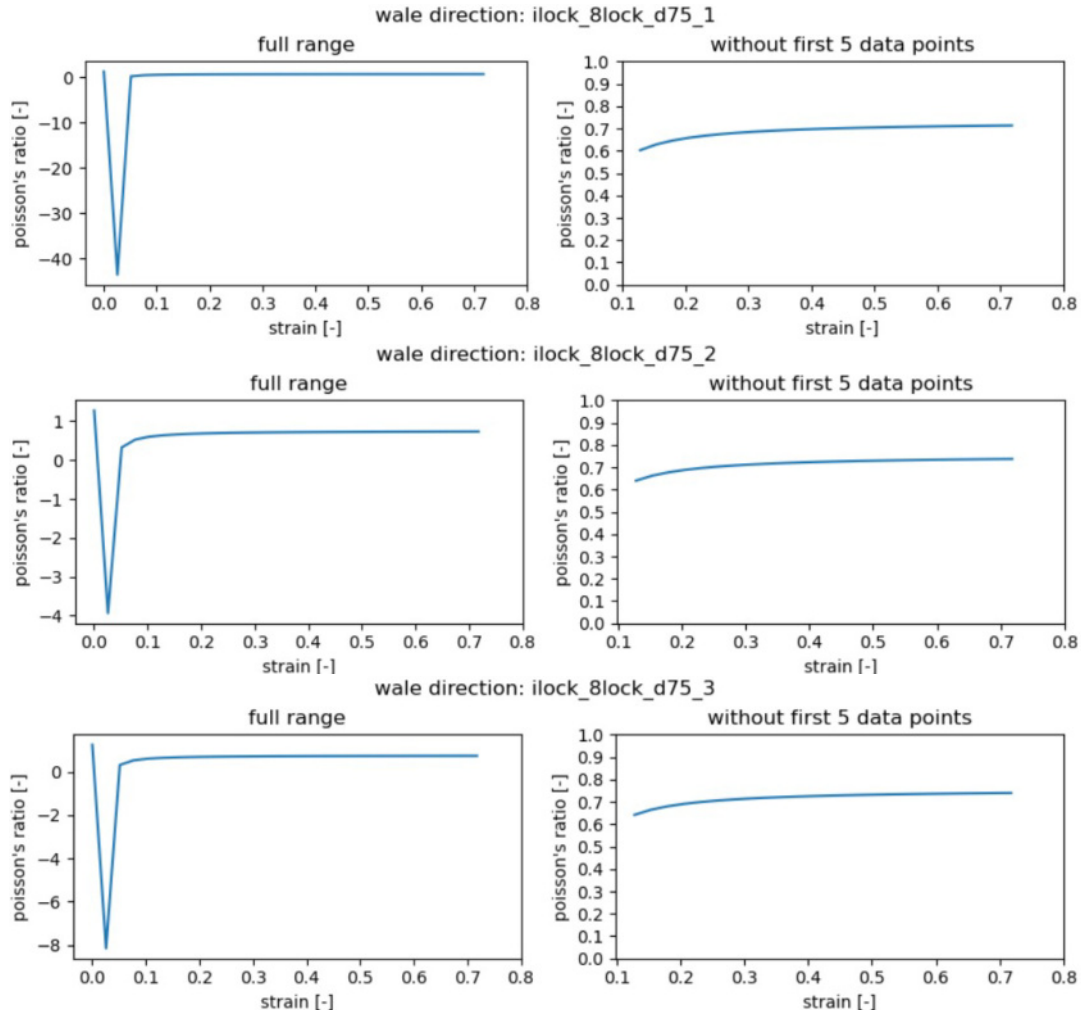

Figure E.14: Interlock_eightlock_d75

Course direction

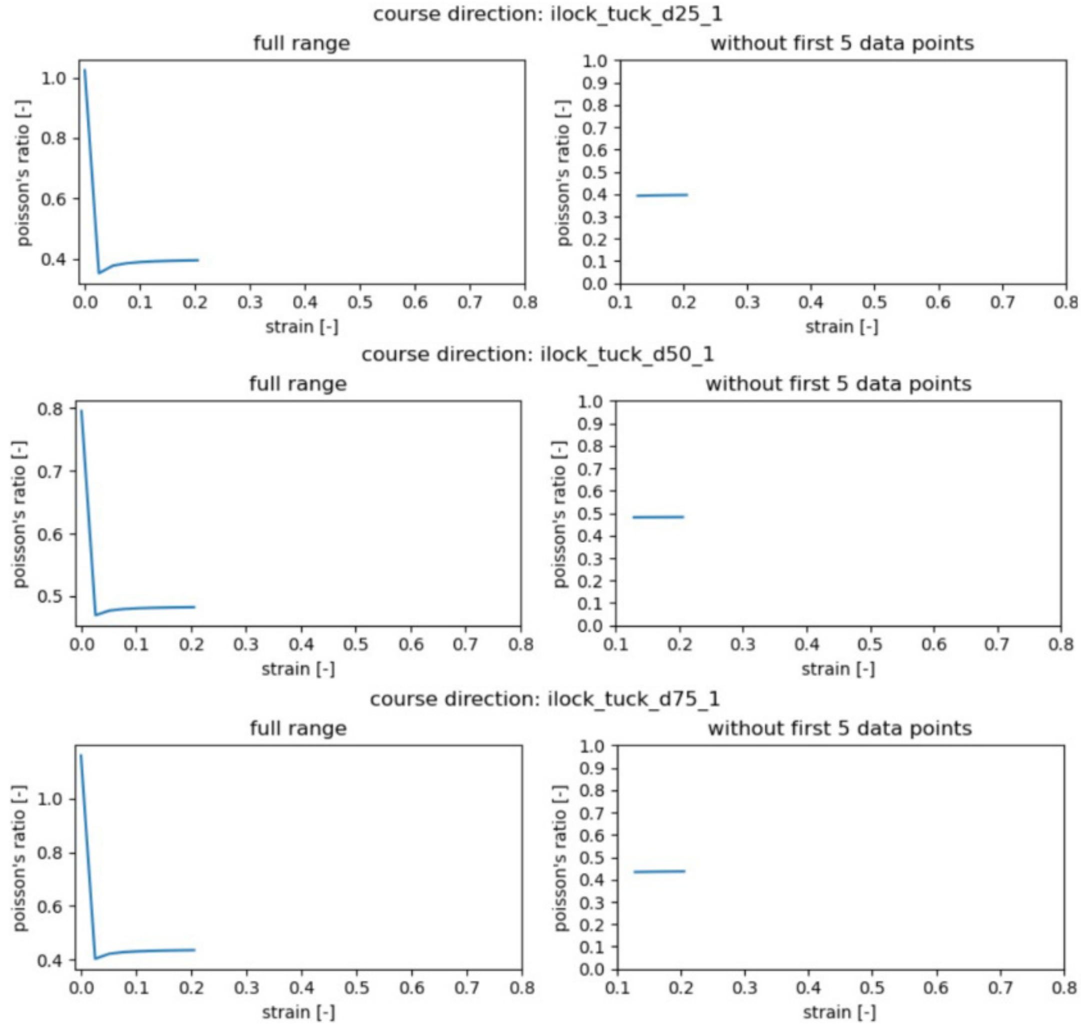

Figure E.15: Interlock_tuck

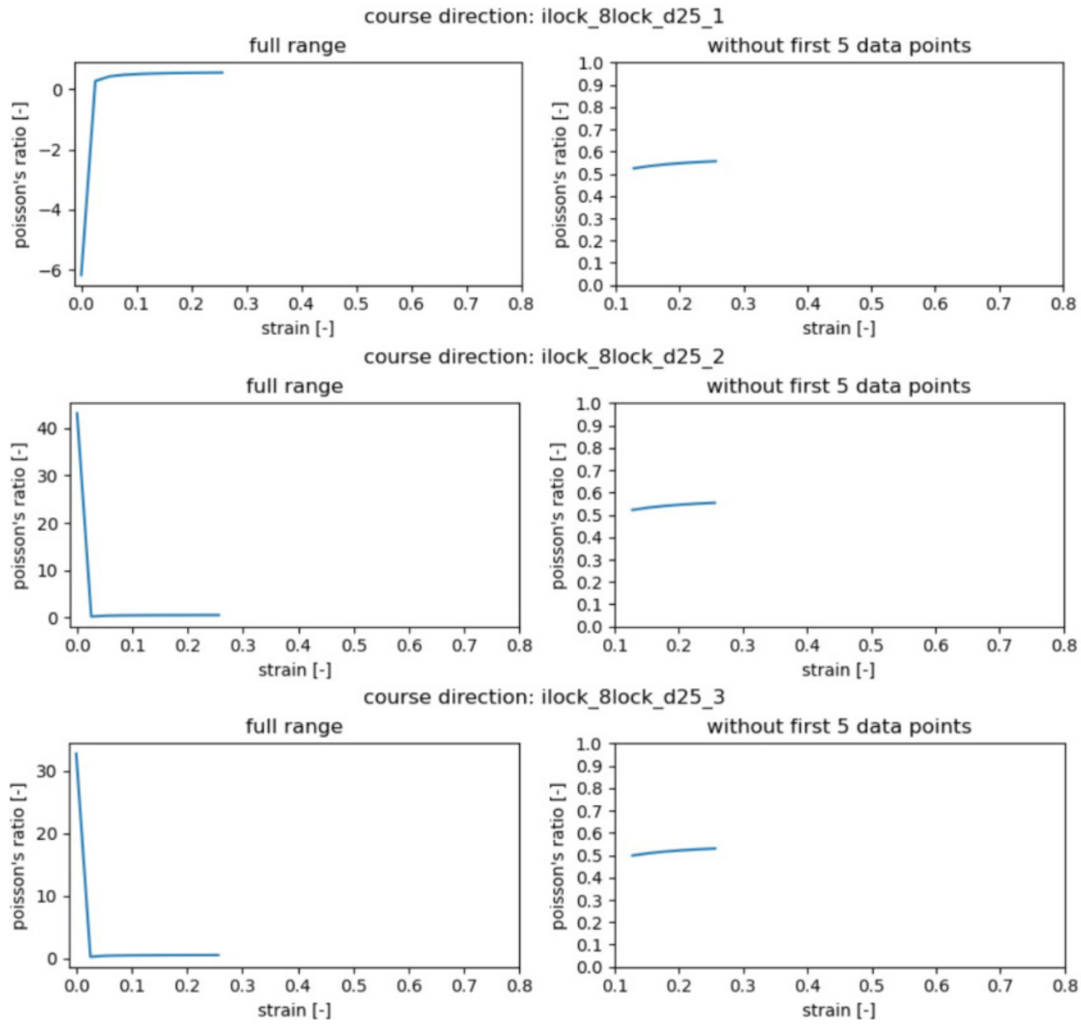

Figure E.16: Interlock_eightlock_d25

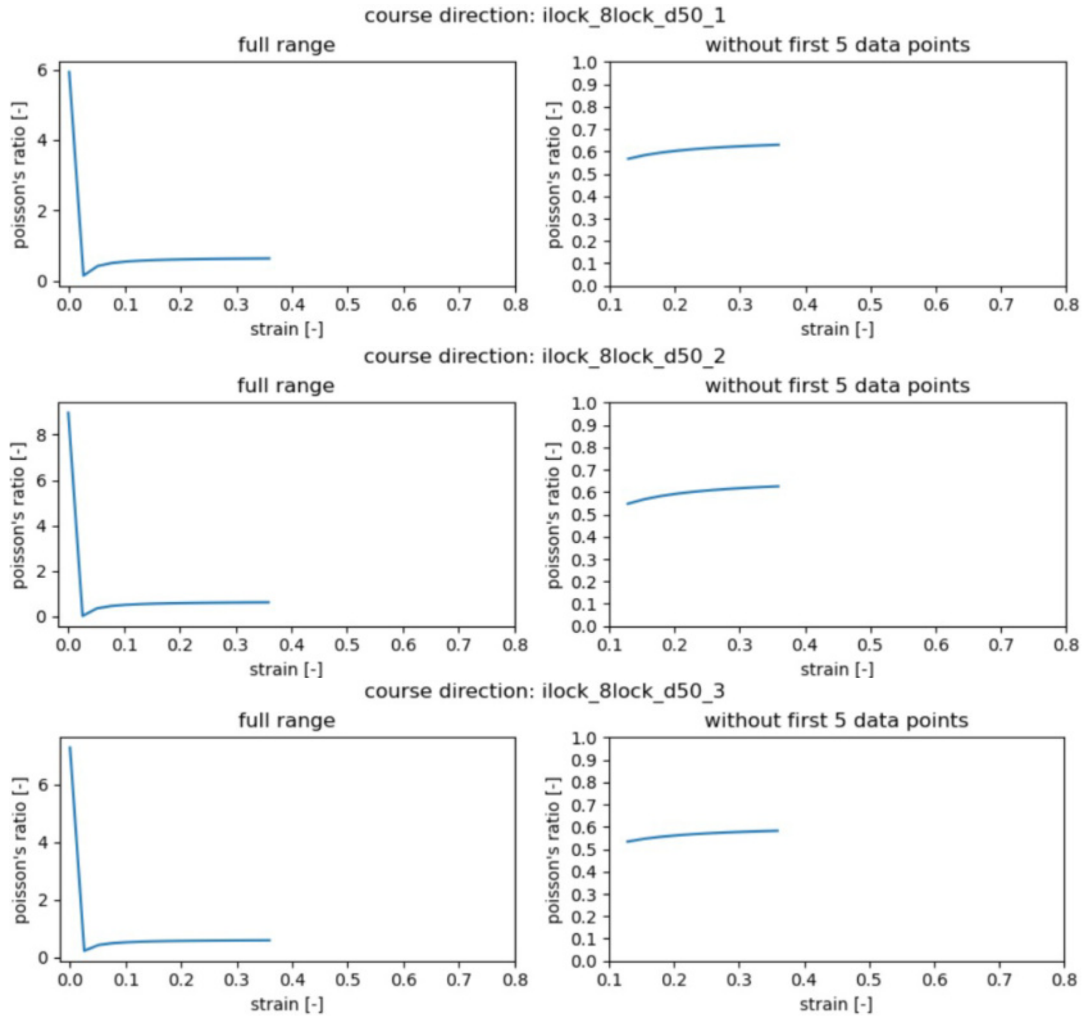

Figure E.17: Interlock_eightlock_d50

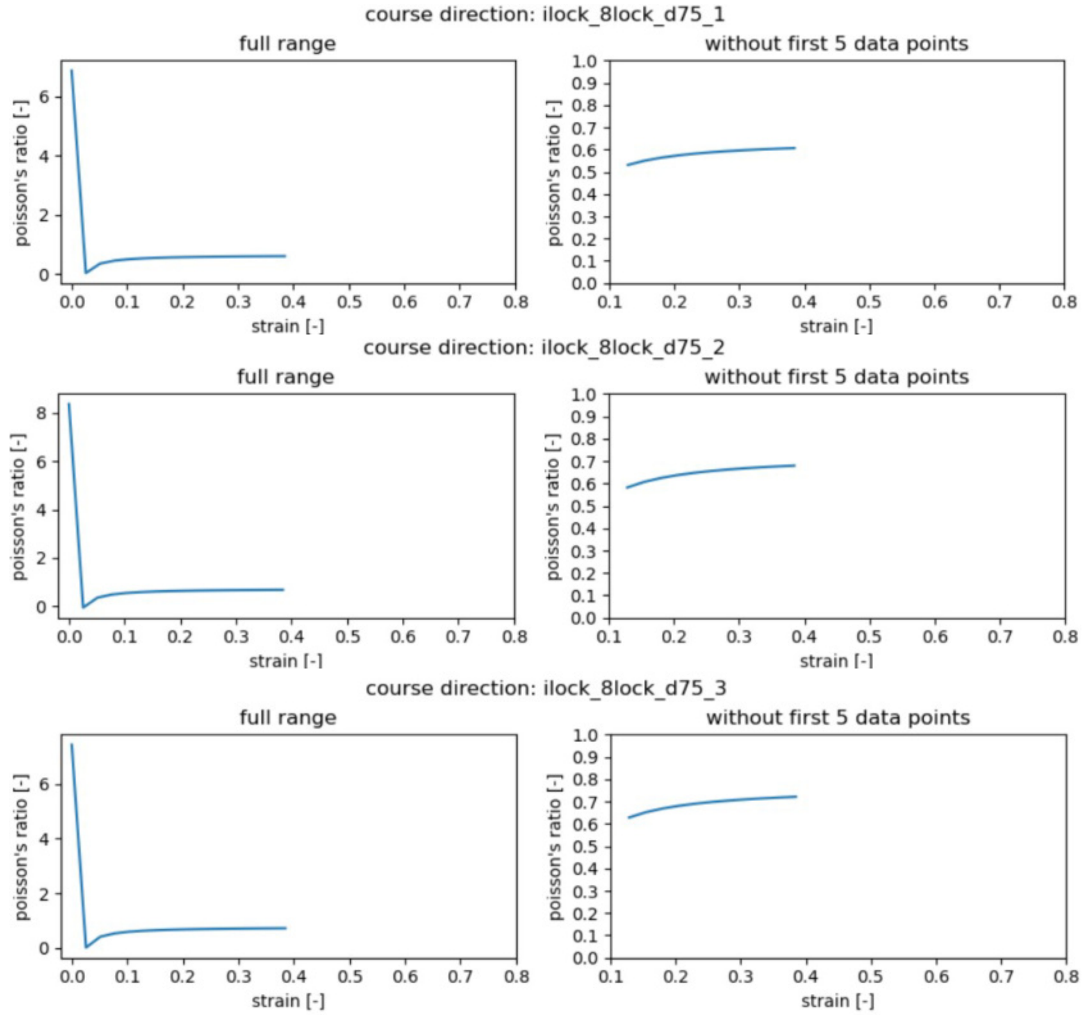

Figure E.18: Interlock_eightlock_d75

F

Area determination

Since the thickness of knitted fabrics is very small, this is not simply measurable with a ruler. Therefore the area is determined based on the weight of the fabrics. The method of determining the area based on the weight is shown in Equation F.1 and F.2.

This method is dependent on the amount of strain that is applied to the fabric since the length of the fabric in the testing direction depends on the applied strain. For this research, it is chosen to measure the size when the fabric is fully relaxed (see Figure F.1a). For some of the patterns, the fabric is not rectangular. This is caused by a push-pull effect of the knitting stitches that are used to fabricate the pattern. This effect is visible in Figure F.1b for a non-homogeneous fabric. When the fabric is not rectangular, the length is determined at the centre of the fabric.

Table F.1 gives an overview of the properties of all fabrics.

$$\rho = \frac{m}{V} \Rightarrow V = \frac{m}{\rho} \tag{F.1}$$

$$V = A \cdot l \Rightarrow A = \frac{V}{l} \tag{F.2}$$

ρ	:	Density of the material (1.3 g/cm^3)
m	:	Mass
V	:	Volume
A	:	Area perpendicular to testing direction
l	:	Length of fabric in testing direction

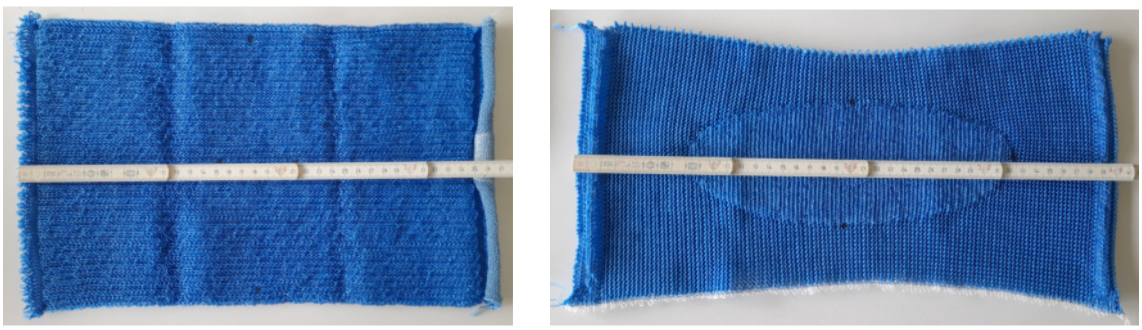

(a) Rectangular fabric

(b) Non-rectangular fabric

Figure F.1: Length determination of fabrics

		Wale direction				Course direction			
	Pattern name	Weight [g]	Length [mm]	Volume [mm^3]	Area [mm^2]	Weight [g]	Length [mm]	Volume [mm^3]	Area [mm^2]
Homogeneous fabrics	interlock1	22.3	378	17154	45.4	21.5	404	16539	40.9
	interlock2	22.0	352	16923	48.1	22.3	410	17154	41.8
	interlock3	22.3	362	17154	47.4	22.3	407	17154	42.1
	eightlock1	19.0	381	14615	38.4	19.2	395	14769	37.4
	eightlock2	18.7	370	14385	38.9	19.6	383	15077	39.4
	eightlock3	18.8	384	14462	37.7	19.5	380	15000	39.5
	hexagon1	13.5	341	10385	30.5	-	-	-	-
	hexagon2	13.5	349	10385	29.8	-	-	-	-
	hexagon3	13.5	344	10385	30.2	-	-	-	-
	tuck1	27.0	351	20769	59.2	20.0	383	15385	40.2
	tuck2	27.3	346	21000	60.7	20.5	393	15769	40.1
	tuck3	27.2	332	20923	63.0	20.5	394	15769	40.0
	interlock_1float1	14.5	392	11154	28.5	21.9	355	16846	47.5
	interlock_1float2	14.1	391	10846	27.7	21.4	356	16462	46.2
	interlock_1float3	14.1	382	10846	28.4	21.4	354	16462	46.5
	interlock_2float1	10.2	372	7846	21.1	-	-	-	-
	interlock_2float2	10.1	383	7769	20.3	-	-	-	-
	interlock_2float3	10.1	385	7769	20.2	-	-	-	-
Non-homogeneous fabrics	ilock_tuck_d25_1	22.5	369	17308	46.9	22.1	400	17000	42.5
	ilock_tuck_d50_1	22.5	357	17308	48.5	22.1	402	17000	42.3
	ilock_tuck_d75_1	22.5	356	17308	48.6	22.2	404	17077	42.3
	ilock_8lock_d25_1	21.6	354	16615	46.9	22.0	394	16923	43.0
	ilock_8lock_d25_2	21.1	357	16231	45.5	21.9	398	16846	42.3
	ilock_8lock_d25_3	21.2	354	16308	46.1	21.9	393	16846	42.9
	ilock_8lock_d50_1	22.0	354	16923	47.8	21.8	390	16769	43.0
	ilock_8lock_d50_2	21.8	369	16769	45.4	21.7	395	16692	42.3
	ilock_8lock_d50_3	21.8	356	16769	47.1	21.7	394	16692	42.4
	ilock_8lock_d75_1	23.0	359	17692	49.3	21.6	386	16615	43.0
	ilock_8lock_d75_2	22.8	356	17539	49.3	21.4	386	16462	42.6
	ilock_8lock_d75_3	22.8	356	17539	49.3	21.3	390	16385	42.0

Table F.1: Fabric properties

G

Force-strain diagrams

G.1. Homogeneous fabrics

Wale direction

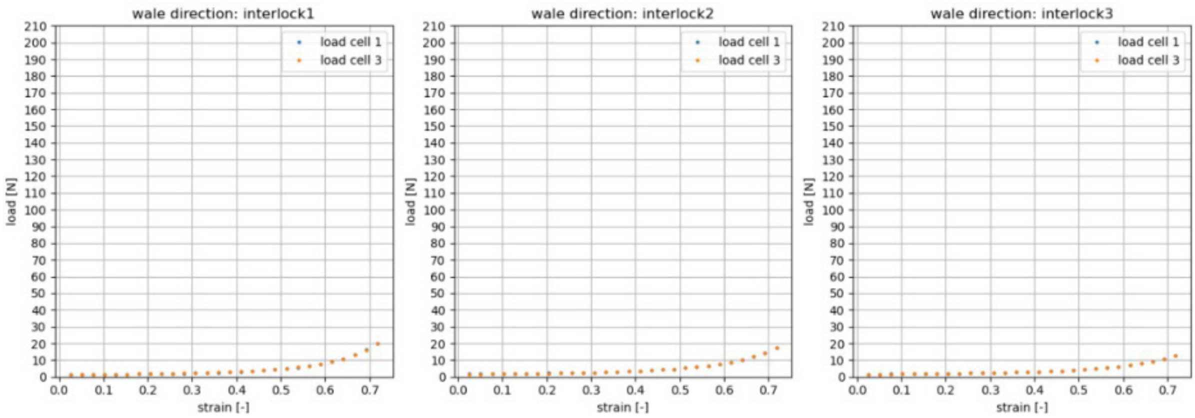

Figure G.1: Interlock

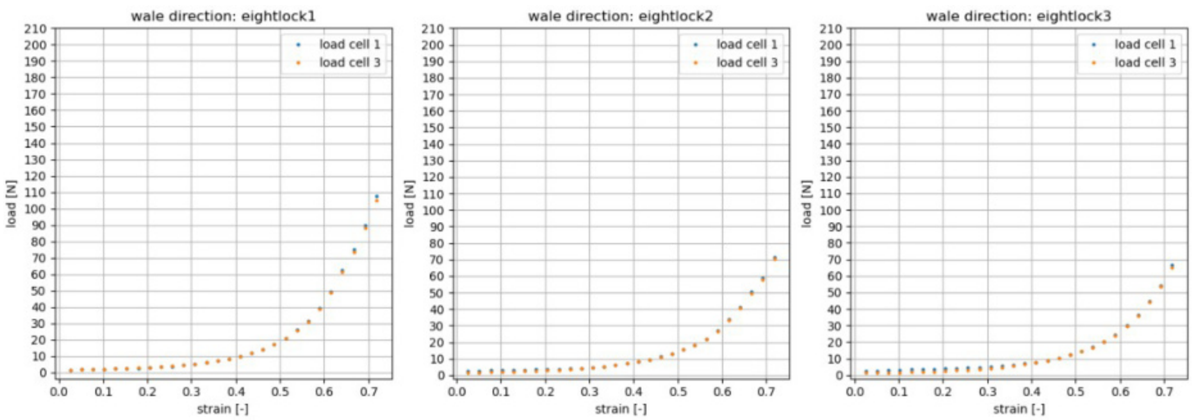

Figure G.2: Eightlock

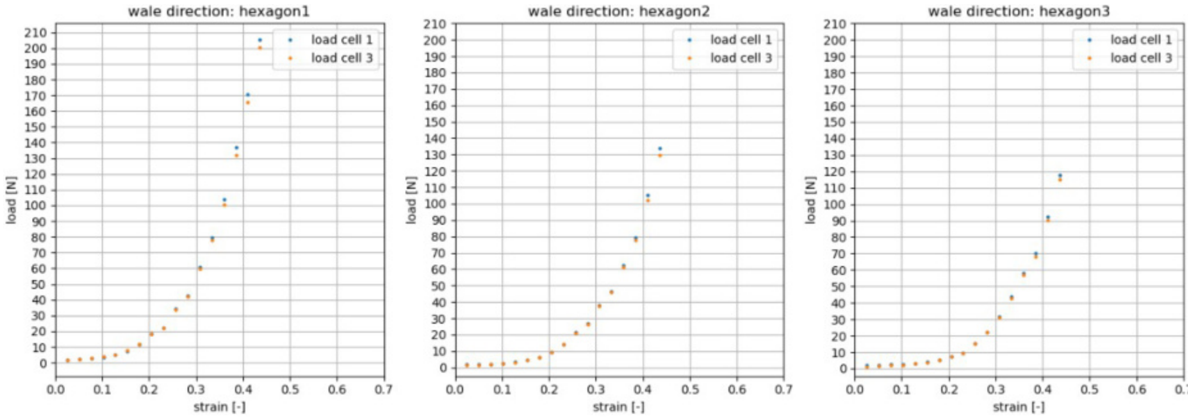

Figure G.3: Hexagon

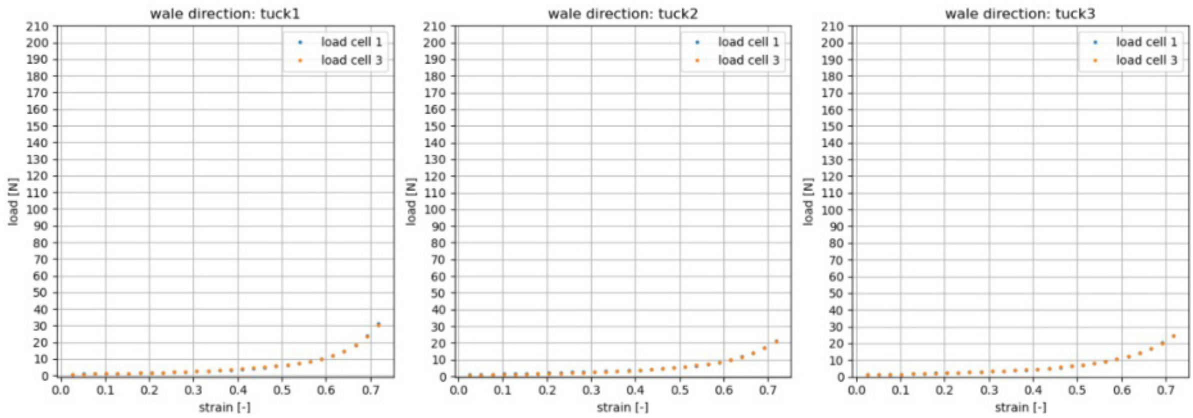

Figure G.4: Tuck

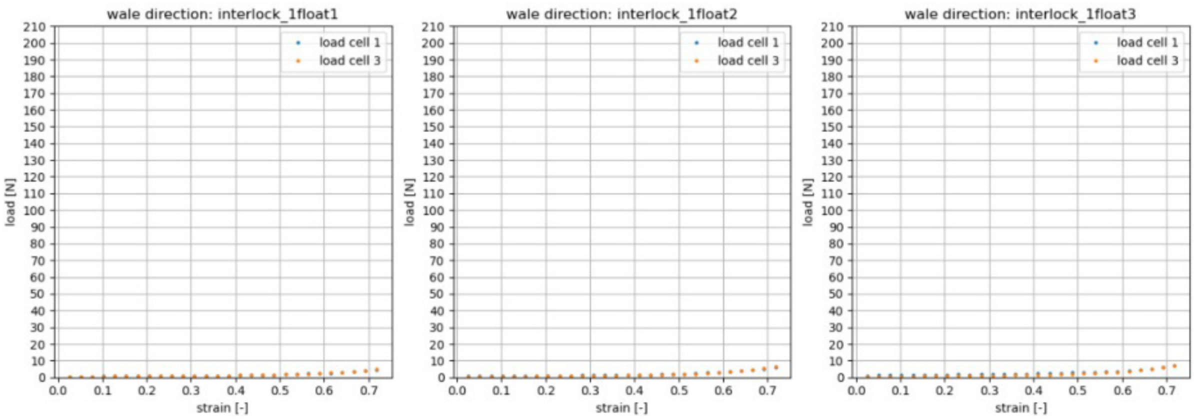

Figure G.5: Interlock_1float

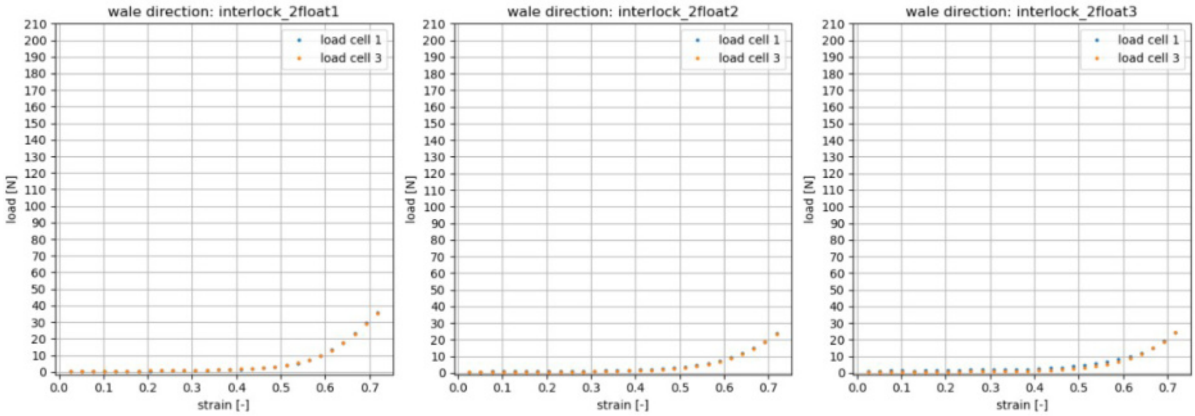

Figure G.6: Interlock_2float

Course direction

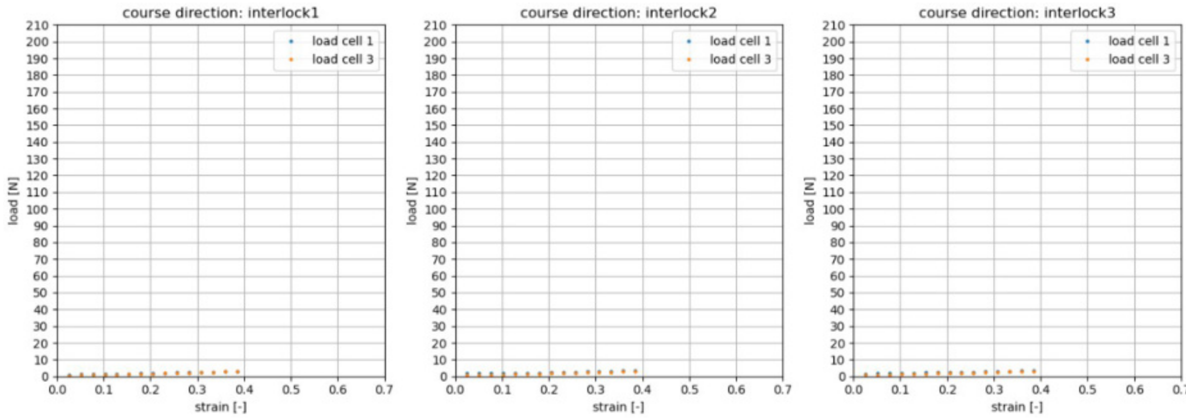

Figure G.7: Interlock

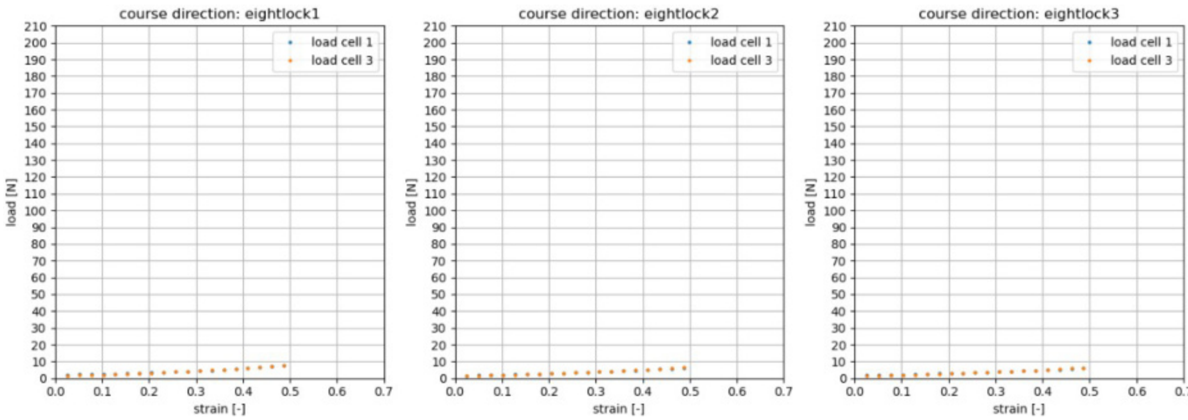

Figure G.8: Eightlock

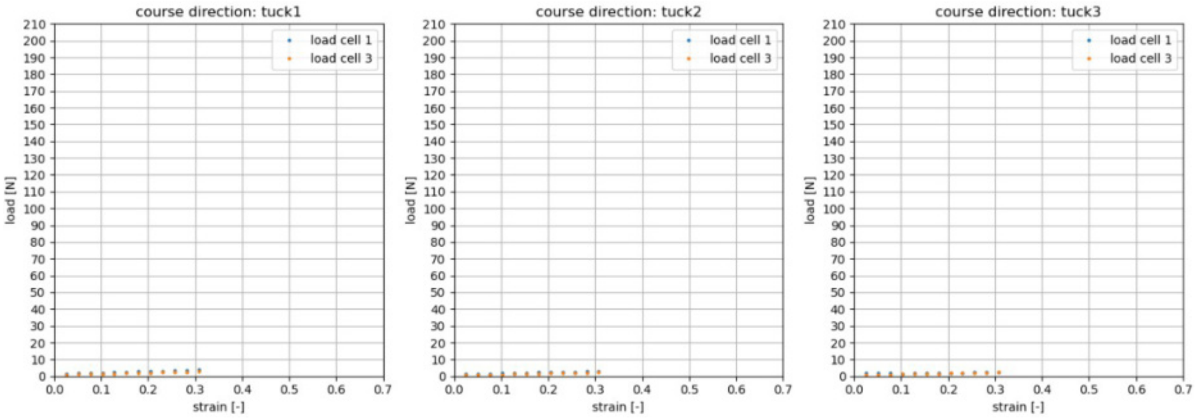

Figure G.9: Tuck

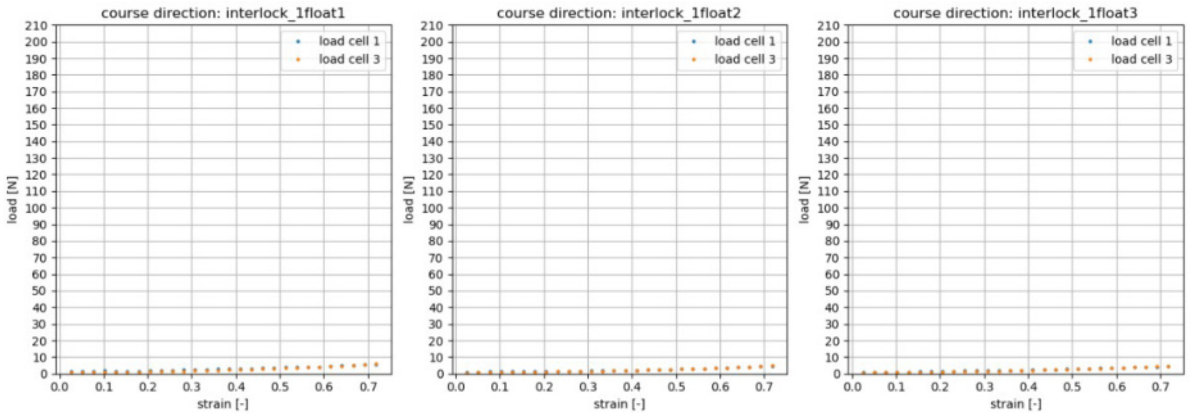

Figure G.10: Interlock_1float

G.2. Non-homogeneous fabrics

Wale direction

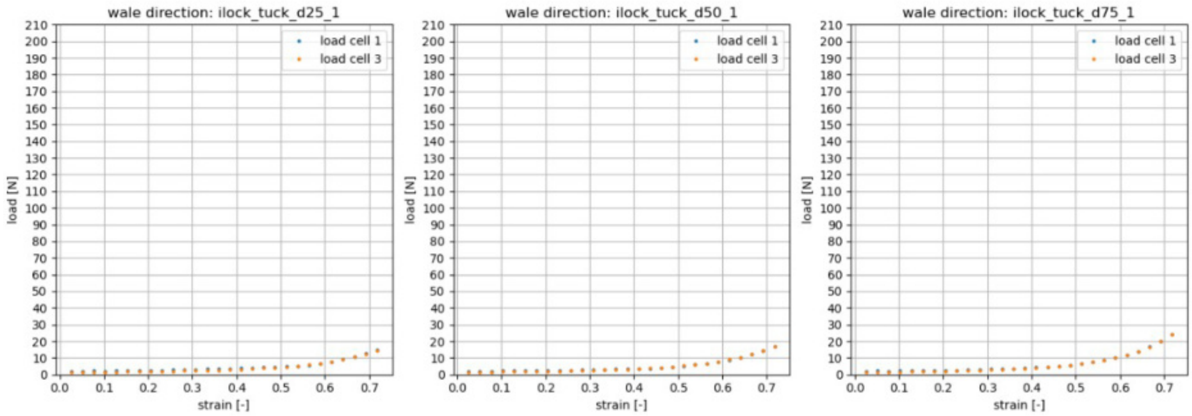

Figure G.11: Interlock_tuck

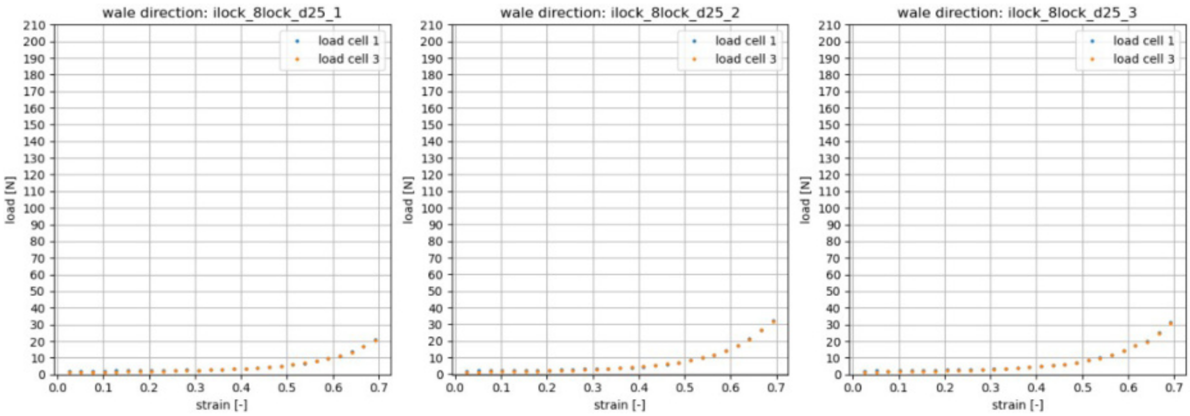

Figure G.12: Interlock_eightlock_d25

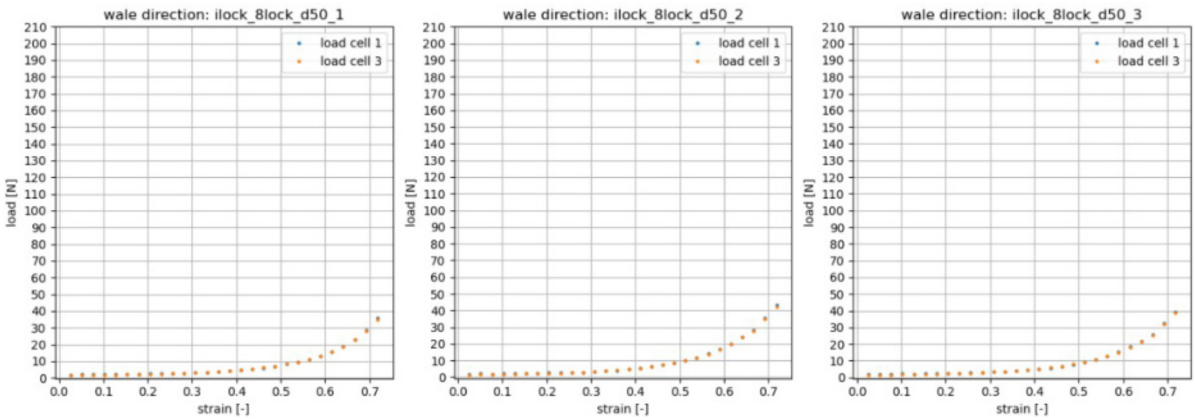

Figure G.13: Interlock_eightlock_d50

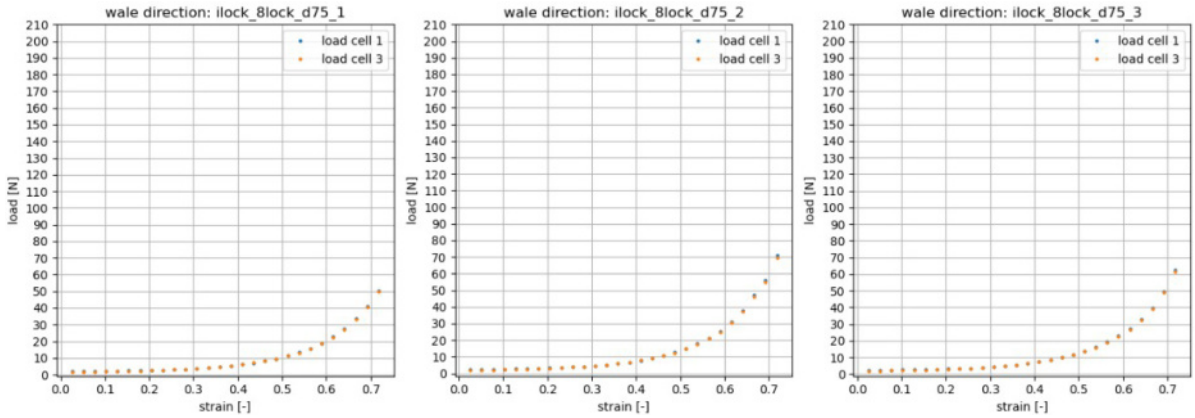

Figure G.14: Interlock_eightlock_d75

Course direction

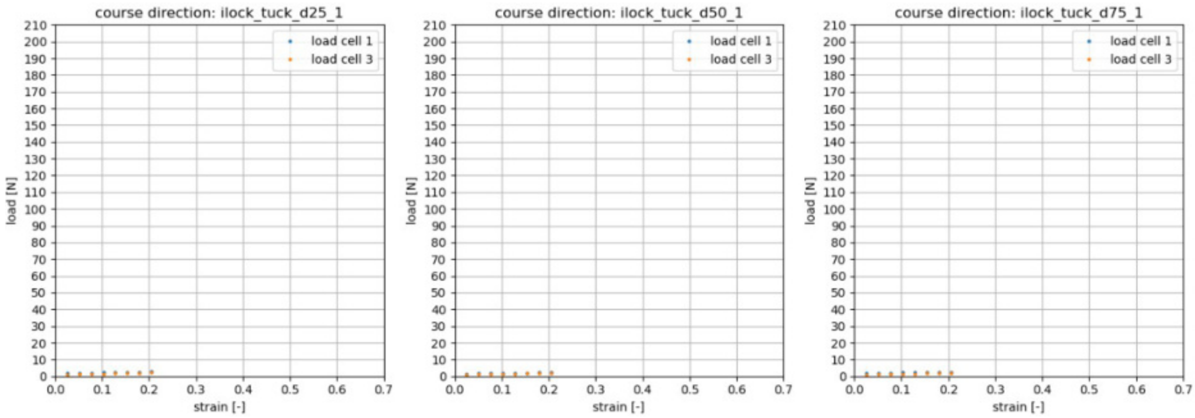

Figure G.15: Interlock_tuck

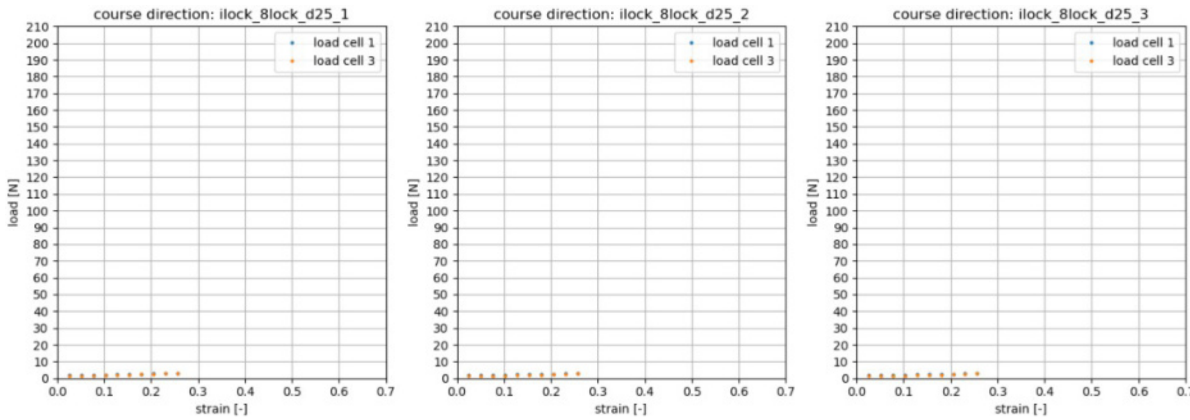

Figure G.16: Interlock_eightlock_d25

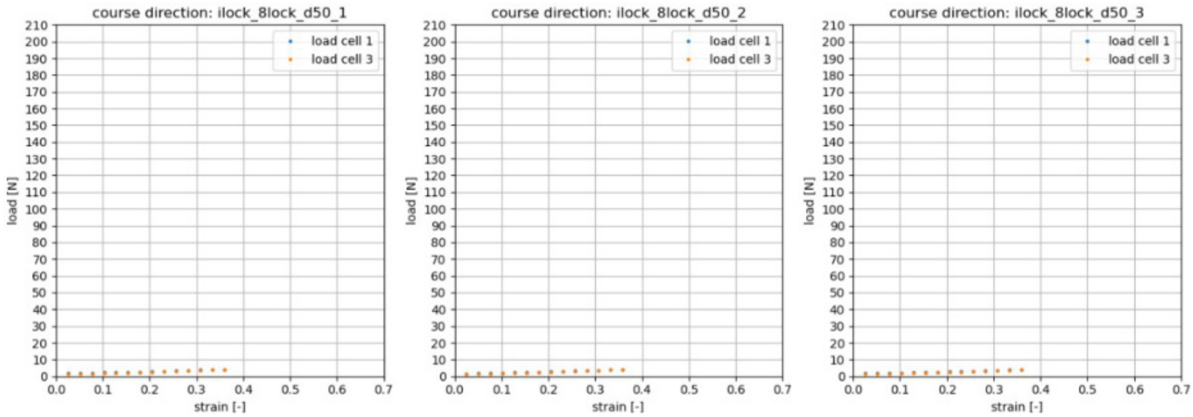

Figure G.17: Interlock_eightlock_d50

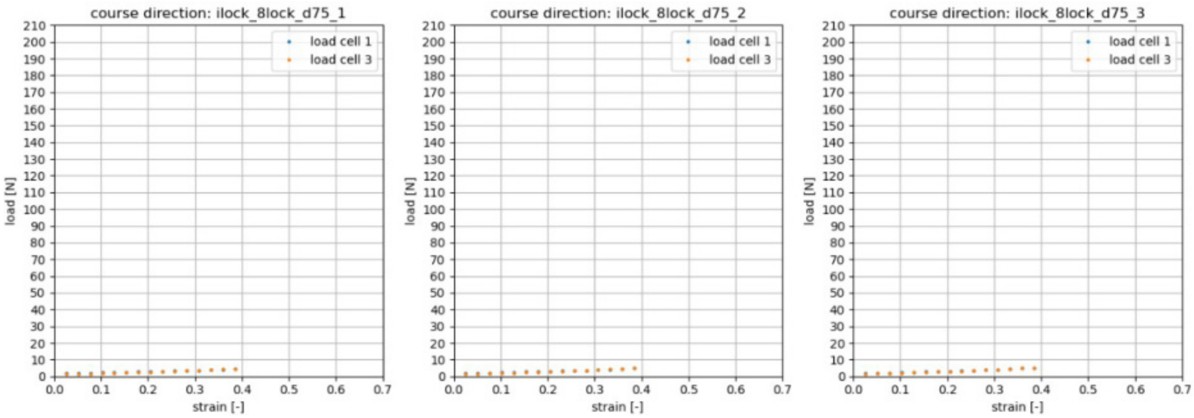

Figure G.18: Interlock_eightlock_d75

H
Young's modulus

H.1. Homogeneous fabrics

Wale direction

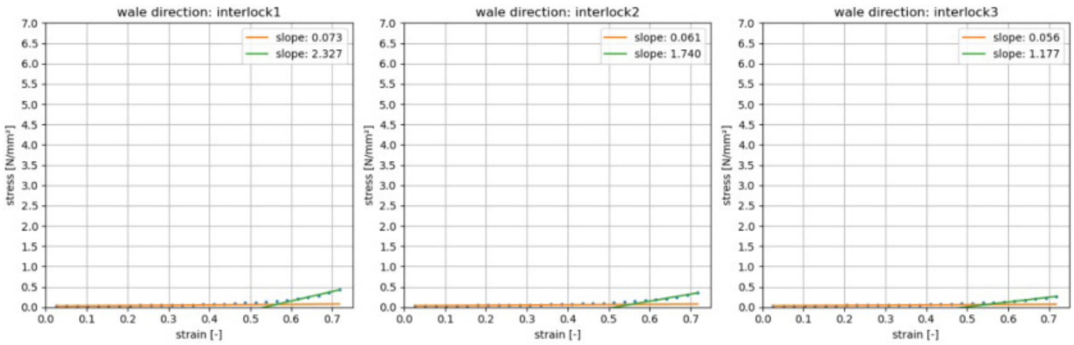

Figure H.1: Interlock

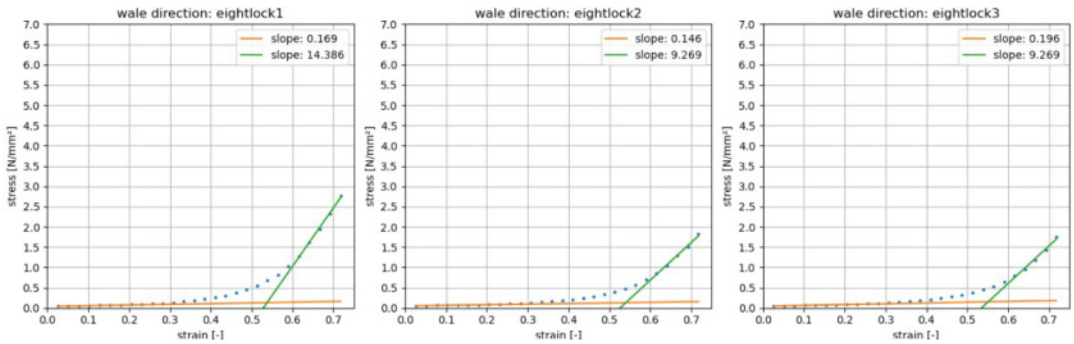

Figure H.2: Eightlock

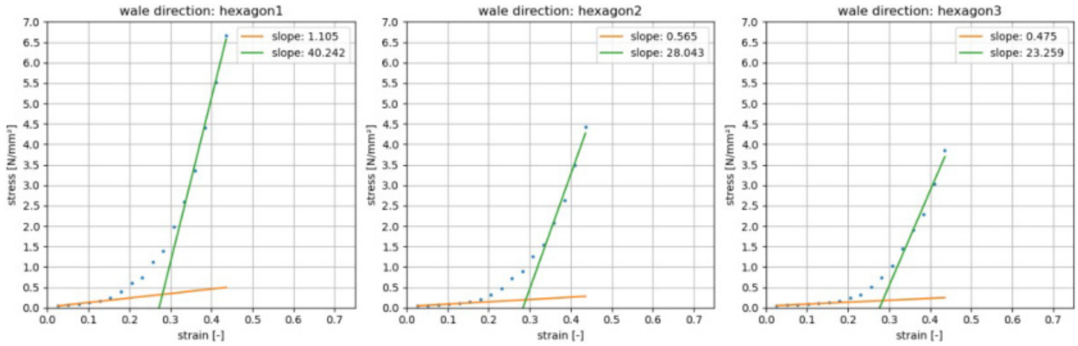

Figure H.3: Hexagon

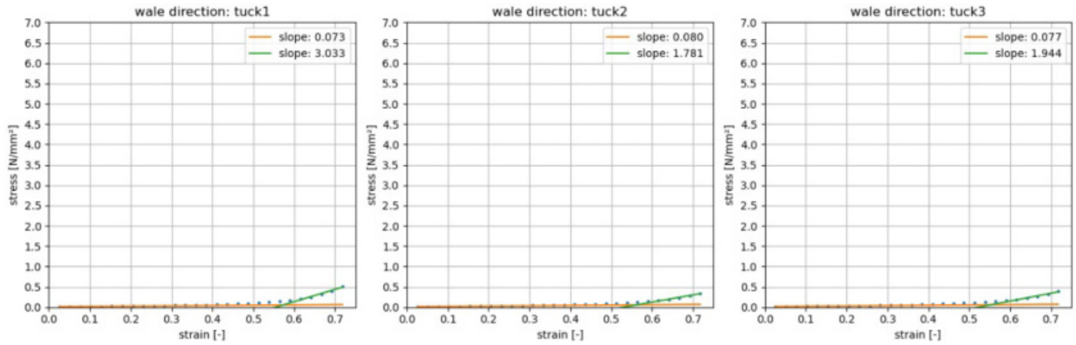

Figure H.4: Tuck

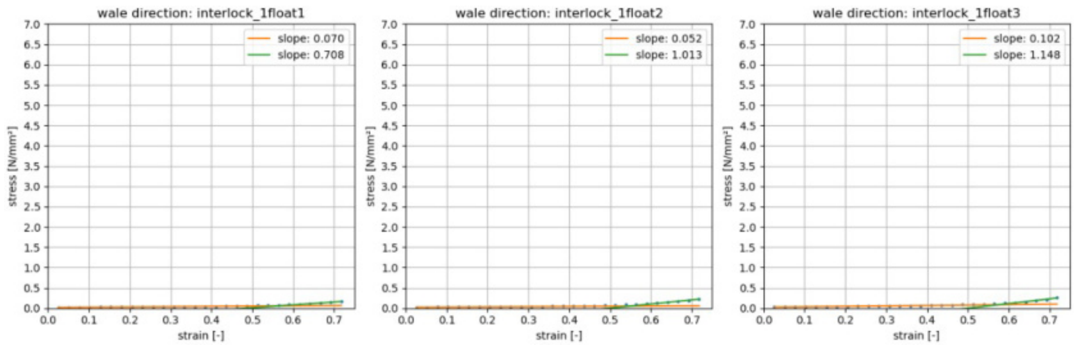

Figure H.5: Interlock_1float

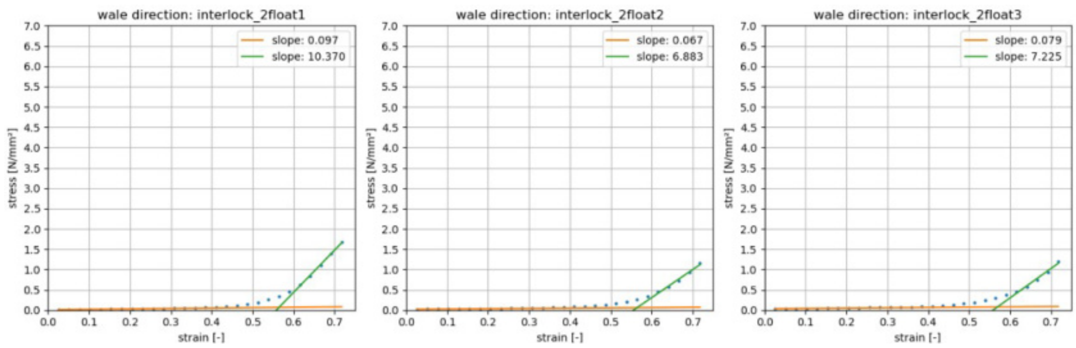

Figure H.6: Interlock_2float

Course direction

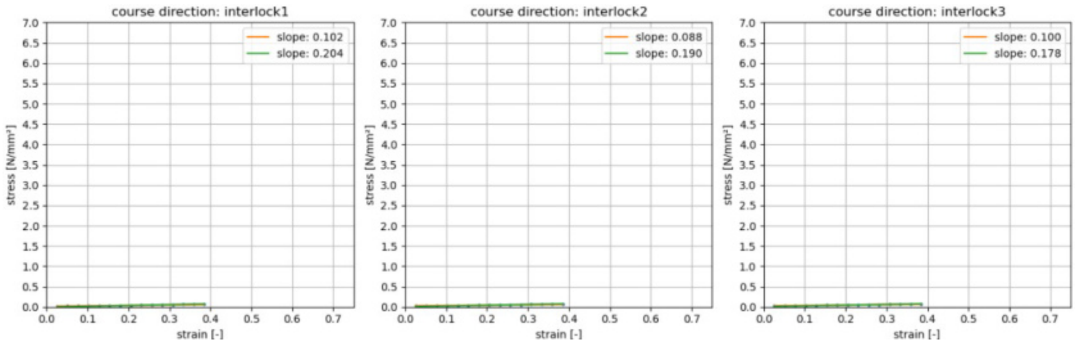

Figure H.7: Interlock

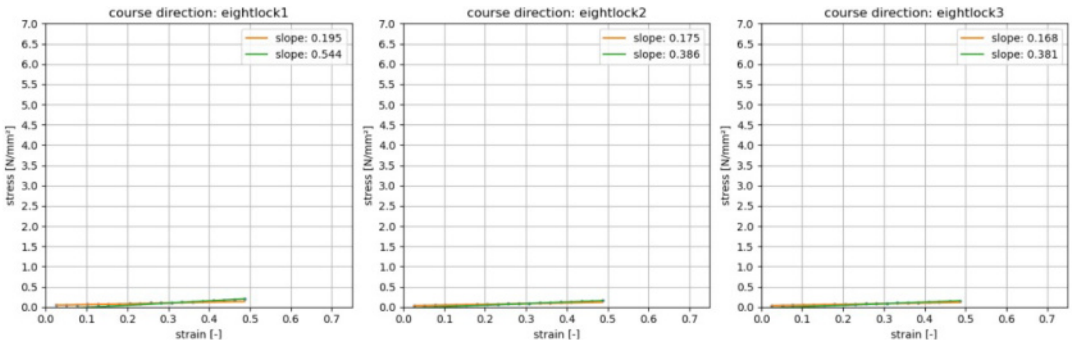

Figure H.8: Eightlock

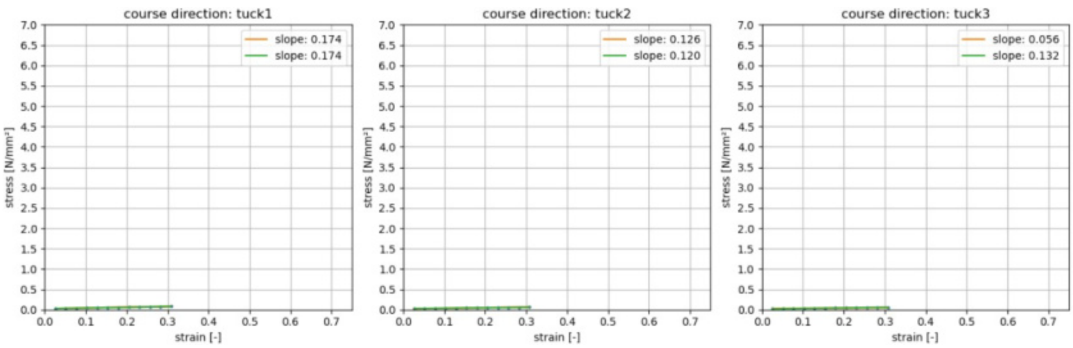

Figure H.9: Tuck

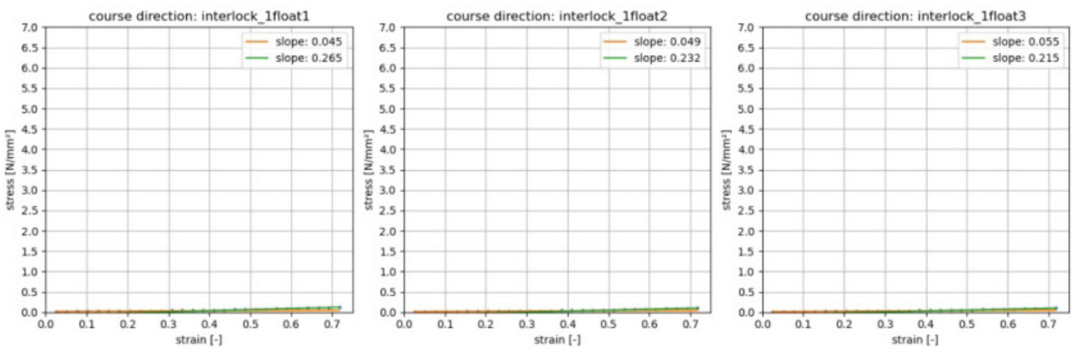

Figure H.10: Interlock_1float

H.2. Non-homogeneous fabrics

Wale direction

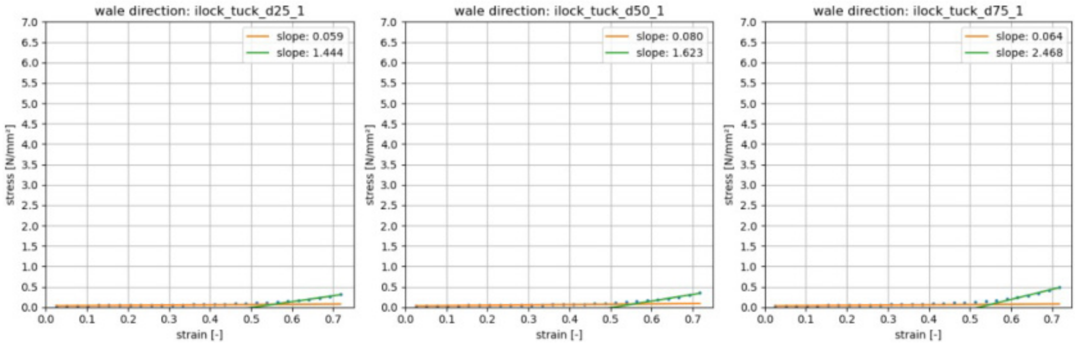

Figure H.11: Interlock_tuck

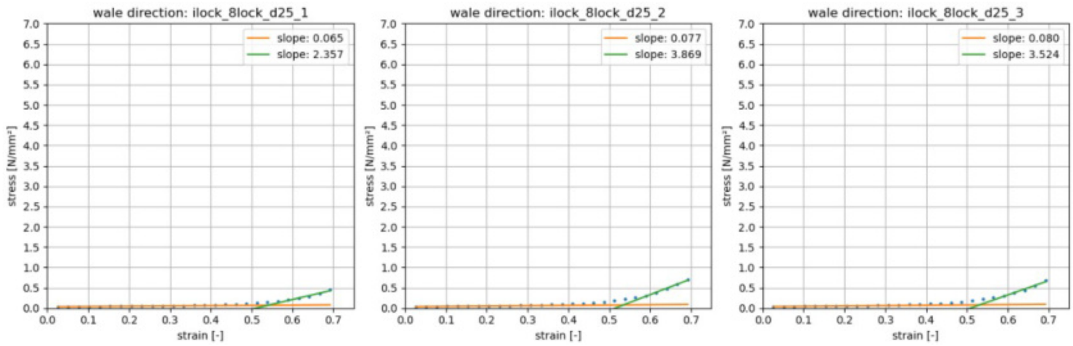

Figure H.12: Interlock_eightlock_d25

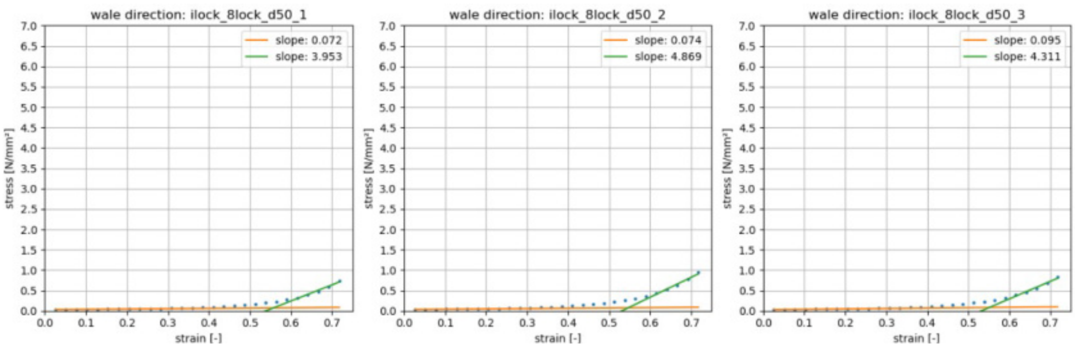

Figure H.13: Interlock_eightlock_d50

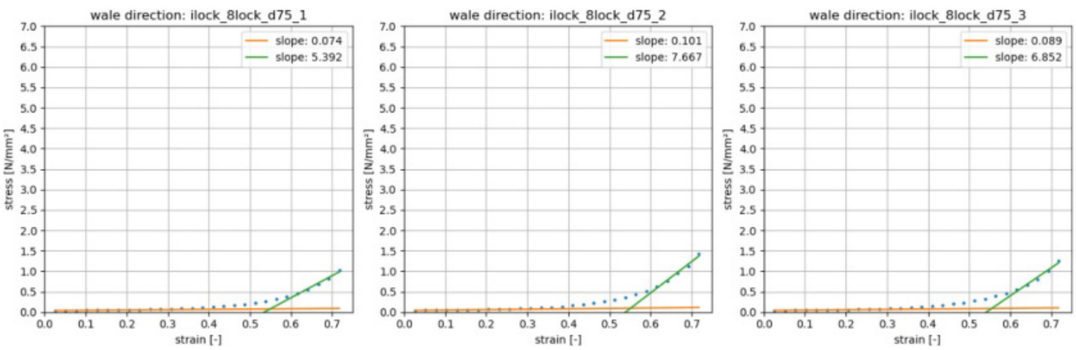

Figure H.14: Interlock_eightlock_d75

Course direction

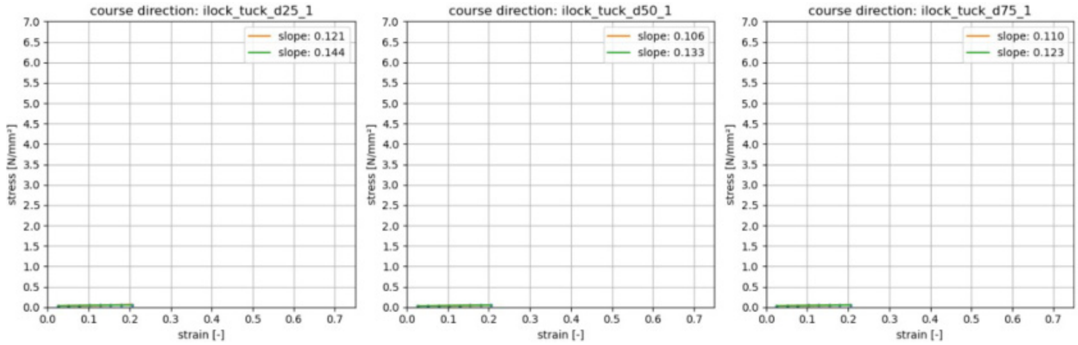

Figure H.15: Interlock_tuck

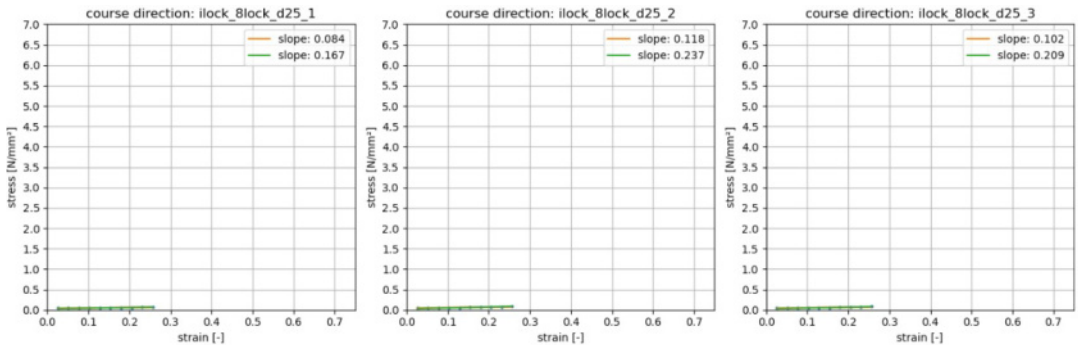

Figure H.16: Interlock_eightlock_d25

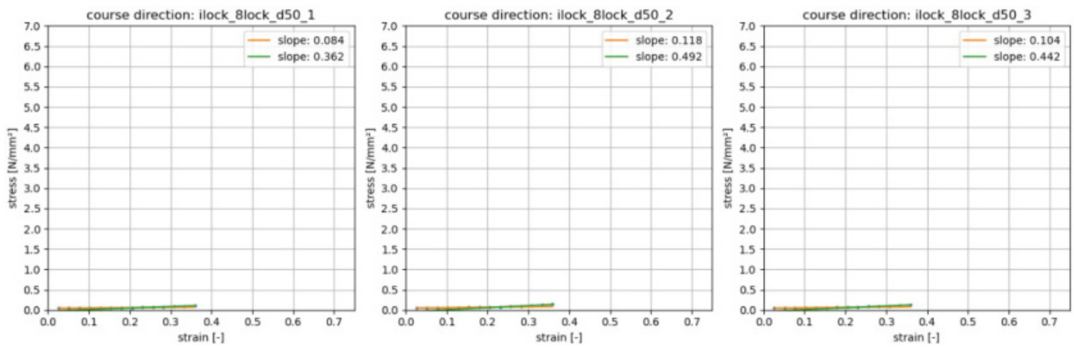

Figure H.17: Interlock_eightlock_d50

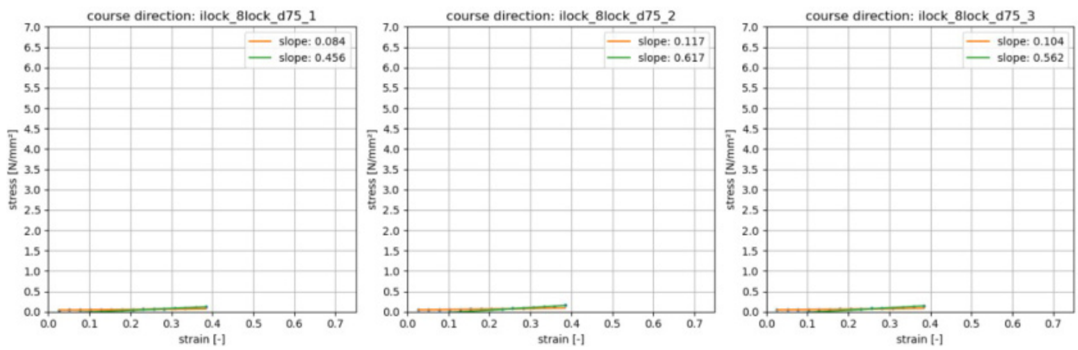

Figure H.18: Interlock_eightlock_d75